1990

Photometry of the Wolf-Rayet star EZ Canis Majoris (EZ CMa)

Lucia Gabriella Adorni-Braccesi
University of Wollongong

Photometry of the Wolf-Rayet Star EZ Canis Majoris (EZ CMa)

A dissertation submitted in partial fulfilment of the requirements for the award of the degree of Master of Science (Honours).

from

Department of Physics

University of Wollongong

by

Lucia Gabriella Adorni-Braccesi, BSc*(Woll)*.

December 1990

Then God said,

"Let lights appear in the sky

to separate day from night

and to show when days, years and seasons begin;

they will shine in the sky

to give light to the earth"

-and it was done.

Genesis 1

ABSTRACT

Previous photometry of the variable WN5 star EZ CMa shows that it has a constant period of 3.7658 ± 0.0007 days, but a light curve that has varied in shape and amplitude over the past 15 years. Subsidiary peaks or possible secondary periods have been observed in this time. These photometric variations may be explained by either binary modulation, pulsation or rotation-related phenomenon. The detection of a long term period of 10.24±0.03 days, is presented, with a montage of all light curves of EZ CMa plotted over the past 15 years.

CONTENTS

INTRODUCTION

Wolf-Rayet stars are massive, hot stars which are thought to be in an evolutionary stage immediately preceeding supernova explosion. Most Wolf-Rayet stars show light variability which is due to intrinsic properties or binary modulation.

The Wolf-Rayet star examined in this thesis, is the WN5 star EZ CMa, (HD 50 896). It has an unusual photometric light curve, which varies in shape and amplitude over a time interval of months. The cause of light variability, either from binarity or some intrinsic property, is not yet known, but it always has a period of 3.76 days. It is thought that EZ CMa is most likely a binary system with the atmosphere of the Wolf-Rayet star enclosing a neutron star (WR + c). If this is the case, EZ CMa will fill the missing link in the evolution of massive binary systems.

Photometric measurements of EZ CMa were taken over 16 nights using the 16 inch Cassegrain telescope of the Department of Physics, University of Wollongong, in an attempt to contribute to the existing photometric information of EZ CMa, and help solve the cause for its variability.

CHAPTER 1: WOLF-RAYET STARS

Wolf-Rayet (W-R) stars are believed to be the final stages in the evolution of massive stars, before they explode into supernovae. They were discovered by the French astronomers Wolf and Rayet in 1867, and consist of a hot central core surrounded by a shell of gas which is expanding rapidly (approximately 1000km/sec). Their spectrum is characterised by wide, multiply-ionized carbon, nitrogen, oxygen and helium emission lines superimposed on the continuum (Jaschek 1987). Surface temperatures range between 15 000K and 100 000K (Rublev 1975), with an absolute magnitude range of -3.4^{m} to -6.3^{m} (Rublev 1975). This places Wolf-Rayet stars among the O-type stars on the Hertzsprung-Russell diagram.

In 1933, Edlen and Payne divided W-R stars into two subtypes; the carbon sequence (WC), whose spectra contain strong carbon and oxygen emission lines; and the nitrogen sequence (WN) containing strong nitrogen emission lines. Each sequence is further divided according to the relative strength of the characteristic emission lines, i.e. from WC4 to WC9 and from WN3 to WN9. The higher number, in WC types only, indicates narrower emission line widths (Jaschek 1987).

Two rules are observed in this classification scheme. Lines from the more ionized elements, for example; N*V*, are narrower than lines of a less ionized element such as N*IV*. Also, the quantity $\Delta\lambda/\lambda$, where $\Delta\lambda$ is the width of the emission lines and λ is the wavelength, is constant for a given ion. (Jascheck 1987).

This classification also applies to line emission in the near infra-red.

The star under observation in this thesis, EZ Canis Majoris (HD 50896), is classified as a WN5 type star. It's spectrum is characterised by emission lines such that: strength of N*III* ~ strength of N*IV* ~ strength of N*V*.

Figure 1.1: Emission lines in WR stars

Carbon sequence		Nitrogen sequence	
He I		He I	
He II	4686	He II	4686
C II	4267	N III	4097, 4640, 5314
C III	3609, 4187, 4325, 4650, 5696	N IV	3483, 4057
C IV	4441, 4658, 4786, 5805	N V	4605, 4622
O II	4134, 4317, 4349, 4366, 4414, 4417		
O III	3714, 3760, 3961		
O IV	3385, 3405, 3412, 3562, 3725, 3736		
O V	5592		
O VI	3815, 3835		

Figure 1.2: Classification of WN spectra

Class		Criteria
WN8	N III ≫ N IV	He I strong with violet absorption edges. N III λ4640 ≈ He II λ4686, N III λ5314 present
WN7	N III ≫ N IV	He I weak, N III λ4640 < He II λ4686.
WN6	N III ≈ N IV	N V present but weak, N III λλ4634–41 band present
WN5	N III ≈ N IV ≈ N V	N III λ4634–41 band present
WN4.5	N IV > N V	N III very weak or absent
WN4	N IV ≈ N V	N III very weak or absent
WN3	N IV ≪ N V	N III absent

Smith 1968

It is important to note that the WN & WC spectral classification does not correspond clearly to evolutionary stages or physical properties of Wolf-Rayet stars. Also, the division into the two types nitrogen and carbon is not exclusive. For example, some carbon emission lines are observed in the WN type stars. There are also a few intermediate types which are a mixture of WC and WN type stars and may be binaries.

The width, $\Delta\lambda$, of the emission lines range from 4A to 100A, and are an indication of the velocities of the expanding shell of gas surrounding the hot core (Lamontagne, Moffat, Lamare 1982). This is because lines emitted by gas travelling towards the observer, will be bunched up or Doppler shifted towards the blue, with respect to gas travelling away from the observer, in which case the emission lines will be red-shifted. The line contribution from the gas expanding towards and away from the observer and in all other directions, add up to the broad line width observed.

The origin of the driving force of the expanding shell of gas is generally conceded to be radiation pressure, although complete agreement between theory and observation is still lacking.

Wolf-Rayet stars are young Population I type stars (stars with a relatively high abundance of elements heavier than hydrogen and helium that have been formed recently). They are helium stars with atmospheres that are enriched with nitrogen and carbon.

Most Wolf-Rayet stars are found along the Galactic plane in the spiral arms, similar to O-type stars, and are thought to have evolved from O-type stars because of this. However, they are not found in the anticentre quadrant: $140 < l < 220$, an effect believed to be due to the low metallicity of the O stars, and/or a steeper I.M.F (Conti 1983).

More than 40% are the exciting stars of ionized hydrogen (HII) regions (Van der Hucht 1981), and some are the central star of ring nebulae which resemble planetary nebulae but are much larger (Lamontagne, Moffat 1982). These nebulae have been

observed only around WN 5,6,8 type Wolf-Rayets (Rublev 1975), and are situated relatively close to them (7 - 10 pc). They are thought to be interstellar matter that has been swept up by gas streaming from the W-R stars, and are still expanding at a rate of 10 to 100 km/s (Johnson & Hogg 1965).

Only 159 Wolf-Rayet stars have been catalogued down to the 15th magnitude. Three are brighter than mag. 6.5, and twenty are brighter than mag. 9 (Lamontagne, 1982).

The mass range of Population I Wolf-Rayet stars is from 8 $M_{\odot}$ to greater than 100 $M_{\odot}$ (Smith & Maeder 1986), and the periods of Wolf-Rayet binaries range from 1.6 days to 20 days.

The majority of Wolf-Rayet stars show some light variability either in the continuum or the emission lines. Possible reasons for this variability have been summarised by Lamontage and Moffat (1987) and include:

1. Formation and ejection of plasma blobs in the strong winds of Wolf-Rayet stars
2. Radial or non-radial pulsations
3. Rotation (eg. of hot or dense clumps confined by a magnetic field)
4. Binary modulation (eg. eclipses, transparency effects, or tidal perturbations).

The first source of variability is expected to occur randomly but can occur periodically if it is connected with pulsations, rotation or a binary modulation of the star. Radial and non-radial pulsations, and rotation would be periodic over short time spans but are unlikely to be persistent for longer time intervals. Binary modulation would show long term periodicity with only one period (Lamontagne, Moffat 1987).

The Evolution of Massive Close Binary Systems

If two stars in a binary system are separated by a distance equal to or less than the radius of the largest star, each star has the effect of changing the structure and evolution of the other star, since some surface material systematically flows from one star to it's companion (Harwit 1973). This system is called a close binary system, and is found in up to 73% of all known variable Wolf-Rayet stars (Kuhi 1973).

The French mathematician, Edward Roche (~1850), discovered that the gravitational domain of each star in a binary system, that is, the area in which material of a star cannot escape from that star and is bound to the star, could be drawn as a three dimensional figure 8 around the system. These are called Roche lobes. Material from a star which crosses over this border or lobe, is not bound to that star, and can escape into space or be caught in the companion star's Roche lobe.

Close binary systems are divided into three classes; detached, in which each star is contained within its Roche lobe; semi-detached, in which the photosphere of one star fills its Roche lobe; and contact binaries, in which both stars are at or over their Roche lobes.

The evolution of both stars in a close binary system is affected in the following way. The more massive star of a detached binary system evolves into the red-giant stage before its companion. The red giant may overflow its Roche lobe and lose mass to the companion star, to become a semi-detached binary system. This decreases the evolutionary time period of the companion star because it has gained mass.

Massive binary systems contain large stars such as O-type stars, which are denoted by O+O.

It is hypothesised (Van den Huevel 1976), that the more massive O star develops into a Wolf-Rayet star after losing mass through either Roch lobe overflow or by its own stellar wind, becoming a WR+O system. The Wolf-Rayet undergoes a supernova explosion and becomes a compact companion, (neutron star or black hole, denoted by "c"). If the binary system loses more than half of its mass in the explosion, then, according to the Virial Theorem, the system becomes unbound and the companion O star becomes a "runaway star", and accelerates out of the Galactic plane (Moffat, Seggewiss 1979). If enough mass from the more massive O star is transferred to the companion O star before the W-R stage and supernova explosion, the system can stay bound, losing less than 50% of its total mass.This is the c+O stage and is relatively short.

The O star then evolves into a Wolf-Rayet star, often times producing a ring nebula in the process, and engulfs its companion to become a contact binary. It is hypothesised that all WR+OB systems become c+WR systems, and that the two Wolf-Rayet stages last for equal time intervals (de Loore, de Greve 1975).

The Wolf-Rayet star finally evolves into a neutron star and the system becomes a runaway, c+c, binary pulsar system.

The proposed evolution of massive binary systems is therefore:

O+O => WR+O => c+O => c+WR => c+c

All stages of the evolution of massive binaries have been observed except the c+WR system. It is thought that EZ CMa is a Wolf-Rayet which has engulfed a neutron companion star, and may be the "missing link" in the evolution of massive binaries.

The Detection of Neutron Stars

Neutron stars are formed during a supernova explosion, when the star's core is compressed so much that normal gas pressure cannot support it. If the remnant mass is less than $1.4M_{\odot}$, the core collapses to become a white dwarf and relies on electron degeneracy pressure[(a)] for support. If the remnant mass is more than $1.4M_{\odot}$, degeneracy pressure cannot support it and it collapses until electrons are forced together with protons to become neutrons. If the remnant mass is greater than $3M_{\odot}$, not even neutron degeneracy pressure[(b)] can support it, and it collapses further to become a black hole.

In a semi-detached or contact binary system where one component is a neutron star (or black hole), mass from its companion falls into the neutron star, is heated, and emits irregular bursts of X-rays. By measuring the X-ray light flux in binary stars and by knowing the mass of the companion star, the existence of a neutron star (or black hole) can be determined.

CHAPTER 2: A HISTORY OF EZ CANIS MAJORIS

EZ Canis Majoris, HD 50896, has a visual magnitude of 6.94, an absolute magnitude of -4.9, and is the sixth brightest Wolf-Rayet star in the sky. It was classified by Smith (1968) as a WN5 type star, and is located at galactic longitude $l = 234.8^{o}$ and latitude $b = -10.1^{o}$ It is four times the average distance from the Galactic plane (Z=280pc, Smith 1968) of young, Population I stars and is therefore, thought to be a "runaway" star which has been accelerated out of the Galactic plane by an impulse received from a supernova explosion, 10^{6}-10^{7} years ago (Moffat 1982). It is 1.59 kpc (Smith 1968) or 5190 light years away and is in the centre of the faint, SNR ring, S308, though considered not be associated with it (Nichols-Bohlin, Fesin 1986; Howarth, Phillips 1986). It was presumed to be a single star, due to lack of evidence of a companion star, until the profile of the strong emission line He II (λ4686) was found to vary in a similar way as the well known Wolf-Rayet binary V444 Cygni. In 1979, the photometric, polarimetric and spectroscopic light curves were found to vary with a period of 3.76 days (Firmani & Mclean 1980) with an amplitude that varies over months or years. This variation is thought to be due to a neutron star companion which is surrounded by an accretion disc, orbiting the W-R star within its extended atmosphere.

The broad width of the emission lines in the spectra of EZ CMa, indicating strong, radially expanding stellar winds, were first reported by Wilson in 1948, then by Smith in 1965. The winds were measured by Barbon in 1965, to have a mean radial velocity of 3000km/s.

Smith, in 1968, noted that the line profile of the strong He*II* (λ 4686) emission line, was occasionally asymmetric. This was confirmed by Irvine and Irvine in 1973. Similar line profiles are found in known binary systems, such as V444 Cygni (WN5 + O6), and EZ CMa was suspected to be a binary system with a period of 13 days (or multiple of 13) as measured by Schmidt in 1974.

Periodicity of EZ CMa

No clear unique period was determined until 1979. Kuhi, in 1967, suggested a period of 1.01 days with the flux of the continuum light varying by 0.3-0.4 magnitudes. Lindgren, in 1975, found a period of 1.03 days in the flux of the emission lines but not in the continuum.

Firmani, in 1979, determined a period of 3.76 days, which was later confirmed by Cherepashchuck (1981), Lamontage, Moffat, Lamarre (1986), and Van Genderin (1987).

The possible existence of a second period was suggested by Gosset and Vreux (Dec 1986), to be, besides the 3.76 day high maximum, a 1.26 day maximum of lower amplitude. A 62 night photometric run of EZ CMa was taken by Drissen, Lamontage, Moffat (DLM) in 1988, and the best period determined to be 3.77 days, with other possible periods of 1.26 days and 0.75 days. In 1989, a second period of 1.18 days was found by Balona in 1989.

The Light Curve

The light curve of EZ CMa is highly variable in amplitude and phase but always has the same 3.76 day period.

Below is a montage of the photometric light curve for EZ CMa over a period of 13 years.

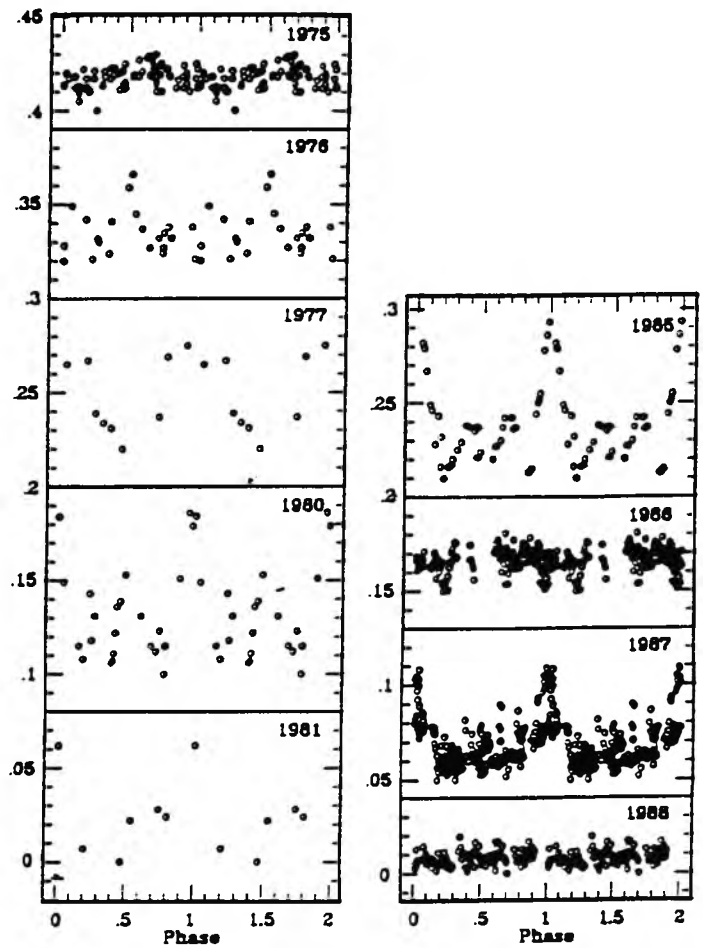

A montage of all available photometry for HD 50896. The period is 3.7658 d. the epoch of phase zero is JD 2440000.500.

Figure 2.1: Balona, Egan, Marang 1989

The amplitude of the light curve in 1975 and 1976 was small (0.008mag), with the possibility of the main period being absent, and the observed peaks being secondary periods. In 1977, the amplitude increased to 0.05mag., and in 1980 and 1985, the amplitude was 0.08mag. It became low again in 1986 and December 1988.

The 62 night photometric run, taken by DLM (early 88),gave a smooth light curve over an interval of two weeks, but its shape changed on a longer timescale.

During the first two weeks, the light curve was similar to that obtained in 1980 and 1985, i.e. one narrow maximum of amplitude 0.085mag. and some secondary maxima. Cherepashchuck (1980) suggested that the sharp maximum, approximately 1.2 days wide, and the wide minimum, approximately 2.5 days wide, were as a result of the asymmetric brightness distribution in the atmosphere of the Wolf-Rayet star due to the presence of a neutron star.

During the third and forth weeks, the light curve was similar to the 1977 curve obtained by Firmani (1980), with a rapid increase in brightness, followed by a slow decrease.

The final part of the data is less certain, but is similar to the 1986 data obtained by Van Genderin (1987) with a phase shift in the light curve of ~0.35.

The DML Light Curve of EZCMa (1988)

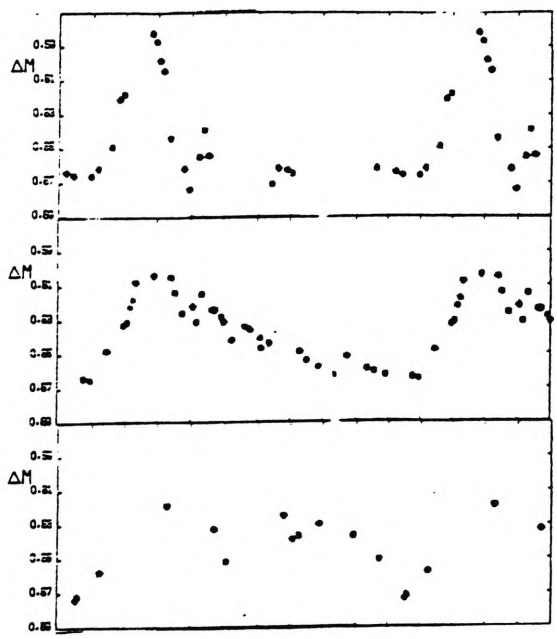

Figure 2.2: Drissen, Lamontage, Moffat 1988

Light Curve of EZCMa (1986)

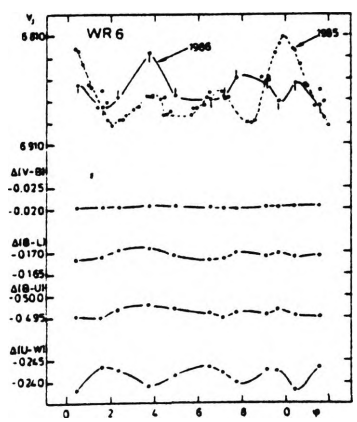

Figure 2.3: Van Genderin 1986

Variations of the light curve in the X-ray portion of the spectrum have also been observed. Moffat (1982), pointed out that similar variations were seen in V444 Cygni, and are produced from collisions of winds from the component objects. White and Long (1986) reported that the X-ray flux changed by a factor of 2 within 30 minutes, and Pollock (1987) observed a change by a factor of three over two years. White and Long suggested that the X-ray flux comes from accretion from the W-R star onto a white dwarf or from an accretion wake extending away from a black holein the wind of the W-R star. They avoided the suggestion of the presence of a neutron star since the X-ray luminosity of EZ CMa is (1.3 - 3 keV) 32 erg/s and is comparable to single hot stars (O or W-R) or significantly less than that seen among massive X-ray binaries.

EZ CMa as a Binary System

Despite the lack of X-rays, a feasible explanation for the variations in the light curve of EZ CMa, is the presence of a companion star orbiting the W-R star within its extended atmosphere.

The following is a diagram of the proposed structure of the EZ CMa system.

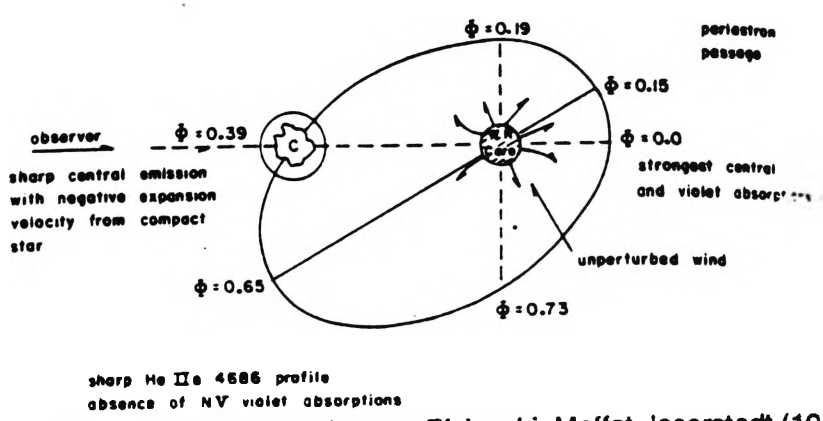

Figure 2.4: Firmani, Koenigsberger, Bisiacchi, Moffat, Isserstedt (1980)

It was constructed by comparing emission line profile variations of EZ CMa to other known binary systems with similar line variations.

During phases ~0.4 -0.6, the profile of the prominent He*II* (λ 4686) emission line has a sharper peak and more extended wings. This is similar to CQ Cep (WN7 + O7) when the O7 star is in front of the W-R star.

At phase 0.0±0.2, the N *V* (λ 4604) absorption lines are most intense, and at phase 0.3-0.8 almost disappear. This is similar to the V444 Cygni (WN5 + O6) system where the WN5 star is in front when the N V lines are most intense, and behind the O6 star when they disappear.

This is evidence that EZ CMa is a contact binary system, with the W-R in front of a possible neutron star companion at phase 0.0, and behind near phase 0.5.

With a period of 3.765±0.002 days, eccentricity e = 0.34 ± 0.08, and an inclination i equal to $71^{o}\pm 3^{o}$, Firmani (1980) determined the mass of the W-R component by analogy with the orbit of the WN5 component of V444 Cygni, to be $m_{W\text{-}R} = 10\ M_{\odot}$ giving the mass of the companion as $m_{c} = 1.32 + 0.15\ M_{\odot}$. This is similar to the mass found for neutron stars in X-ray binaries.

The only problem in confirming that the companion star is a neutron star, is the low X-ray flux. Steven and Willis (1988), calculated the X-ray flux that would be expected if the companion of the W-R star in EZ CMa was a neutron star. They found the flux should be between 10 and 100 times brighter than the flux that is observed.

This factor, and the continual change in the amplitude and length of the maximum of the light curve could be explained by the existence of a slowly precessing accretion disc. X-rays produced from material falling onto the neutron star are absorbed by this accretion disc and are re-emitted at lower frequencies. The compact star and its possible accretion disc, therefore, appear as a low mass, hot object producing continuous optical radiation, surrounded by a wind that produces narrow emission lines (He*II* λ4686, N*IV* λ4058). Changes in the orientation of the accretion disc would produce the variation of amplitude and length of maximum in the light curve.

A recent paper (Willis, Howarth, Smith, Garmany, Conti, 1989), attempted to confirm the existence of the neutron star companion, by observations of the variability of the ultraviolet emission line's P Cygni profile. According to the Hatchett and McCray model (1977), increased ionisation in the stellar wind, which is caused by the X-ray emission of the neutron star situated infront of the Wolf-Rayet star, will weaken the observed P Cygni type absorption lines. At phases 0.0, when the neutron star is behind the Wolf-Rayet, the P Cygni absorption lines will regain their strength and will reflect the normal wind density and velocity of the Wolf-Rayet envelope.

Although strong variations in the absorption lines of N*V* λ1240, C*IV* λ1550, He*II* (λ1640), and N*IV* (λ1718), were observed, there was no significant phase dependence of the variations with the binary period of 3.76 days. The variability of EZ CMa was concluded to be a result of changes in the stellar wind of the Wolf-Rayet star, such as non-radial pulsations, ejection of plasma blobs in the wind, or rotation.

EZCMa As A Single Star

The binary model has three problems associated with it; the weak X-ray flux observed is comparable to single Wolf-Rayet stars, the variations in the profile of the ultraviolet lines show no phase dependence, and the spectroscopic variations can be caused by non-radial pulsations. In view of these factors, models for EZ CMa as a single variable are also considered.

Reasons for variability in single Wolf-Rayet stars can be either; the formation of plasma blobs in the wind, radial / non-radial pulsations, or rotation of hot spots on the Wolf-Rayet star which are confined by a magnetic field.

The occurrence of plasma blobs in the wind of EZ CMa has been found to be low when compared to other single W-R stars. It is therefore, most unlikely to be the cause of such regular periodic variation in the light curve of EZ CMa.

A change in the period, and the existence of more than one period, in B stars is due to non-radial pulsations. Both of the above conditions have been found in EZ CMa, and according to Gosset & Vreux (1986), are a strong argument for the cause of variability of the light curve.

The presence of a rotating semi-stable bright spot in the W-R atmosphere could explain the changes in phase and amplitude of the light curve. A hole in the atmosphere or a region where the hotter layers are exposed would also cause light variability. However, rotation is an unlikely cause of light variation in Wolf-Rayet stars because the hot spots would require a permanent perturbation in the strong stellar

wind, possibly from pockets of plasma that are confined by magnetic fields. Magnetic fields in Wolf-Rayet stars have not been detected. No phase dependent colour variations, which would indicate the presence of rotating hot or cold spots, has been observed for EZ CMa (Van Genderin 1986), so rotation is highly unlikely.

In conclusion, the cause of variability of EZ CMa to date, remains a mystery!

CHAPTER THREE: OBSERVING METHODS AND PROCEDURE

Differential Photometry

The simplest observing method, and the one used for EZCMa, is differential photometry. This is the most accurate technique for measuring small variations in brightness.

In differential photometry, a second star of nearly the same colour and brightness as the variable star is used as a comparison star. All changes in the variable star are determined as magnitude differences between it and the comparison star.

The procedure is to alternate between the variable and comparison stars, measuring them a few times each filter and averaging the counts. A third star, the check star, is measured a few times during the night to test the non-variability of the comparison star. The sky background is then measured through each filter and subtracted from the star readings.

The magnitude difference between the variable and comparison stars in each filter can then be calculated by :

$$m_{var} - m_c = -2.5 \log(I_{var} / I_c)$$

where I_{var} and I_c are the measurements of the variable and comparison stars respectively, with the sky background subtracted.

The advantage of differential photometry, is that it is not necessary to calibrate the

disadvantage is that the actual magnitude and colour of the variable cannot be determined unless the comparison star is standardised.

The Earth's Atmosphere

Starlight coming to us from space is absorbed and scattered by air and water molecules, and by dust particles in the earth's atmosphere. The amount of light lost depends on the angle from the zenith, the wavelength of observation, and the atmospheric conditions. This loss of light is called extinction, and all photometric results must be corrected for this to give the apparent magnitude of the star outside the earths atmosphere.

The largest factor contributing to light extinction is the variation of the air mass that the stars' light must traverse as it moves away from the meridian.

The figure below shows the earth's atmosphere as a plane-parallel slab.

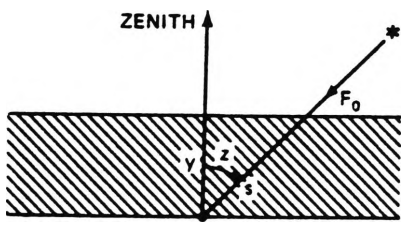

Figure 3.1

The curvature of the earth can be ignored for stars within 60^{o} of the zenith. The loss of light flux in travelling a distance ds in the earth's atmosphere is proportional to the

light flux of the star F_λ; the absorption coefficient α_λ; and the distance travelled through the atmosphere ds.

That is:

$$dF_\lambda = -F_\lambda \alpha_\lambda ds$$

where α_λ is in cm^{-1}, and the minus sign indicates that the light flux, F_λ, is decreasing with distance travelled. This can be written ;

$$dF_\lambda / F_\lambda = - \alpha_\lambda ds$$

and integrated over path length s, travelled in the atmosphere to get:

$$\ln(F_\lambda / F_{\lambda 0}) = - \int_o^s \alpha_\lambda ds$$

where $F_{\lambda o}$ is the light flux at the top of the atmosphere, and F_λ is the flux reaching the ground.

We define the optical depth τ by:

$$\tau_\lambda = \int_o^s \alpha_\lambda ds$$

which is dependent only on the absorption coefficient of the atmosphere, α_λ and the amount of atmosphere the light flux passes through. We can then write:

$$F_\lambda / F_{\lambda o} = e^{- \tau_\lambda}$$

To convert this flux ratio to a magnitude difference, we get,

$$m_\lambda - m_{\lambda o} = -2.5 \log (F_\lambda / F_{\lambda o})$$

$$= -2.5 \log (e^{-\tau_\lambda})$$

where m_λ and $m_{\lambda o}$ are the apparent magnitude of the star at the earth's surface and above the atmosphere, respectively. This becomes:

$$m_\lambda - m_{\lambda o} = 2.5 (\log e)\, \tau_\lambda$$

or

$$m_{\lambda o} = m_\lambda - 1.086\, \tau_\lambda$$

This equation can be placed in a more useful form if we show the variation of τ_λ with location in the sky. By figure 3.1, we get

$$\cos z = y / s$$

where z is the zenith angle, y is the thickness of the atmosphere at zenith, and s is the path length of the light. This can be written:

$$s = y \sec z$$

and

$$ds = dy \sec z$$

so that the optical depth

$$\tau_\lambda = \int_o^s \alpha_\lambda ds$$

becomes

$$\tau_\lambda = \sec z \int_o^y \alpha_\lambda dy$$

Therefore,

$$m_{\lambda o} = m_\lambda - 1.086 \sec z \int_o^y \alpha_\lambda\, dy$$

or

$$m_{\lambda o} = m_\lambda - k_\lambda' \sec z$$

where k_λ' is the principle extinction coefficient in units of magnitudes per airmass, and the subscript 0 is used to denote a magnitude outside the atmosphere.

Also secz is the mass of the air traversed by the starlight. When the star is directly overhead, z=0, and secz=1 in units of airmass. Secz can be determined by the following equation; $X = secz = (\sin\varphi\sin\delta + \cos\varphi\cos\delta\cos H)^{-1}$

where, φ = observer's latitude

δ = declination of the star

H = hour angle (from meridian) in degrees

The values of the extinction coefficient can then be found by taking photometric measurements of a (non-variable) star with changing airmass. By plotting magnitude versus airmass, the slope of the line is the extinction coefficient, k', and the y-intercept the extra-atmospheric magnitude.

For differential photometry, the differential magnitude of the variable star is calculated from: $\Delta m_\lambda = -2.5 \log (I_{var} / I_c)$

With the first order extinction coefficient, this becomes

$$\Delta m_{\lambda o} = \Delta m_\lambda - k_\lambda'(X_{var} - X_c)$$

where X_{var} and X_c are the airmasses for the variable and comparison star at each filter.

There are two types of particles in the atmosphere that cause first order extinction, and each have different wavelength dependencies. The major constituent is the air molecule which absorbs and scatters light by Rayleigh Scattering. The first order

coefficient k', varies as λ^{-4},where λ is the wavelength of light, and is in the range 3000A to 4500A.

Larger particles such as dust or water droplets cause scattering called aerosol scattering. Aerosols with diameters comparable to the wavelength of light produce extinction which is roughly inversely proportional to the wavelength (λ^{-1}), while particles much larger than the wavelength of light produce extinction which is independent of λ.

Figure 3.2 shows the change in the first order extinction coefficient with wavelength.

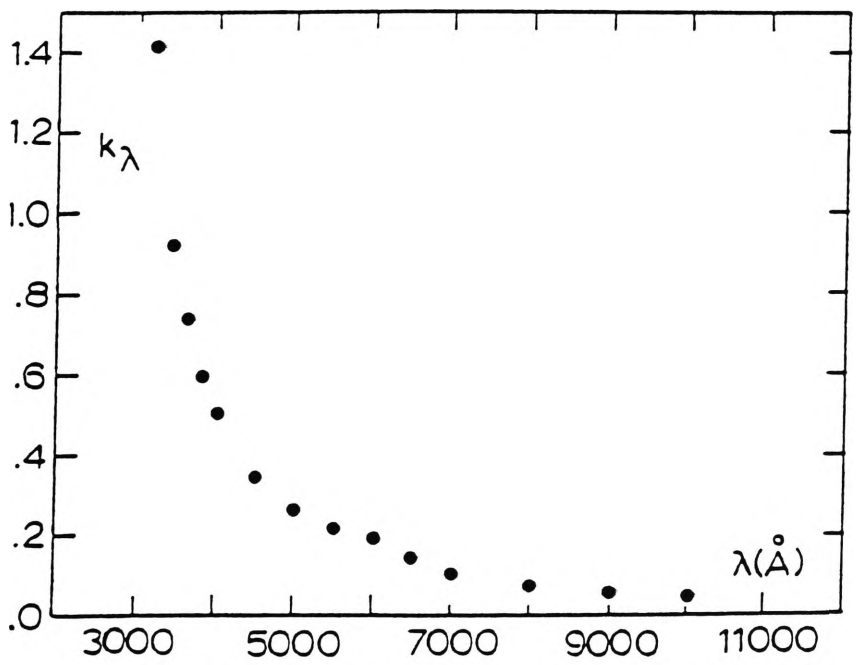

Figure 3.2: D.S.Hall, R.M. Genet (1982) pp9-6

In general, blue wavelengths are absorbed and scattered more than red wavelengths. This produces a problem when the same extinction coefficient, k', is applied to stars of different colours. The $\Delta m_{\lambda o}$ of the red star will have too much

extinction, and the blue star too little, giving a too small and a too large differential magnitude, respectively. This error, which is dependent on the star's colour and the airmass through which it is observed, is corrected for by the second order coefficient

of extinction k", so that; $$k_\lambda' = k_\lambda' + k_\lambda''(m_{\lambda 1} - m_{\lambda 2})$$

giving $$m_{\lambda o} = m_\lambda - k_\lambda' X - k_\lambda'' (m_{\lambda 1} - m_{\lambda 2})X$$

To obtain the colour dependent extinction coefficient k", a comparison of two close stars of different colours, such as the check star and comparison star, is required. The airmass may be taken as the average between the two stars because they are

close, so that; $$V_{01} - V_{02} = [V_1 - k_v' X - k_v''(B-V)_1 X] - [V_2 - k_v' X - k_v''(B-V)_2 X]$$

or $$\Delta V_0 = \Delta V - k_v''\Delta(B-V)X$$

which gives $$\Delta V = k_v'' \Delta(B-V)X + \Delta(B-V)_0$$

where V_{01} is the extra-atmospheric magnitude of star 1 through the Johnson V filter, and $(B-V)_1$ is the colour index of star 1.

By plotting ΔV against $\Delta(B-V)X$, the slope is the second order coefficient of extinction, k''_v, for the V filter.

For differential photometry, the extra-atmospheric, differential magnitudes for the visible and blue filters, respectively are:

$$\Delta V_0 = \Delta V - k_v'(X_{var} - X_c) - k_v'' \times \Delta(B-V)$$

$$\Delta B_0 = \Delta B - k_B'(X_{var} - X_c) - k_B'' \times \Delta(B-V)$$

where X is the average airmass for the variable and its comparison star.

Sky Background

There are six factors that contribute to the light of the night sky.

1- Integrated starlight from distant galaxies

2- Integrated starlight from within our galaxy

3- Zodiacal light which is caused by sun reflecting off dust in the plane of the solar system. It increases in brightness going towards the sun, and is confined to the ecliptic plane. Within 50^o of the sun, the zodiac light in the ecliptic plane is brighter than the brightest part of the Milky Way seen from earth, and is brighter than integrated starlight over most of the sky. It is relatively uniform across arc minutes.

4- Night airglow is the fluorescence of the atoms and molecules in the air from photochemical excitation. It occurs in a layer 100km above the earth and is variable depending in sky conditions, local time, latitude, season and solar activity. The light is made up of emission lines caused by atomic oxygen (λ5577 Å), sodium (λ5892 Å), molecular oxygen (λ7619, λ8645 Å), hydroxl OH^- (I.R) , and a continuum caused by nitrous oxide and other molecules.

5- Aurora is caused by the fluorescence of atoms and molecules from charged particles coming from the sun. These particles become trapped in the earth's geomagnetic field and spiral towards the poles where they excite air molecules. The main aurora emission lines are; atomic oxygen (λ5577,λ6300,λ6364 Å), hydrogen (λ6563 Å), and molecular nitrogen (IR). Brightness varies according to solar activity, latitude (concentrating around the poles), and time of year (peaking in March and October).

6- Twilight emission lines are caused from the illumination of sodium atoms contained in the upper atmosphere. The sodium D line (λ5892 Å), is the only emission line and appears when the solar depression angle (distance at which the sun is below the horizon) is between 7^0 and 10^0.

Photometric Systems

Photometric systems or light filters are divided into three types depending on the width of the bandpasses; wide-band, intermediate band and narrow band.

Wide-band systems have filter widths of about 900Å. The most commonly used is the Johnson UBV system.

The visual filter (V) is yellow with a transmission wavelength range of 4600Å to 7400Å and a peak transmission around λ5500Å. It was chosen to match the old visual magnitudes and is almost identical to the yellow-green portion of the spectrum where the human eye is most sensitive.The long wavelength cut-off is either

determined by the frequency response of the photometer for a 1P21, blue sensitive photocell, or, as in my case, by a specialised V filter (λ5000-λ6600Å), using a red sensitive diode.

The transmission wavelengths of the blue filter (B) range from 3600Å to 5600Å and is centred around λ4300Å. It corresponds to the peak sensitivity of a photographic emulsion. This filter consists of a blue and an ultraviolet blocking filter. The latter filter is used to prevent the B magnitude from being affected by the Balmer discontinuity (i.e. the sharp drop in the continuum spectrum due to bunching up of the hydrogen absorption lines in the star's atmosphere.)

The ultraviolet filter (U) transmits wavelengths from 3000Å to 4200Å and is centred on 3500Å but has two problems. It transmits some light in the near infrared which must be blocked by a second filter, or the red light must be measured and subtracted. The second problem is that the short wavelength cut-off is set by the earth's atmospheric conditions. Thus the UBV system is not totally defined by the filter's wavelength.

A wide band system is useful, for example, to observe how the slope of the continuum changes with temperature, or the way the Balmer discontinuity is influenced by temperature and gravity.

The UBV system was extended to bandpasses in the infrared. The UBVRIJKLMN system has a wavelength range from λ3650 Å to λ102000 Å, with the filters J through to N requiring special cooled detectors.

Intermediate-band systems have filter widths of a few hundred angstroms, and the most commonly used is the Stromgren system.

The Stromgren (ybvu) system is almost totally filter defined. The yellow (y) filter matches the visual (V) magnitude and is centred at 5500 Å. The blue (b) filter is centred on 4700 Å which is 300 Å to the red of the Johnson B filter, to reduce the effects of blanketing from the absorption lines of metals in stars later than A0 type. For early type stars, the b and y filters are free from blanketing, but in later type stars the two filters are affected almost equally.

The violet (v) filter is centred in a region of strong blanketing, but towards the red of the Balmer discontinuity, the ultraviolet (u) filter measures both the blanketing and the Balmer discontinuity.

In general, the Stromgren system provides a visual magnitude, a measure of the strength of metal lines, and a measure of the Balmer discontinuity. Furthermore, it's wavelength range is filter defined and independent of the detector, and it's bandpass is small enough so that the second-order, colour dependent coefficient of extinction k", can be ignored.

The filters used to study EZ CMa were filters suggested by Carmelle Robert of the Montreal University, Canada. They are the Johnson B and V filters, and the Stromgren b filter which is used to isolate the strong, HeII (λ4686Å) emission line characteristic of WN5 Wolf-Rayet stars.

Effective Wavelengths and Bandwidths of Photometric Systems
(in Microns)

	λ	Δλ		λ	Δλ		λ	Δλ
U	0.365	0.068	R	0.70	0.22	u	0.350	0.034
B	0.440	0.098	I	0.90	0.24	v	0.411	0.020
V	0.548	0.089	J	1.25	0.38	b	0.467	0.016
			K	2.20	0.48	y	0.547	0.024
			L	3.41	0.70			
			M	5.00	-			
			N	10.20	-			

Figure 3.3: D.S. Hall, R.M. Genet (1982) pp10-3

Telescope Set-up

The 16-inch Cassegrain telescope of the University of Wollongong, Department of Physics, was used with a silicon PIN diode photometer (model SSP-3). Observations were recorded automatically on an Apple II computer and also on a printer. An amplifier gain of 100 was required for all star and sky readings. The time for all observations was between 1am and dawn, with most nights attaining best photometric conditions approximately one hour before dawn.

Diagram of the Telescope and Photometer Setup

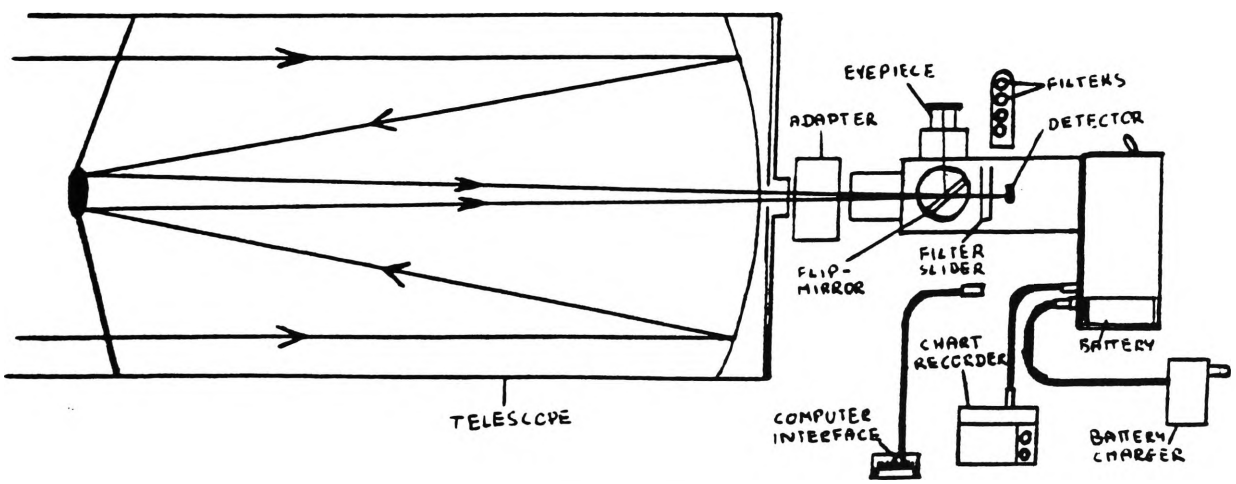

Figure 3.4

Observing Procedure

JULIAN DATE:

The number of days that have elapsed since 12 noon, 4713 BC January 1 is called the Julian date and is the current dating system used in astronomy. The Julian date at midnight from the years 1901 to 2099 is calculated in the following way:

The Gregorian calendar date is in year (Y), month (M), day (D).

For $M>2$ then $y = Y$ and $m = M-3$;

$M \leq 2$ then $y = Y-1$ and $m = M+9$. Then

$$\text{JULIAN DATE} = 1721103.5 + \text{INT}(365.25y) + \text{INT}(30.6m + 0.5) + D$$

where INT means to consider only the whole part inside the brackets.

The Julian date for day 1 of observations was calculated to be:

2 448 145 = 11 Sept 1990 (noon)

CHOICE OF COMPARISON STARS:

Two comparison stars for any variable are usually chosen- one to be the comparison star for the variable, the other to check the variability of the comparison. If the variations between the comparison and the check star are larger than the nightly error, either the comparison or the check star are variable. The variable is determined by either comparing the nightly standardisation of the comparison, or by deciding which star gives a light curve for the variable that has the smallest scatter.

Factors to consider when choosing a comparison star for the variable are that the comparison star is;

1- not varying

2-less than 1^{o} from the variable star to minimise the value ΔX which can become significant at large Z.

3-of similar colour to minimise the colour dependent extinction coefficient k". A colour index difference of 0.1mag is best, 0.5 mag is tolerable, and 1.0 mag should be avoided.

4-equal in magnitude so that both stars can be observed with the same coarse gain setting on the amplifier.

5-preferably not red in colour, as red stars are almost always variable and are likely to be flare stars.

The comparison stars for EZ CMa were recommended by Carmelle Roberts (Montreal Uni. 1988). They are;

STAR	RA (2000)	DEC(2000)	v	colour index
HD 50 711 (comp)	$6^{h}\,53^{m}\,22.1^{s}$	$-24^{o}\,41'\,3"$	7.5	-0.2
HD 50 853 (check)	$6^{h}\,53^{m}\,55.2^{s}$	$-24^{o}\,32'\,21"$	6.2	0.6
HD 50 896 (var)	$6^{h}\,54^{m}\,12.9^{s}$	$-23^{o}\,55'\,42"$	~6.86	-0.3

which clearly meet all the criteria.

The observing sequence used for EZ CMa and suggested by Carmelle is;

sky - check star - variable - comparison - variable - check star - sky.

Each star was observed through three filters in the order of; Stromgren b, Johnson B, Johnson V, for five lots of 10 second integrations, then averaged with a standard deviation error reading using the PHOTOM programme of Moore/Ihnat. The standard deviation error reading and percentage error were determined by:

$$SDEV = \sqrt{\frac{\sum_{N} (x_i - \bar{x})^2}{N-1}}$$

$$\% \text{ ERROR} = \frac{SDEV}{\bar{x}.\sqrt{N}} \times \frac{100}{1}$$

Observations with an error greater than 2% were discarded.

CHAPTER 4: DATA REDUCTION AND DISCUSSION

Data was obtained over 16 nights in groups of approximately 5 nights each, due to bad weather which disrupted continuous observation. Each group covered the proposed 3.76 day period of EZ CMa.

The photometric programme, PHOTV, of G. Moore, was used to reduce the data. This programme interpolates the value of the night sky at the beginning and end of the sequence, to the expected sky value at the time of flux measurements of the variable and comparison stars. The interpolated sky background is subtracted from both star readings, and the difference in the flux counts are converted to differential magnitudes by the equation:

$$\Delta m_{\lambda} = -2.5 \log (I_{var} / I_{c})$$

where I_{var} and I_{c} are the light flux counts through the filter λ, for the variable and comparison stars, respectively.

First order extinction corrections, which vary nightly depending on the moisture and dust content of the atmosphere, were made by firstly, plotting the magnitude of the comparison star for each filter, after the sky background has been subtracted, versus the changing airmass as the star rises. These plots are illustrated in plates 3 to 7. The slope is the first order extinction coefficient, k', and the corrected differential magnitude is:

$$\Delta m_{o} = \Delta m - k'(X_{var} - X_{c})$$

for each filter, where X_{var} and X_c are the airmass of the variable and comparison stars, respectively.

The coefficients of extinction were calculated separately for each night and applied to the differential magnitudes.

To estimate likely periods, a phase dispersion minimisation programme was used. The programme is outlined in a paper by Stellingwerf (1978), and is based on Lafler and Kinman's (1965) computerised version of the classical PDM technique, in which the period that produces the least observational scatter about a mean (derived) light curve, is chosen as the best period. This method works well on irregularly spaced data and can be used in non-sinusoidal time variations.

A general outline of the PDM technique follows.

The variance of a number (N) of observations such as stellar magnitude (**x**) and observation times (**t**), is given by:

$$o^2 = \frac{\sum^{N} (x_i - \bar{x})^2}{N-1} \qquad (A)$$

where $\bar{x}$ is the mean of the magnitudes. This also applies to any subset of x_i giving sample variances s^2.

If the distinct samples are chosen having their individual variances s_j^2 (j=1,M) and containing n_j data points, the overall variance for all samples is given by:

$$s^2 = \frac{\Sigma (n_j - 1)\, s_j^2}{\Sigma n_j - M} \qquad (B)$$

We require minimising the data with respect to the mean light curve. If Π is a trial period, phase vector **ø** becomes $ø_i = t_i / \Pi - [t_i / \Pi]$, where the brackets indicate the integer part.

We now choose M samples from **x**, using the condition that all members of sample j have similar $ø_i$. Usually, the full phase interval is divided into "bins", but samples may be chosen in any way that satisfies the condition. All points need not be chosen or one point can belong to many samples. The variance of these samples, gives a measure of the scatter around the mean light curve defined by the means of the x_i in each sample, and is considered as a function of ø.

We define significance $Ç = s^2 / o^2$

where *s* is given by equation (B) and *o* is given by equation (A). If Π is not a true period, then $s^2 \sim o^2$, and Ç ~ 1. If Π is a correct period, Ç will reach a local minimum compared with neighbouring periods, and approximate to 0.

The PDM programme is a type of least-squares fitting programme that fits to a mean curve defined by the means of each bin, rather than to a given curve such as a Fourier component. It finds all components of a period including subharmonics or aliases which can be identified by their narrow line widths or a doubly periodic mean curve.

The phase dispersion minimisation programme, PDMRS, was used to estimate likely

periods and their significance. The periods were then plotted as amplitude versus phase, using the programme GPLOT, an adaption of PERPLOT, of G.Moore which is used for long period variables, and the best period investigated. Note that each period is plotted twice for visual effect.

Plates 8 to 10 show the light curve of EZ CMa observed through the Johnson V, B and Stromgren b filters, respectively, with the first order coefficients applied. Each point is the average of five lots of 10 second integrations, with a percentage error of less than 1% (mag. 0.01) - the area of the point on the graph.

All observations of the comparison star, HD 50 711, a known non-variable star (Lamontagne, Moffat, Lamarre 1985), are shown in plates 11 to 13, when it is compared with the check star HD 50 853, for a typical night. The scatter is less than mag. 0.03 for each filter.

Plates 14, 15 and 16 give the results of the period finding programme. They list the most probable periods for the Johnson V, B and Stromgren b filters. A significance close to 0 indicates a correct period, and a significance of 1, an incorrect period.

Plates 17 to 62 show the observations plotted as a function of phase for all periods listed in plates 14, 15 and 16.

Ninety possible periods were found, and each were analysed, with the aid of the significance for each period, and tested for consistency in other colours. Best periods were estimated by inspection of the plots in plates 17 to 62 coupled with the most significant period listed in plates 14 to 16.

Consider, firstly, data taken through the Johnson V filter. It was necessary to eliminate all data points taken on nights 1, 6 and 15 due to bad photometric conditions which resulted in standard deviation errors greater than 1% (see plate 2 for details of weather conditions).

The most significant period found was the 3.74±0.02 day period shown in plate 18, with an amplitude of mag 0.12±0.03, and a half-period alias of 1.87 days - plate 23. This is equivalent to the previously determined period of 3.76 days, within the uncertainty of my determination. There is also a significant period of 2.13±0.01 days shown in plate 21, with an amplitude of mag. 0.08±0.03, which has a possible half period alias of 1.07 days shown in plate 26. The light curve, on inspection, suggests that one-day aliasing is a possible but an unlikely explanation of this unusual period. Also present is a 0.79±0.01 day period shown in plate 27, with an amplitude of mag. 0.10±0.03 which has a double period alias of 1.59 days shown in plate 24. This period may be the 0.75 day period previously discovered by Drissen, Lamontage and Moffat in 1988. Of lowest significance is a 1.36±0.02 day period of plate 24 with an amplitude of mag.0.10±0.03, which has a double period alias of 2.76 days shown in plate 20, and a possible half-period alias of 0.68 days shown in plate 28.

For data taken through the Johnson B filter, days 6, 9 and 13 were eliminated.

The 3.74±0.02 day period illustrated in plate 35, with an amplitude of mag.0.10±0.03 is present with multiple period aliases of 15.00 and 1.87 days shown in plates 30 and 42, respectively. The shape of the light curve is similar to the curve obtained in 1986 and 1988 by Gosset, Vreux and Drissen, Lamontage, Moffat, with one high maximum

and a possible secondary low maximum. Also present are a 0.72±0.03 day period given in plate 44, with an amplitude of mag.0.06±0.03, and a 1.34±0.02 day period shown in plate 43, with an amplitude of mag.0.06±0.03 which has multiple-period aliases of 13.95, 5.50 and 2.76 illustrated in plates 31, 33 and 37, respectively. There is also an unusual 1.60±0.01 day period shown in plate 42, with an amplitude of mag.0.1±0.02 which has a double period alias of the 0.79 day periods found in the Johnson V and Stromgren b filters. Finally, there is a 2.14±0.01 day period shown in plate 40, with an amplitude of mag.0.10±0.03 of low significance and probably not real.

For data taken through the Stromgren b filter, days 6, 9 and 13 were eliminated.

The 3.74±0.02 day period given in plate 52, is again present in this filter, with an amplitude of mag. 0.10±0.02, and multiple-period aliases of 15.00, 11.28, 7.32 and 1.89 days shown in plates 46, 47, 49 and 58, respectively. The shape of the light curve is similar to the Johnson B filter, with one high maximum and a possible secondary low maximum. A significant 3.58±0.03 day period of plate 54, is evident with multiple period aliases of 14.15, 10.68 and 1.77 days given in plates 46, 47 and 58, respectively. This may be a consequence of averaging the high maximum and low maximum of the 3.74±0.02 day period, and since it is not found in any other filter, and is considered not real. There is a significant 1.39±0.03 day period shown in plate 60, with an amplitude of mag.0.08±0.03 which has a double period alias of 2.75 days given in plate 56. A 0.78±0.01 day period shown in plate 62, with an amplitude of 0.08±0.03 is also present with good multiple-period aliases of 4.68, 2.32 and 1.57 days illustrated in plates 51, 57 and 59, respectively.

CONCLUSION

Previous observations of EZ CMa (HD 50896) have determined its period to be 3.7658±0.0007 days, with a light curve that varies in amplitude and shape over a time interval of months.

From my photometric data, the best period found is 3.74±0.02 days for the three filters; Johnson V, Johnson B and Stromgren b, with the light curve displaying a high maximum and a secondary low maximum in the Johnson B and Stromgren b filters. Possible secondary periods of relatively lower significance, are present and include a 1.36±0.02 day period and a 0.78±0.01 day period.

The presence of these secondary periods supports the theory that non-radial pulsations cause the light variability of EZ CMa, as proposed by Gosset and Vreux (1986). If EZ CMa is considered a binary system, they indicate that a more complicated phenomenon occurs, in which the accretion disc surrounding the compact companion maybe changing orientation i.e. precessing, or that a third body is present in the system.

Further confirmation and analysis of these shorter periods is required to crack the mystery of the variation in the light curve of EZ CMa.

FOOTNOTES

(a) Electron degeneracy pressure arises from the Pauli exclusion principle, which says that no two electrons can be in exactly the same quantum state. The electron gas has all of its electrons in the lowest energy states allowed by the exclusion principle. The energy of the electrons in the lowest energy state will be higher than the energy of electrons in an ordinary gas. These high energy electrons have high momenta and exert a higher pressure than the pressure exerted in an ideal gas. This pressure is called electron degeneracy pressure.

(b) Neutrons have spin properties similar to those of electrons, they therefore obey the Pauli exclusion principle and are capable of exerting a degeneracy pressure if the pressure is high enough.

REFERENCES

Balona L.A, Egan J., Marang F.: 1988. Mon. Not. R. astr. Soc 240, 106

Cerepashchuk A.M.: 1981. Mon. Not. R. Astr. Soc. 194,755

Conti P.S.: 1983 Astrophys. J. 274, 302

De Loore C., De Greve J.P.: 1975. Ap. Sp. Sci. 35,241

Firmani C., Koenigsberger G., Bisiacchi G.F., Moffat A.F.J.: 1980. Astrophys. J. 239,607

Gosset E., Vreux J.M.: 1987. Astron. Astrophys. 178, 153

Hall D.S., Genet R.M.: 1982. *Photoelectric Photometry of Variable Stars.* I.A.P.P.P.

Hatchett, McCray S.P.: 1977. Astrophys.J. 211, 552

Henden A., Kaitchuck R.H.: 1982.*Astronomical Photometry.* Dept. of Astronomy Indiana University: Van Nostrand Reinhold Company Inc.

Harwit M.: 1973. *Astrophysical Concepts.* John Wiley and Sons.

Howarth I.D., Phillips A.P.: 1986. Mon. Not. R. astr. Soc. 222, 809

Jaschek C., Jaschek M.: 1987. *The Classification of Stars.* Cambridge University Press.

Johnson H.M., Hogg D.E.: 1965. Astrophys.J. 143, 1033

Kuhi L.V., Bappu M., Sahade J.: 1973. *IAU Symposium 49* , 237

Kutner M.L.: 1987. *Astronomy: A Physical Perspective.* Rensselaer Polytechnic Inst. Harper & Row Publishers Inc.

Lafler J., Kinman T.K.: 1965. Astrophys. J. Suppl. 11, 216

Lamontagne R., Moffat A.F.J.: 1982. *IAU Symposium 99, Wolf-Rayet Stars: Observations, Physics and Evolution.* ed. C.W.H. de Loore and A.J Willis

Lamontagne R., Moffat A.F.J., Lamarre A.: 1985 .Astron.J. 91(4), 925

Lamontagne R., Moffat A.F.J.: 1987. Astron. J. 94(4), 1008

McLean I.S.: 1980. Astrophys. J. 236, L149

Mikulasek: 1969. Bull. Astron. Inst. Czech 20, 215

Moffat A.F.J., Drissen L., Lamontagne R., Carmelle R.: 1988. Astrophys. J. in press

Moffat A.F.J., Seggewiss W.: 1979. A.A. 77, 128

Moffat A.F.J., Shara M.M.: 1986. Astron. J. 92(4),952
Nichols-Bohlin. J, Fesin R.S 1986. Astrophys. J. 92,642

Norton's 2000.0 *Star Atlas and Reference Handbook.* ed. Ridpath.Longman Scientific and Technical.

Payne C.H.: 1933. Z. f. Astrophys. 7, 1

Pollock A.M.T.: 1987 Astrophys. J. 320, 283

Rublev S.V.: 1975. I*AU Sumposium No. 67.Variable Stars and Stellar Evolution.* ed. Sherwood and Plaut.

Schmidt G.D.: 1974. Astron. Soc. Pacific 86, 767

Schulte-Ladbeck R.E.: 1988. Astron.J. 97(5), 1471

Smith L.F.: 1968. Mon. Not. R. Astron. Soc. 138, 109

Smith L.F., Maeder.: 1986 A.A 176

Stellingwerf R.F.: 1978. Astrophys. J. 224, 953

Van Genderin A.M., Van der Hucht K.A., Steemers W.J.G.:1987. Astron. Astrophys. 185, 131

Vreux J.M., Andrillat.Y.: 1974. A.A.Suppl. 54, 437

White R.L., Long K.S.: 1986. Astrophys. J. 310, 832

Willis A.J., Howarth I.D., Smith L.J., Garmany C.D., Conti P.S.: 1989. Astron. Astrophys. Suppl.Ser. 77, 269

ACKNOWLEDGMENTS

I would like to thank Glen Moore, for his supervision; Peter Inhat for his assistance with the operation of the telescope; and Vincent MacIntyre, Mark Suters, Philip Randal for their instruction in the use of the PC. Thanks also to my parents for their support and prayers; my sister Maria for the use of her car while observing; and the De Battista family for their kindness. I would also like to acknowledge Andre Varga who sees past the stars.

PLATE INDEX

PLATES 17-29: Plots of singificant periods (Johnson V filter).

PLATES 30-45: Plots of singificant periods (Johnson B filter).

PLATES 46-62: Plots of singificant periods (Stromgren b filter).

PLATE 63: Data points (Johnson V filter).

PLATE 64: Data points (Johnson B filter).

PLATE 65: Data points (Stromgren b filter).

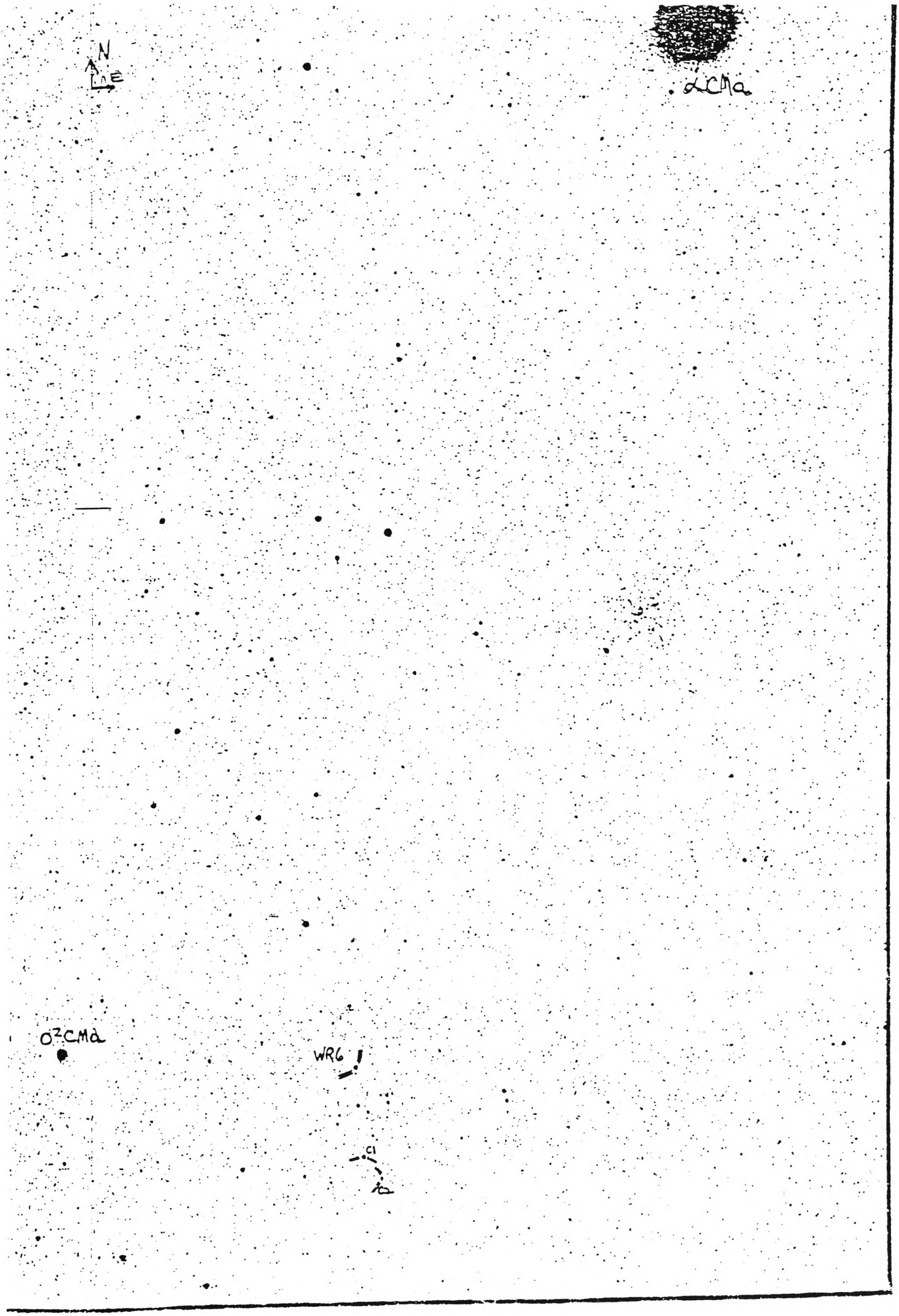
N
E
2 CMa
O² CMa
WR6
C1

DAY OF OBSERVATION	WEATHER CONDITIONS
1	Good conditions, 2% cloud cover, moon in last quarter
6	Scattered cloud (approx.10%), no moon
7	Excellent conditions, no moon
8	Good conditions, moderately humid, no moon
9	Reasonable conditions, humid with air pollution, no moon
13	Good conditions, moderately humid, no moon
14	Excellent conditions, no moon
15	Bad conditions, high wind, warm moist air, no moon
16	Excellent conditions, no moon
17	Good conditions, slightly humid, cool (~11^{o}C),no moon
20	Good conditions, cool (~12^{o}C), first 1/4 moon set after 1hr. observing
21	Good conditions, light southerly wind carrying some pollution from BHP, cool (~11^{o}C), moon set before readings taken.
22	Excellent conditions, cold night (~10^{o}C), moon set after 1 hr. observing
23	Good conditions, 5% cloud cover, bright sky from moon,cold (~10^{o}C)
24	Reasonable conditions, 10% cloud cover, warm (~15^{o}C), humid

Determination of the First Order Extinction Coefficient

Day	John. V Filter	John. B Filter	Strom. b Filter
1	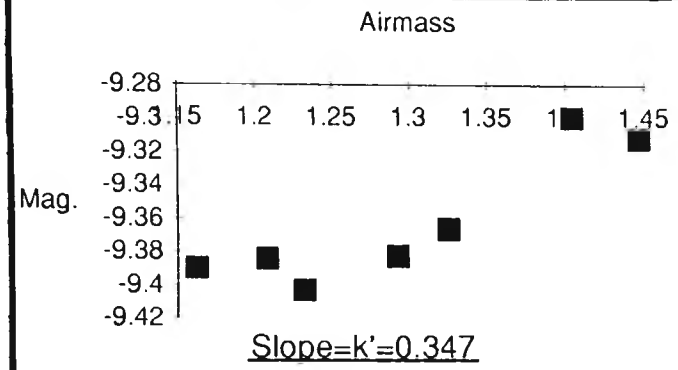 Slope=k'=0.347	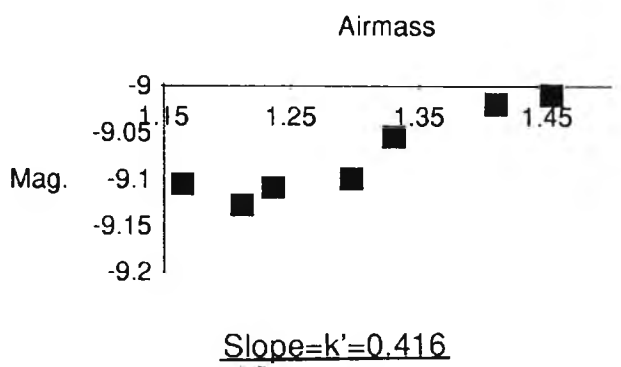 Slope=k'=0.416	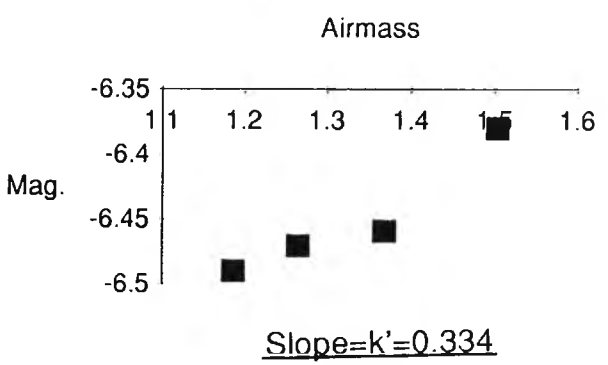 Slope=k'=0.334
6	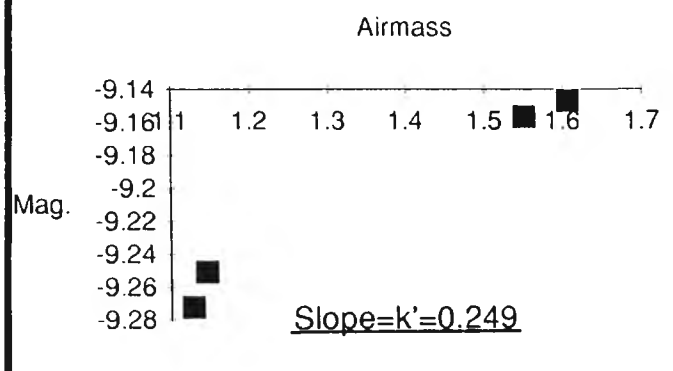 Slope=k'=0.249	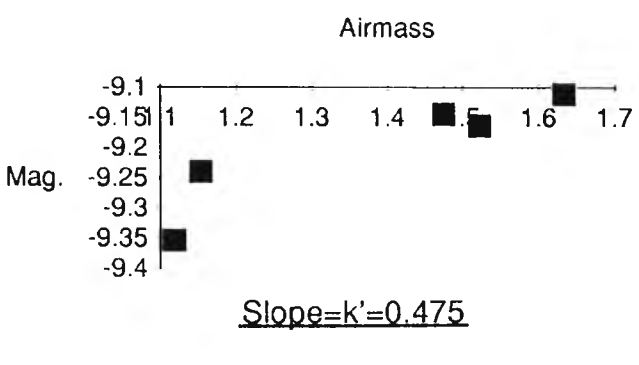 Slope=k'=0.475	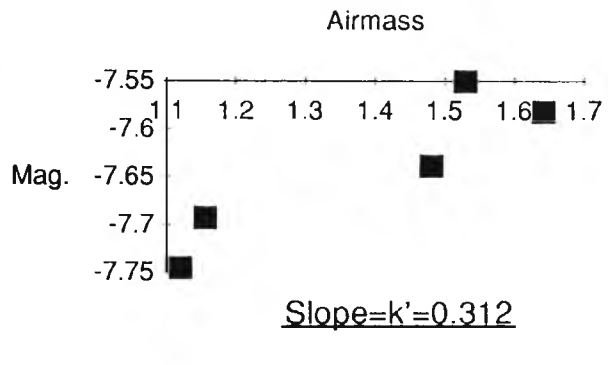 Slope=k'=0.312
7	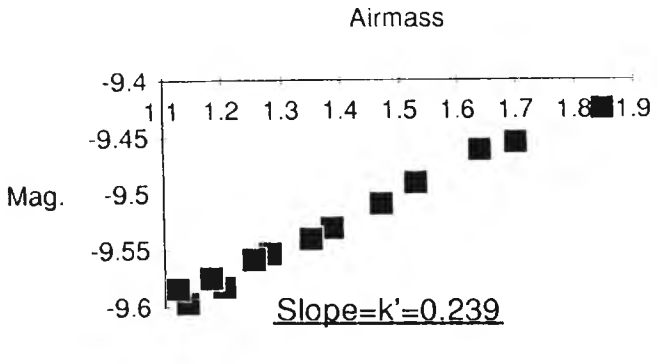 Slope=k'=0.239	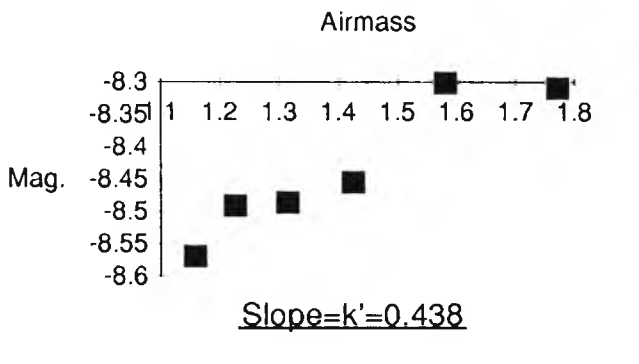 Slope=k'=0.438	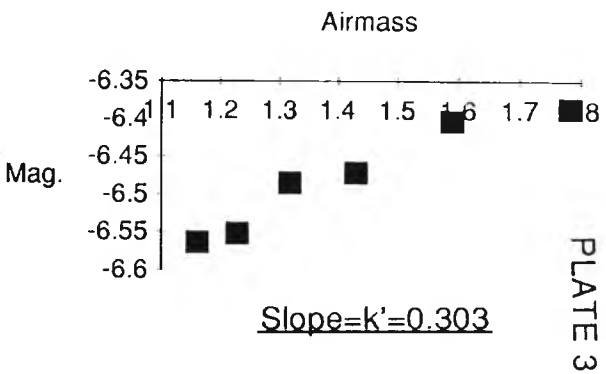 Slope=k'=0.303

PLATE 3

Determination of the First Order Extinction Coefficient (cont.)

Day	John. V Filter	John. B Filter	Strom. b Filter
8	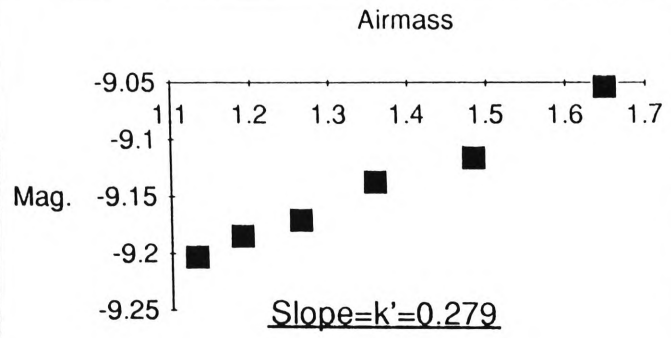 Slope=k'=0.279	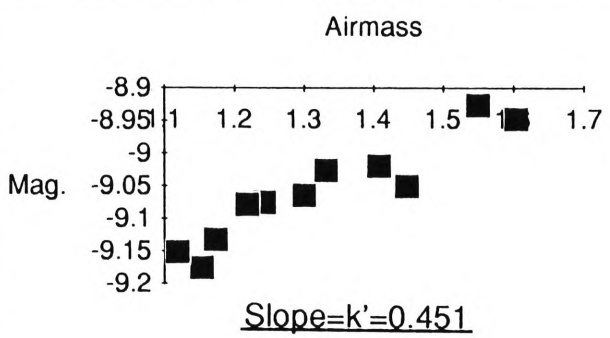 Slope=k'=0.451	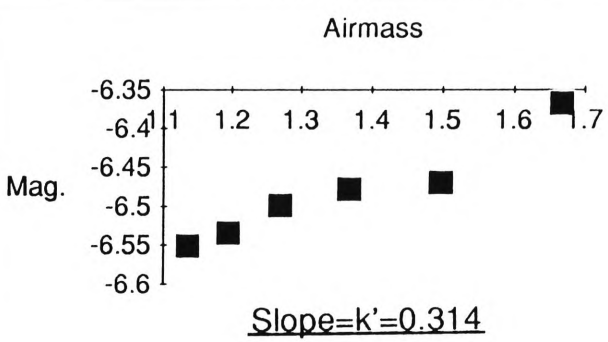 Slope=k'=0.314
9	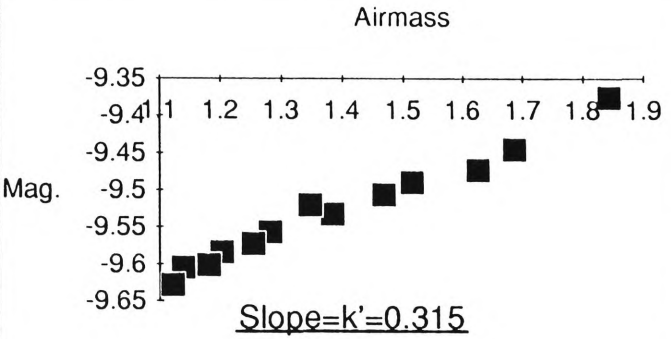 Slope=k'=0.315	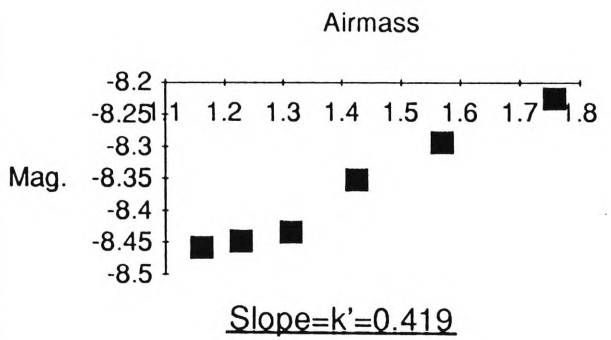 Slope=k'=0.419	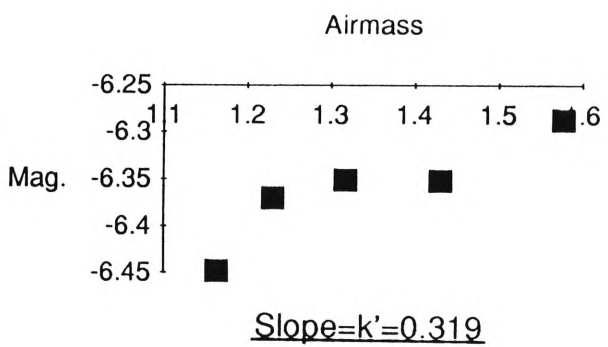 Slope=k'=0.319
13	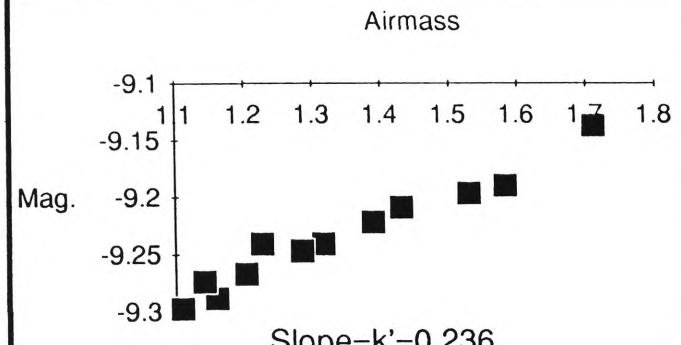 Slope=k'=0.236	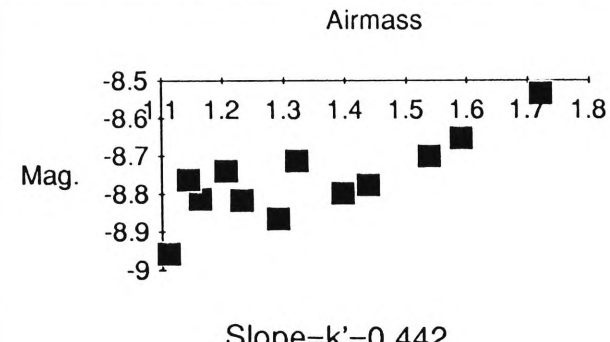 Slope=k'=0.442	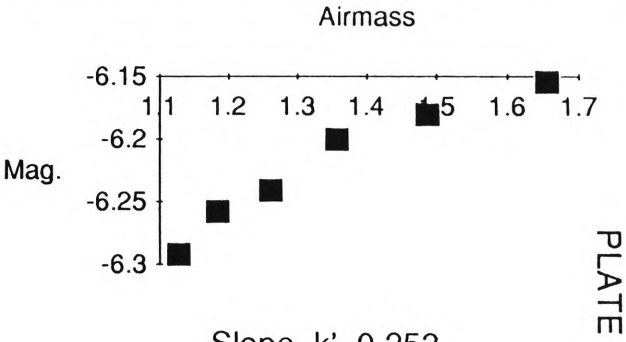 Slope=k'=0.253

PLATE 4

Determination of the First Order Extinction Coefficient (cont.)

Day	John. V Filter	John. B Filter	Strom. b Filter
14	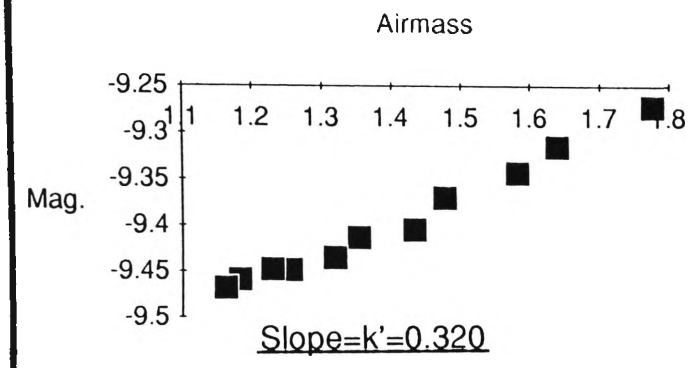 Slope=k'=0.320	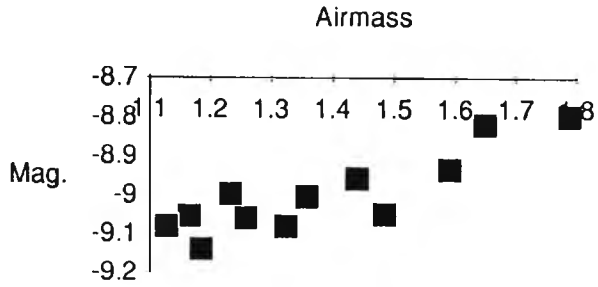 Slope=k'=0.441	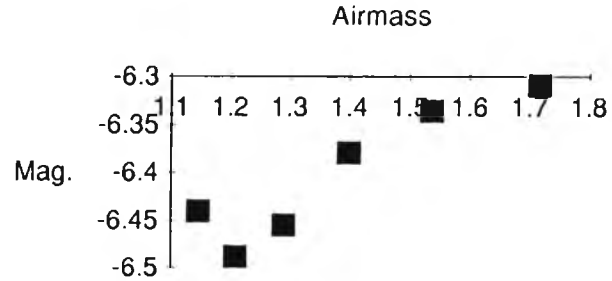 Slope=k'=0.307
16	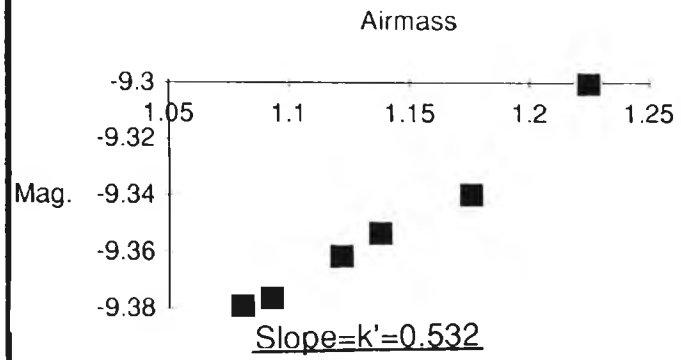 Slope=k'=0.532	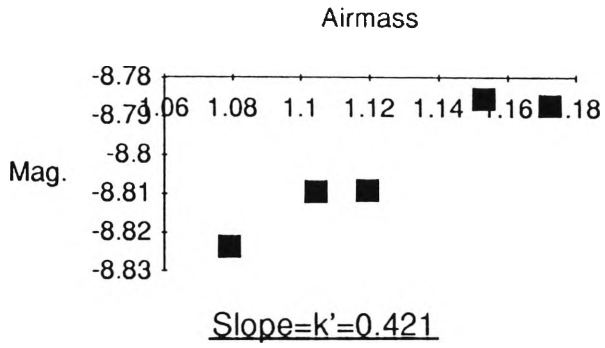 Slope=k'=0.421	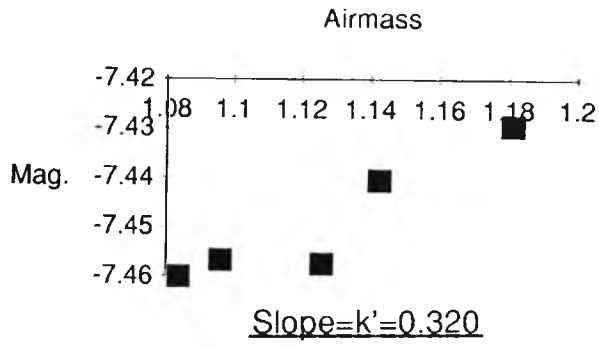 Slope=k'=0.320
17	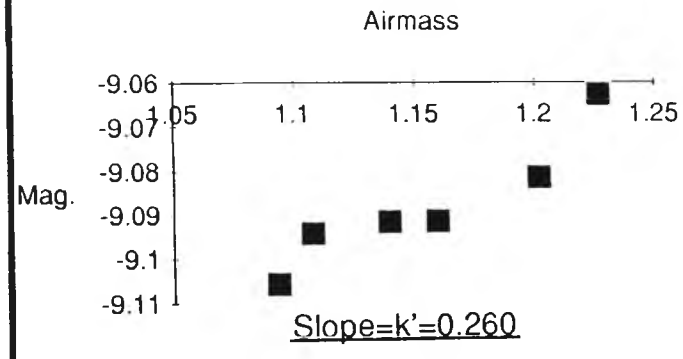 Slope=k'=0.260	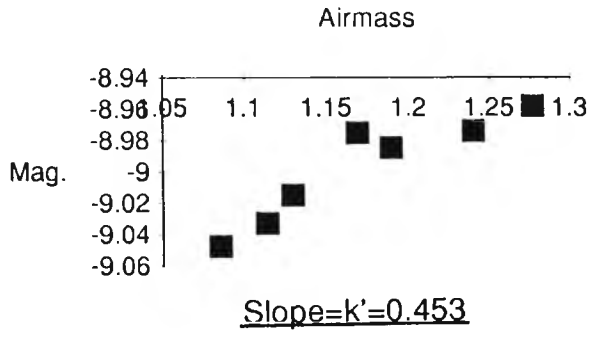 Slope=k'=0.453	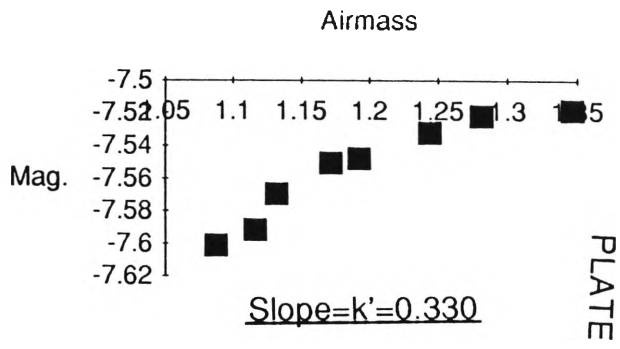 Slope=k'=0.330

PLATE 5

Determination of the First Order Extinction Coefficient (cont.)

Day	John. V Filter	John. B Filter	Strom. b Filter
20	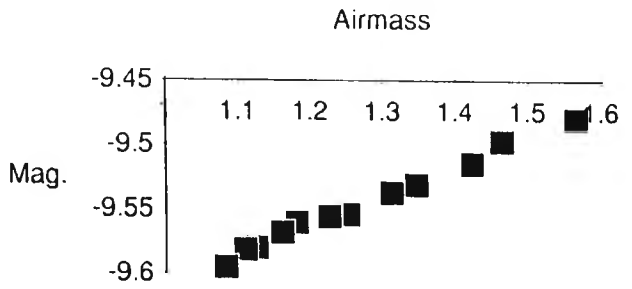 Slope=k'=0.228	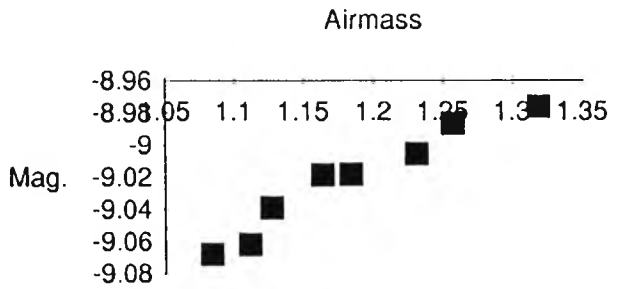 Slope=k'=0.402	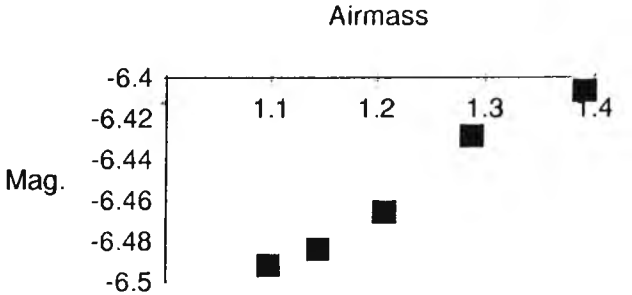 Slope=k'=0.310
21	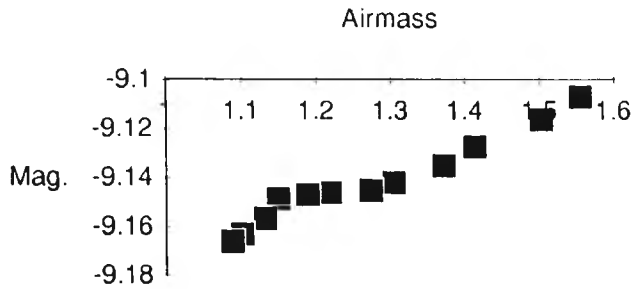 Slope=k'=0.271	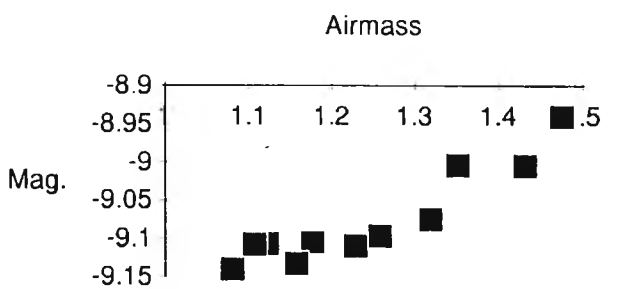 Slope=k'=0.438	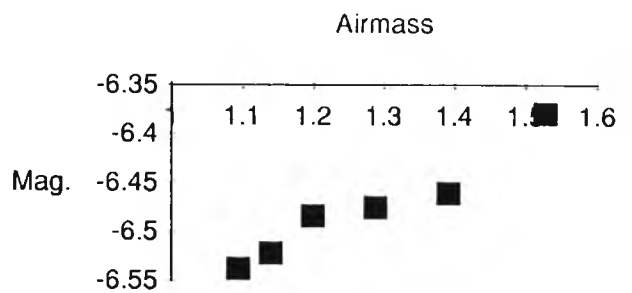 Slope=k'=0.328
22	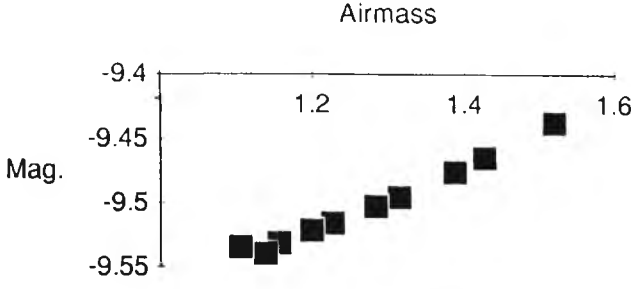 Slope=k'=0.245	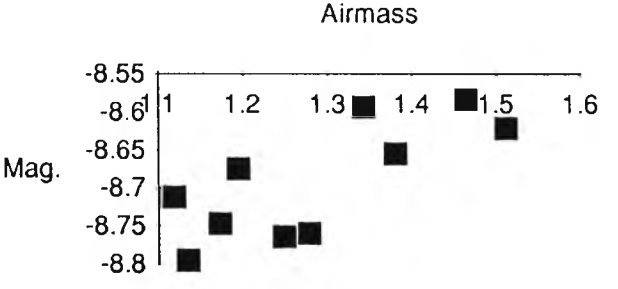 Slope=k'=0.423	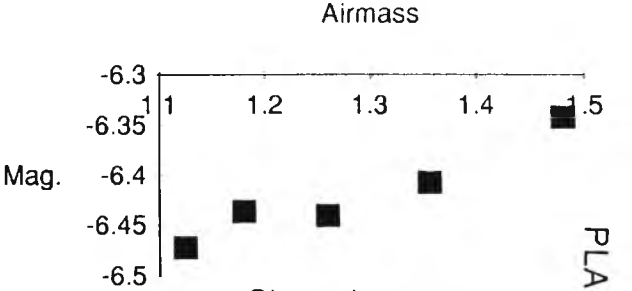 Slope=k'=0.332

PLATE 6

Determination of the First Order Extinction Coefficient (cont.)

Day	John. V Filter	John. B Filter	Strom. b Filter
23	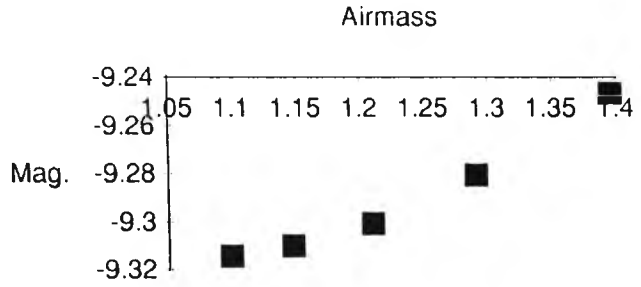 Slope=k'=0.231	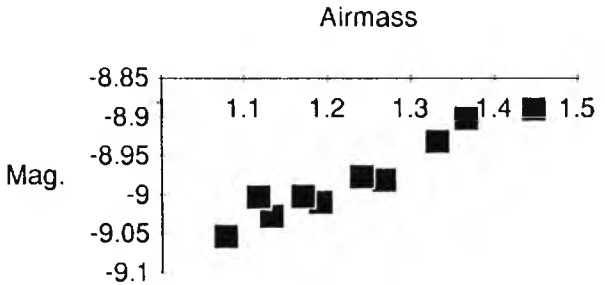 Slope=k'=0.436	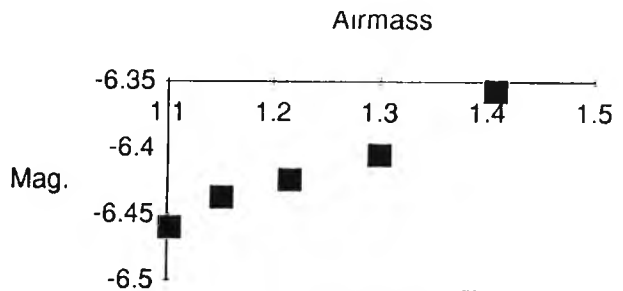 Slope=k'=0.317
24	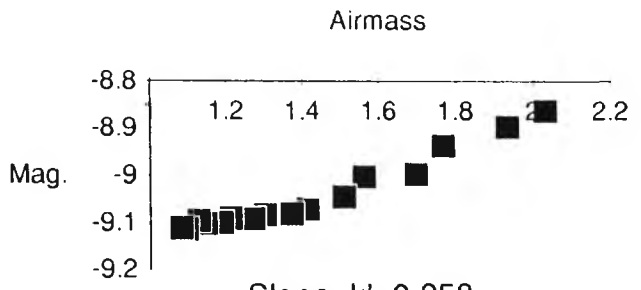 Slope=k'=0.258	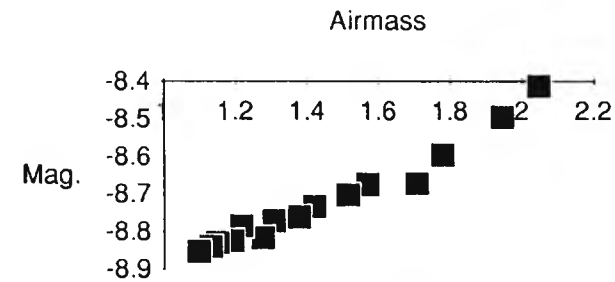 Slope=k'=0.420	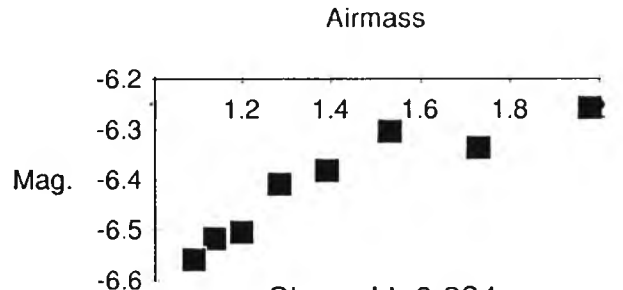 Slope=k'=0.324

PLATE 7

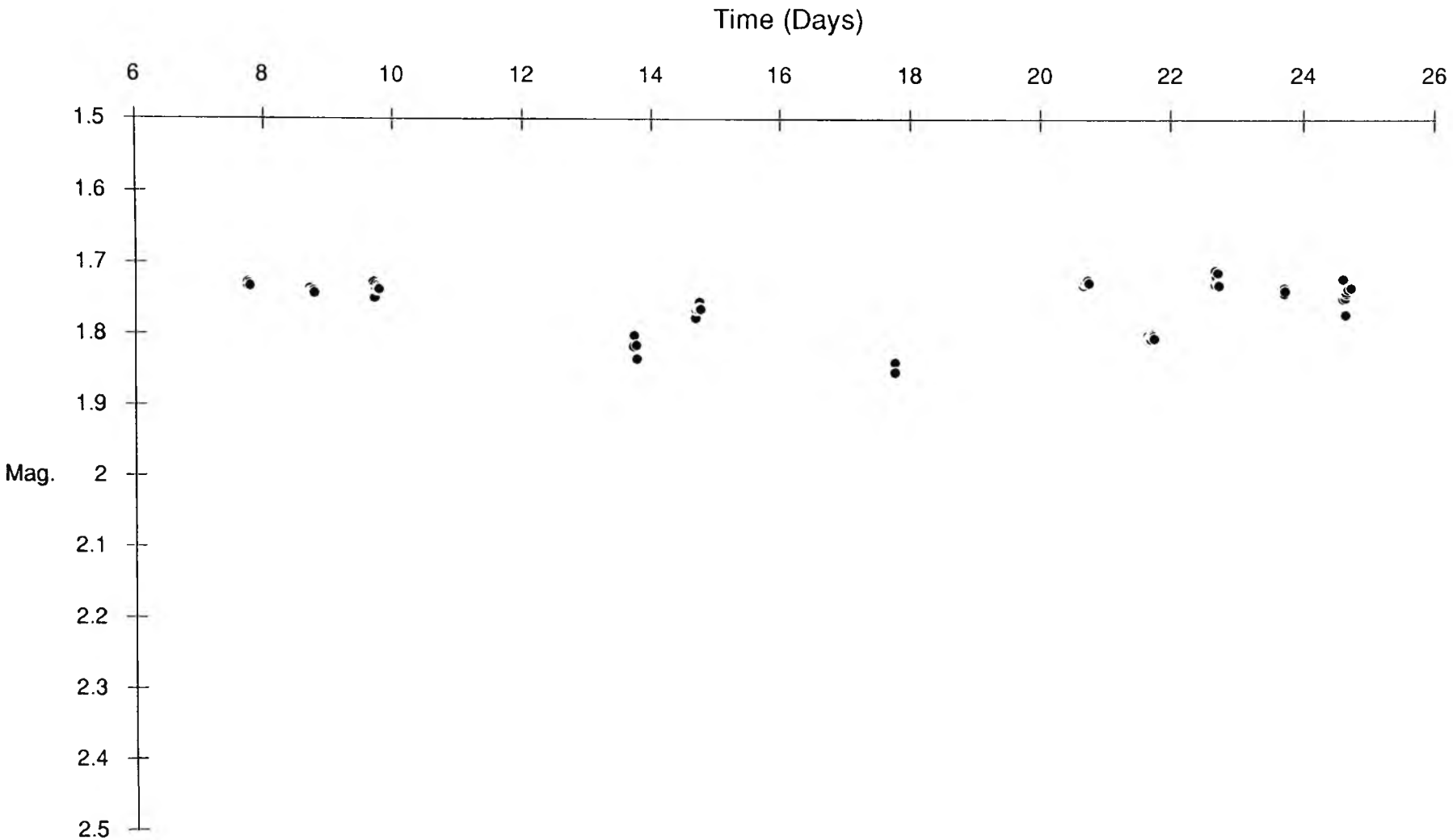

Light Curve of EZCMa (John. V Filter)

PLATE 8

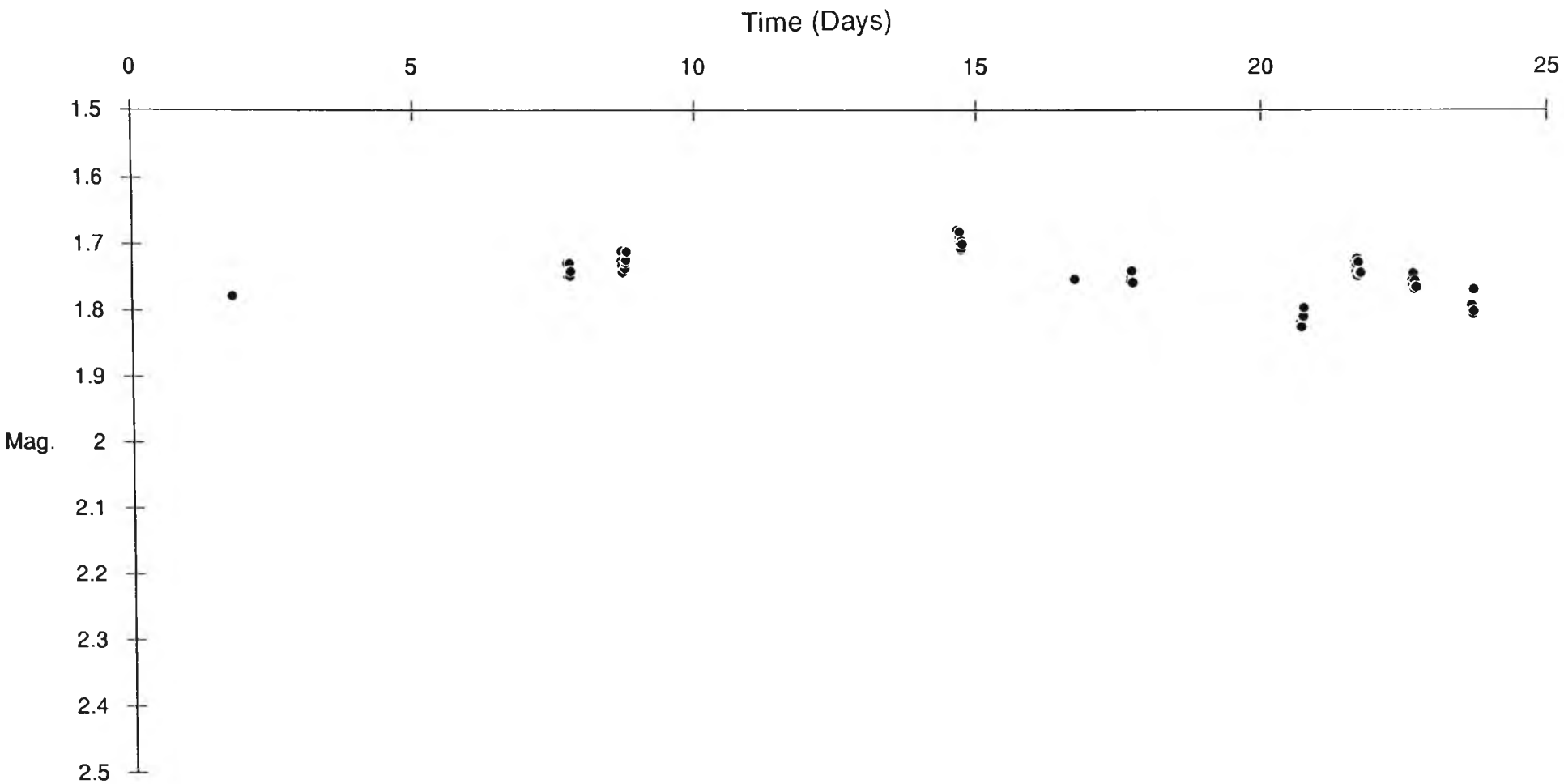

Light Curve of EZCMa (John. B Filter)

PLATE 9

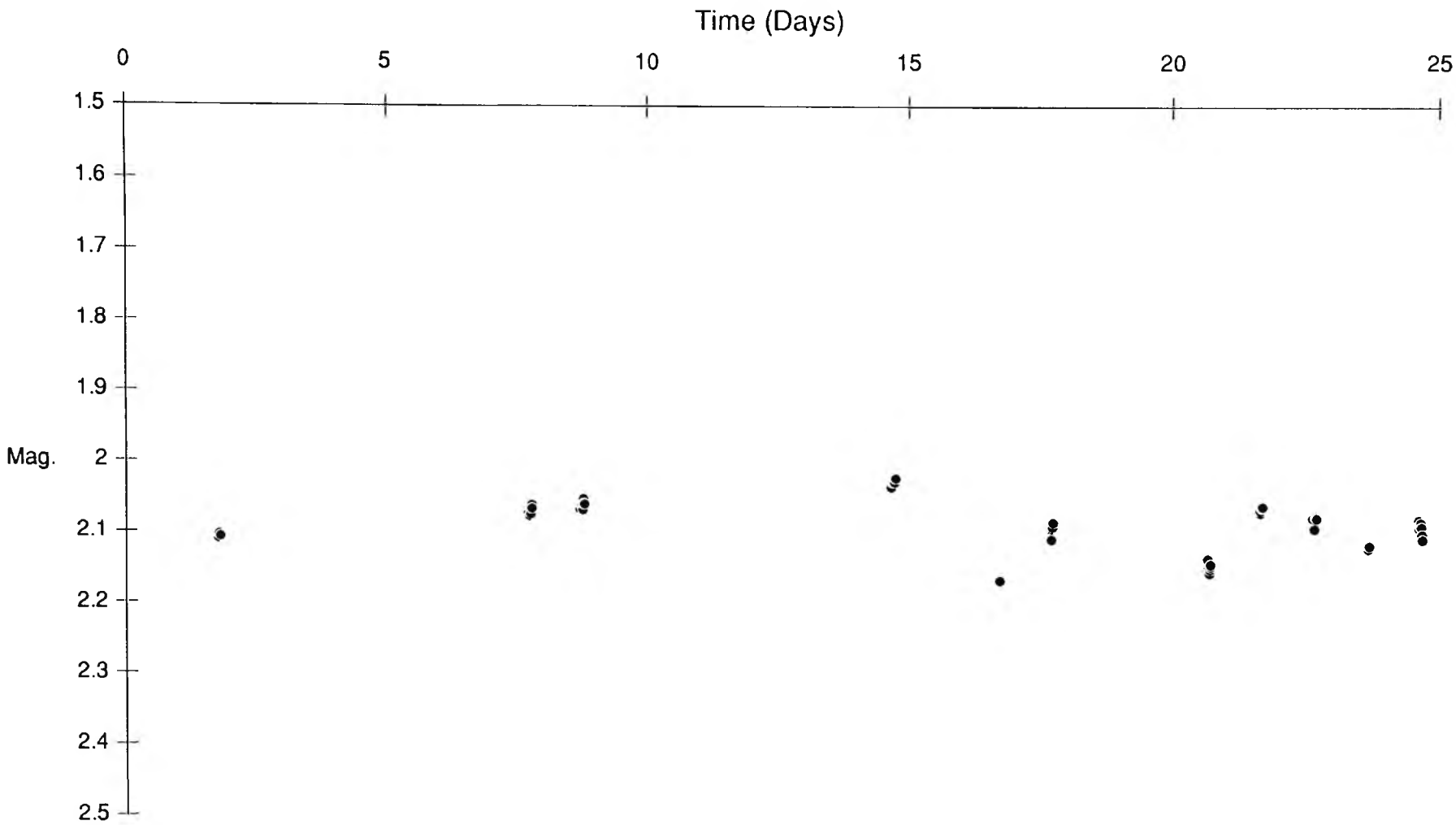

Light Curve of EZCMa (Strom. b Filter)

PLATE 10

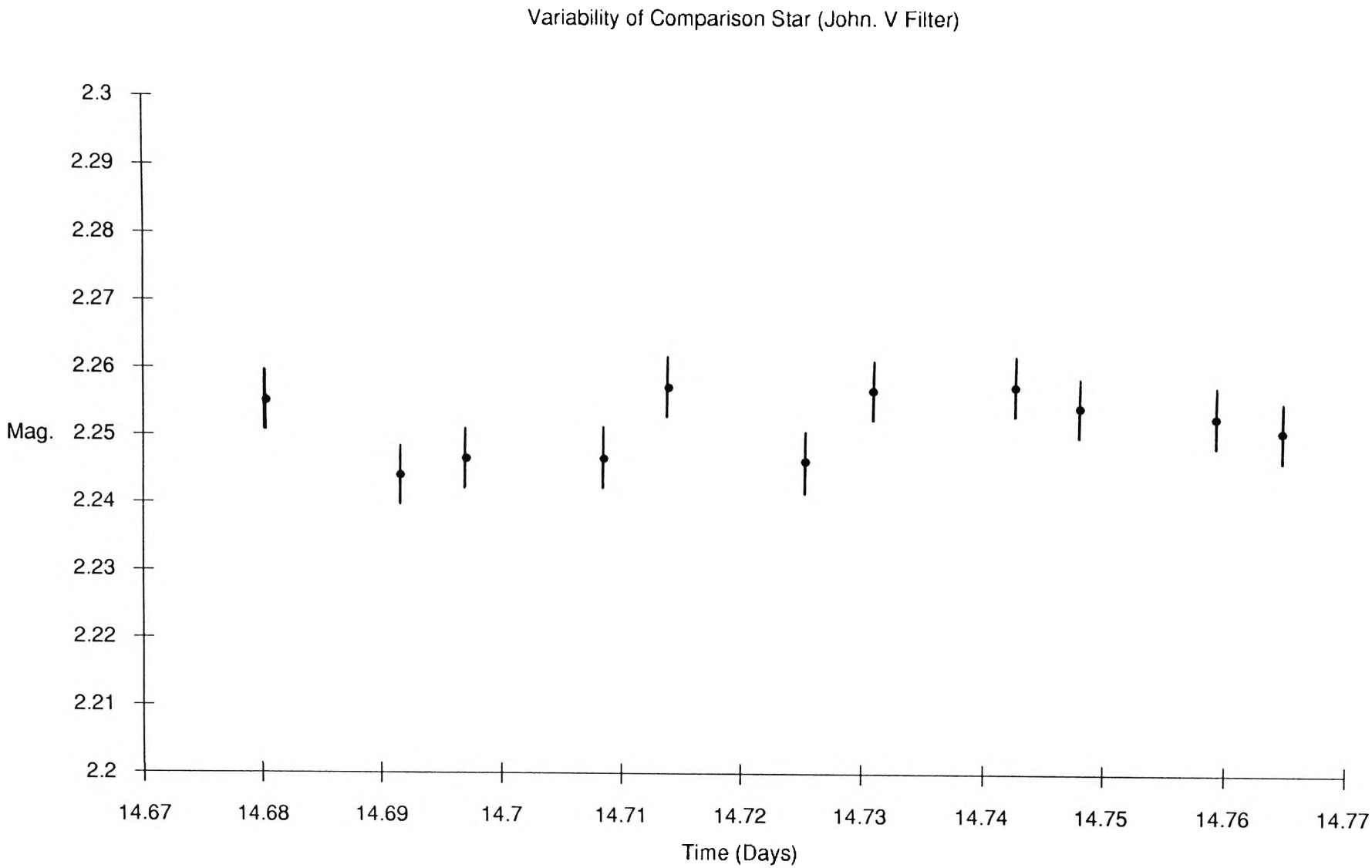
Variability of Comparison Star (John. V Filter)
Mag.
2.3
2.29
2.28
2.27
2.26
2.25
2.24
2.23
2.22
2.21
2.2
14.67
14.68
14.69
14.7
14.71
14.72
14.73
14.74
14.75
14.76
14.77
Time (Days)

PLATE 11

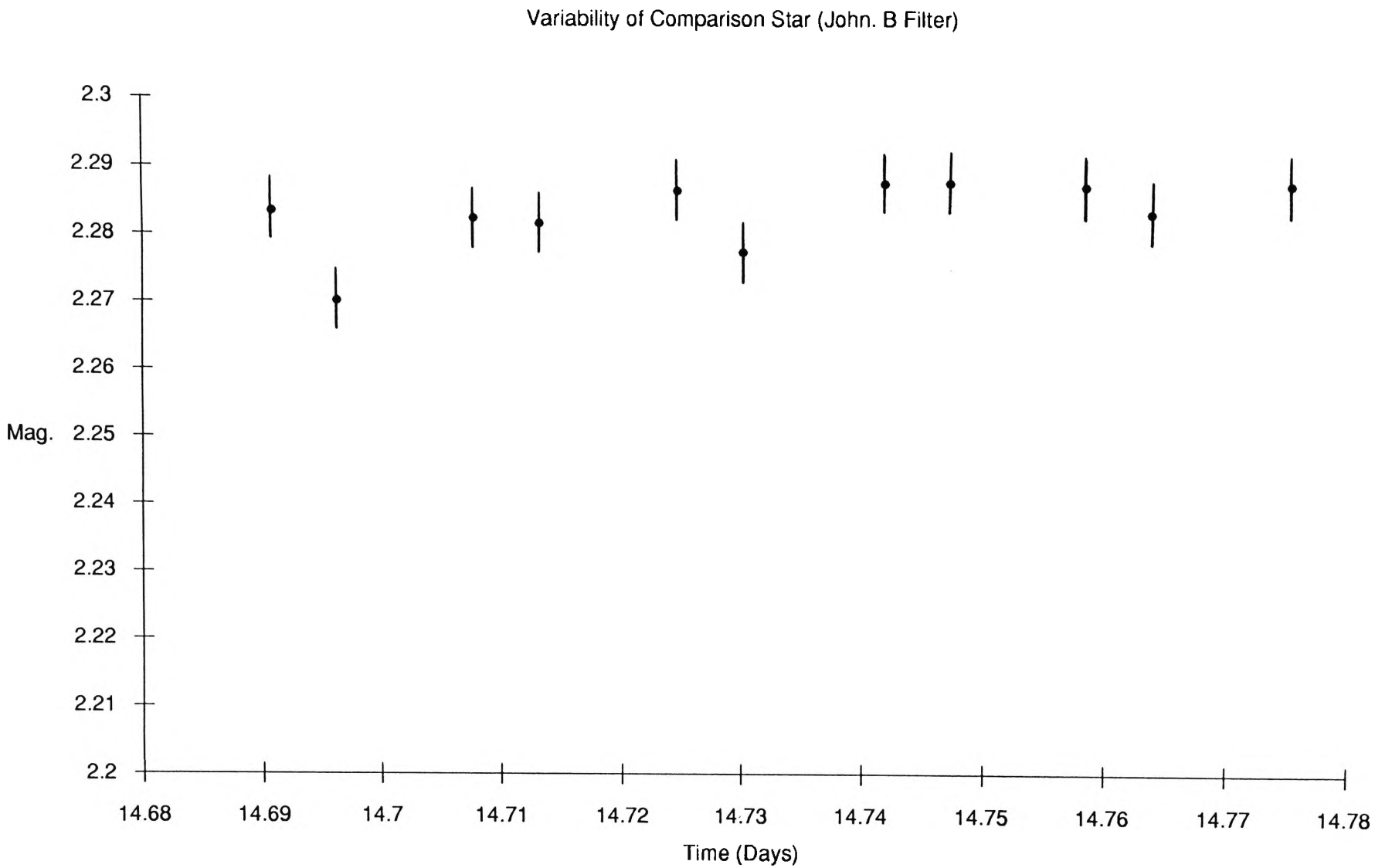
Variability of Comparison Star (John. B Filter)
Mag.
2.3
2.29
2.28
2.27
2.26
2.25
2.24
2.23
2.22
2.21
2.2
14.68
14.69
14.7
14.71
14.72
14.73
14.74
14.75
14.76
14.77
14.78
Time (Days)

PLATE 12

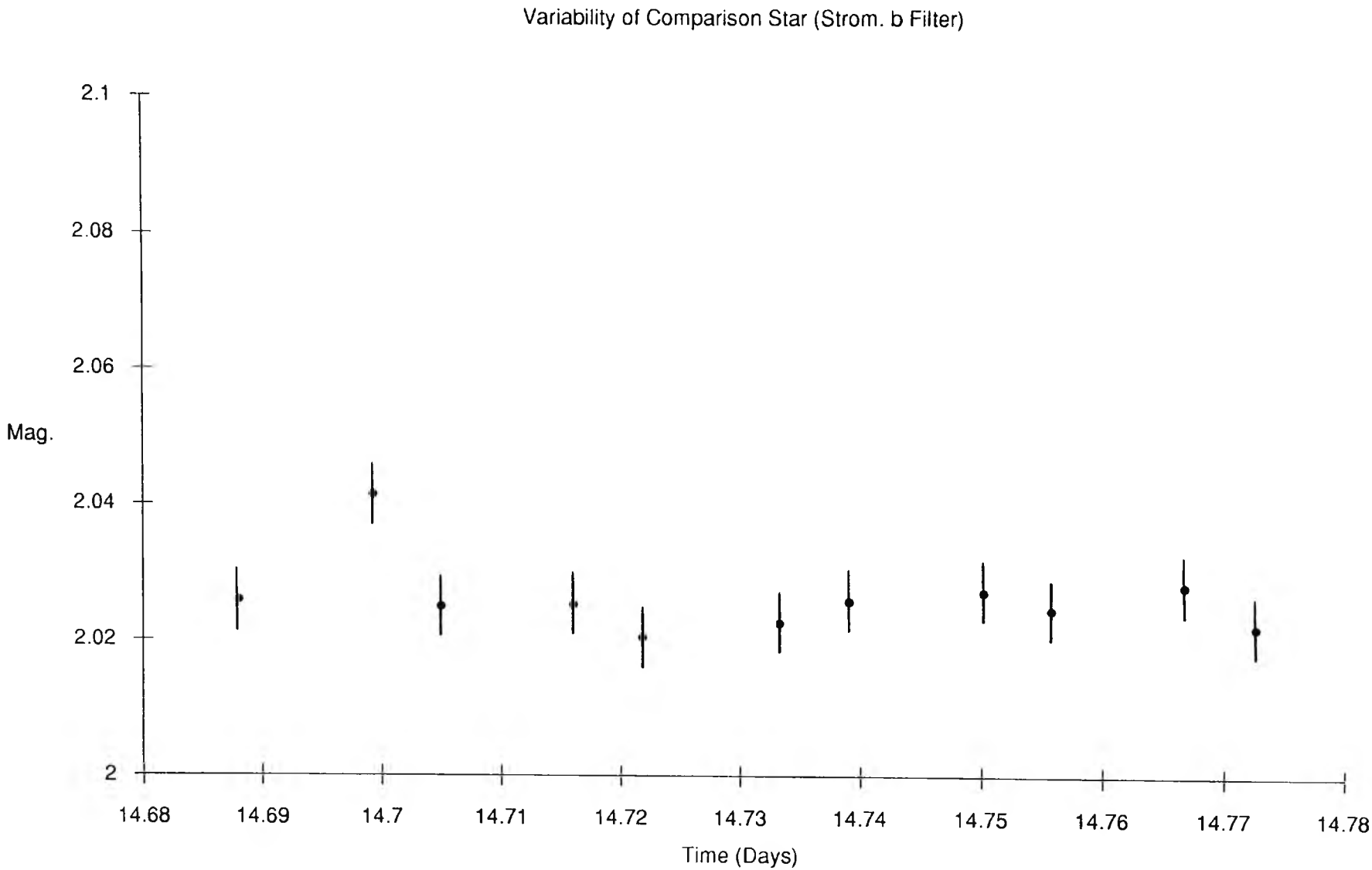
Variability of Comparison Star (Strom. b Filter)
2.1
2.08
2.06
2.04
2.02
2
Mag.
14.68
14.69
14.7
14.71
14.72
14.73
14.74
14.75
14.76
14.77
14.78
Time (Days)

PLATE 13

Significance of Periods (Johnson V filter)

Note: 0 = Most probable period

1 = Least probable period

PERIOD	SIGNIFICANCE
14.78	0.43 e-5
3.82	0.40 e-8
3.76	0.25 e-9
3.74	0.53 e-11
3.67	0.10 e-7
2.81	0.30 e-1
2.76	0.51 e-1
2.14	0.47 e-9
2.13	0.12 e-10
2.10	0.17 e-7
1.90	0.82 e-9
1.88	0.85 e-10
1.87	0.65 e-10
1.86	0.13 e-7
1.59	0.15 e-2
1.36	0.82 e-5
1.34	0.15 e-3
1.32	0.40 e-4
1.07	0.22 e-2
0.94	0.45 e-2
0.93	0.47 e-2
0.79	0.14 e-9
0.76	0.12
0.68	0.51 e-4
0.65	0.84 e-7
0.64	0.11 e-1

Significance of Periods (Johnson B filter)

Note: 0=Most probable period

1=Least probable period

PERIOD	SIGNIFICANCE
15.00	0.67 e-9
14.56	0.20 e-8
13.95	0.12 e-7
13.57	0.80 e-7
13.22	0.55 e-6
12.55	0.35 e-4
5.50	0.46 e-3
5.42	0.60 e-3
3.91	0.38 e-1
3.87	0.19 e-1
3.76	0.22 e-1
3.74	0.27 e-1
3.71	0.29 e-1
3.68	0.23 e-1
3.65	0.37 e-1
2.84	0.12 e-3
2.78	0.10 e-6
2.76	0.26 e-6
2.75	0.29 e-6
2.73	0.14 e-5
2.72	0.24 e-4
2.15	0.39 e-3
2.14	0.17 e-3
2.13	0.68 e-3
1.89	0.53 e-3
1.88	0.11 e-5
1.87	0.13 e-4
1.60	0.43 e-8
1.34	0.35 e-1
0.76	0.12 e-6
0.72	0.70 e-20
0.68	0.50 e-1
0.65	0.21 e-2
0.61	0.87 e-1

Significance of Periods (Stromgren b filter)

Note: 0=Most probable period

1=Least probable period

PERIOD	SIGNIFICANCE
15.00	0.49e-4
14.15	0.19 e-3
11.28	0.49e-2
10.68	0.49 e-2
7.54	0.14 e-4
7.43	0.18 e-6
7.32	0.22 e-7
7.21	0.18 e-4
7.11	0.64 e-5
7.01	0.44 e-5
4.68	0.55 e-4
3.82	0.66 e-4
3.74	0.20 e-6
3.71	0.63 e-7
3.65	0.16 e-8
3.68	0.18 e-8
3.60	0.13 e-9
3.58	0.40 e-10
3.55	0.54 e-10
3.51	0.15 e-8
3.49	0.17 e-7
2.75	0.97 e-5
2.73	0.12 e-5
2.32	0.63 e-5
1.89	0.79 e-2
1.77	0.86 e-4
1.58	0.20 e-3
1.57	0.12 e-3
1.39	0.11 e-9
1.06	0.72 e-4
1.05	0.32 e-3
1.04	0.76 e-3
0.78	0.11 e-5
0.73	0.81 e-3

John. V Filter

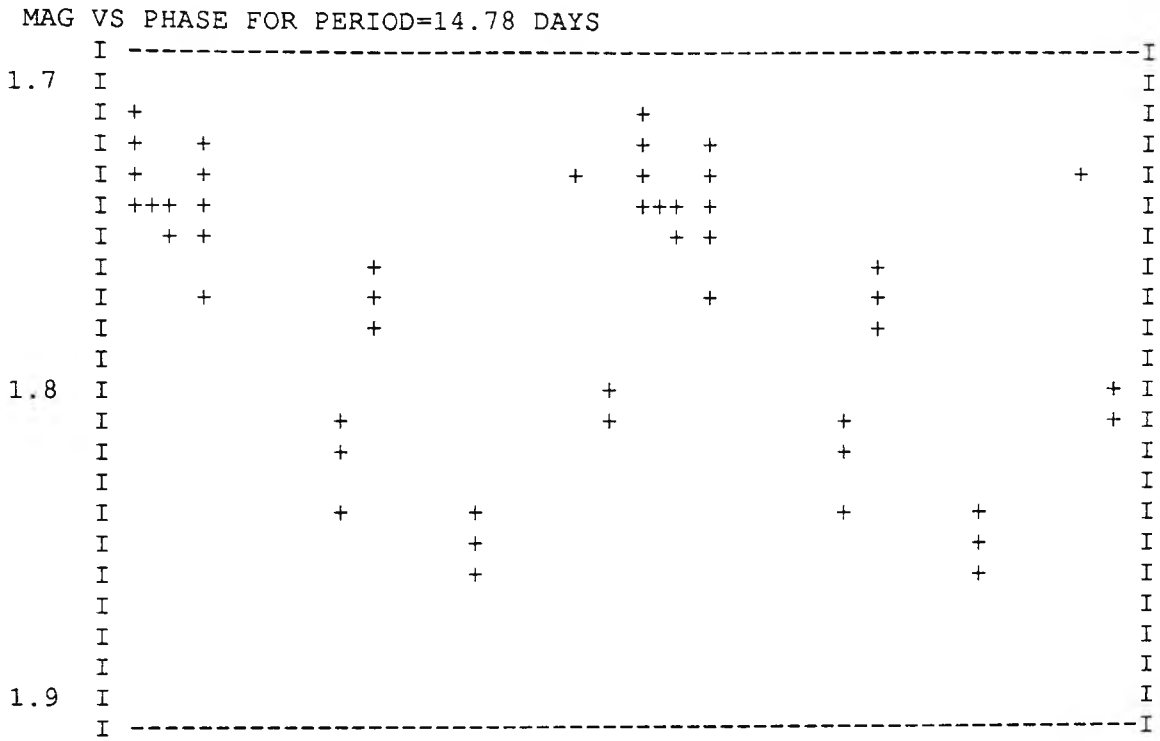

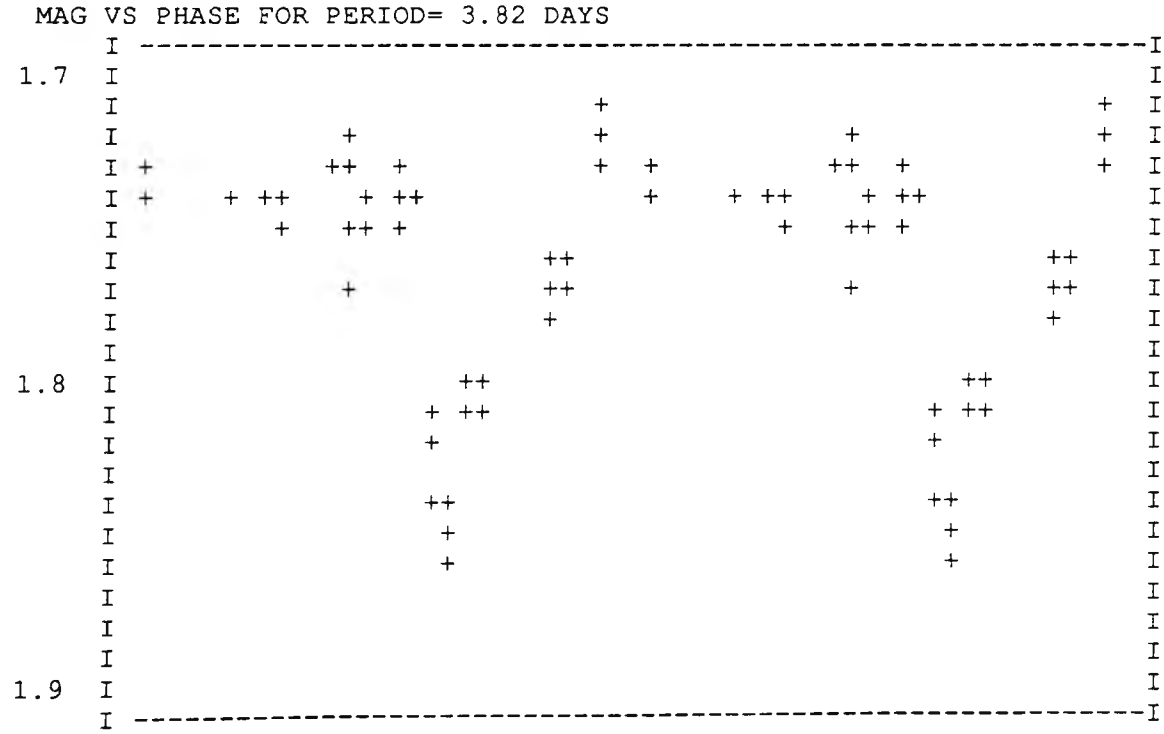

John. V Filter

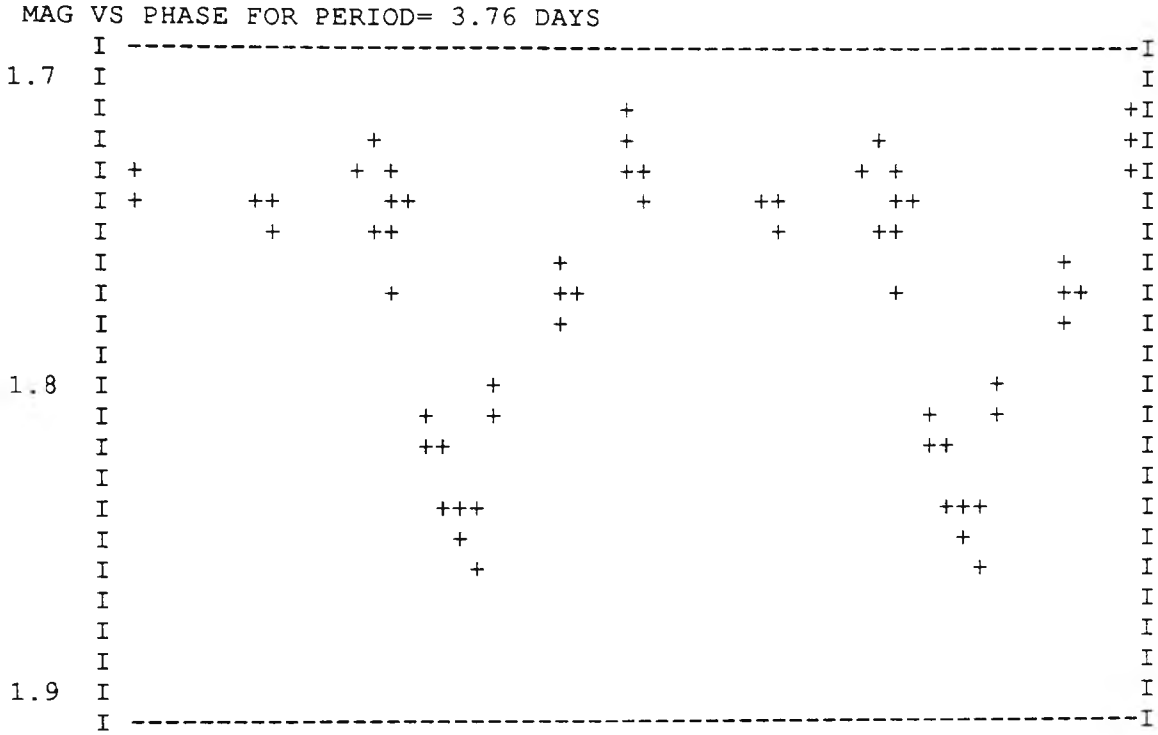

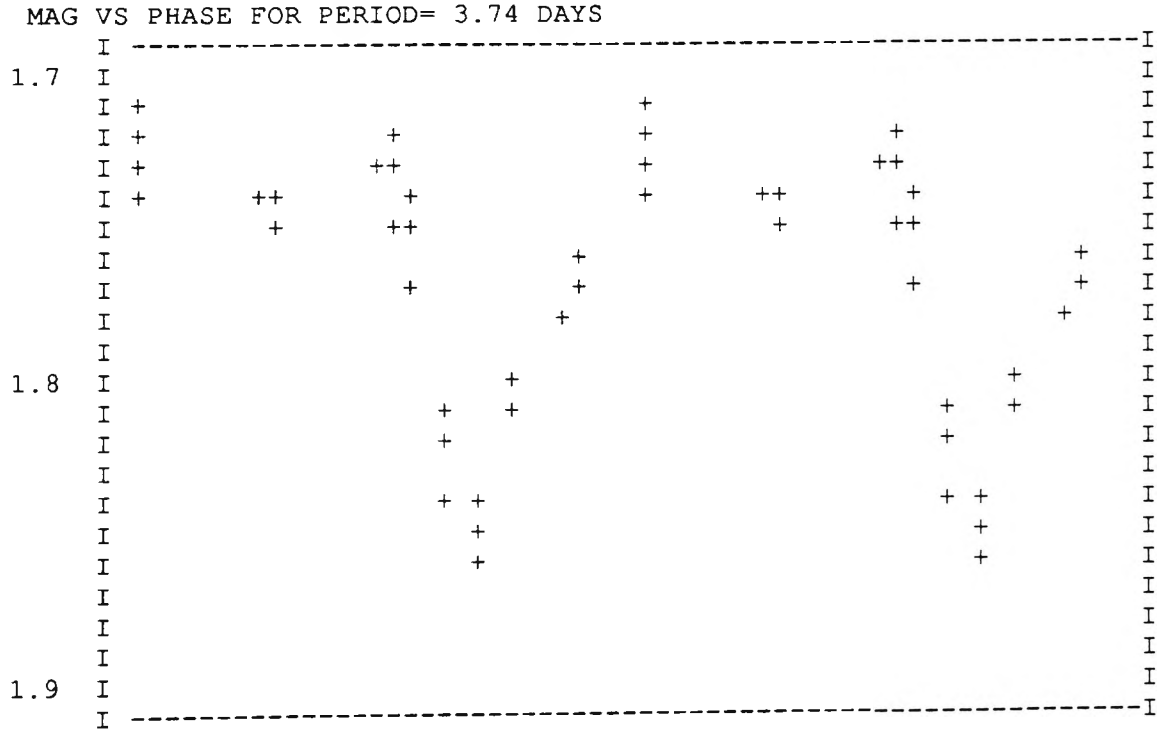

John. V Filter

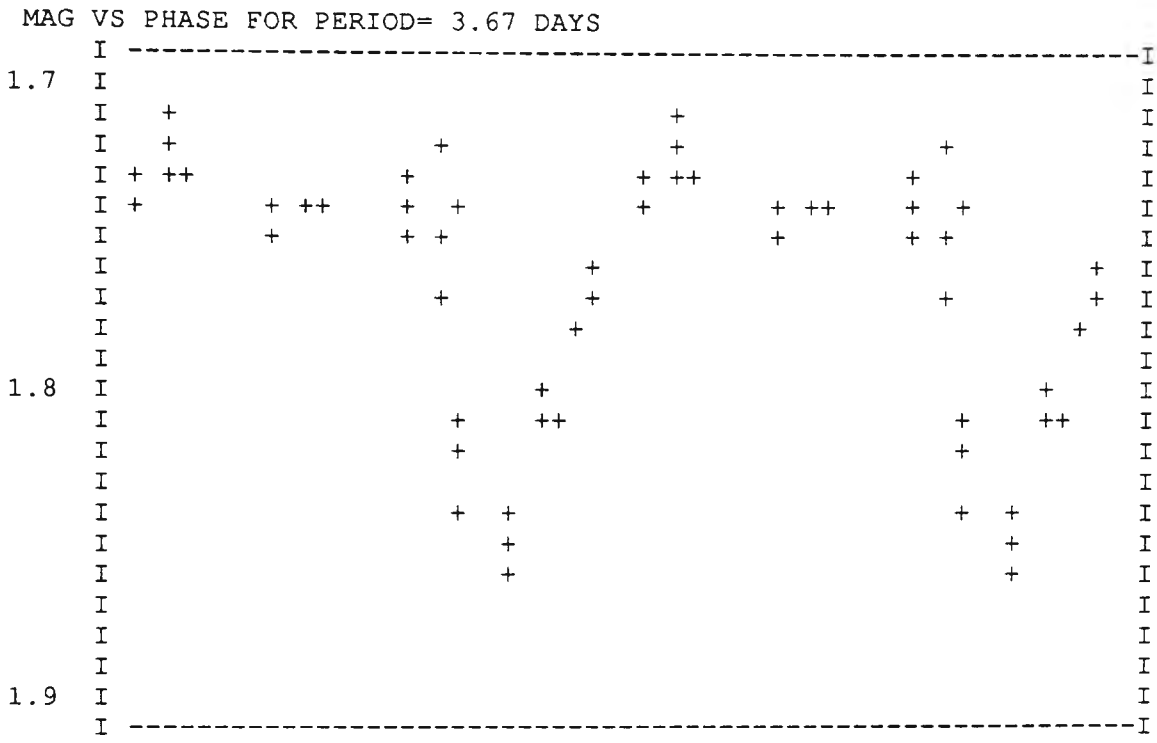

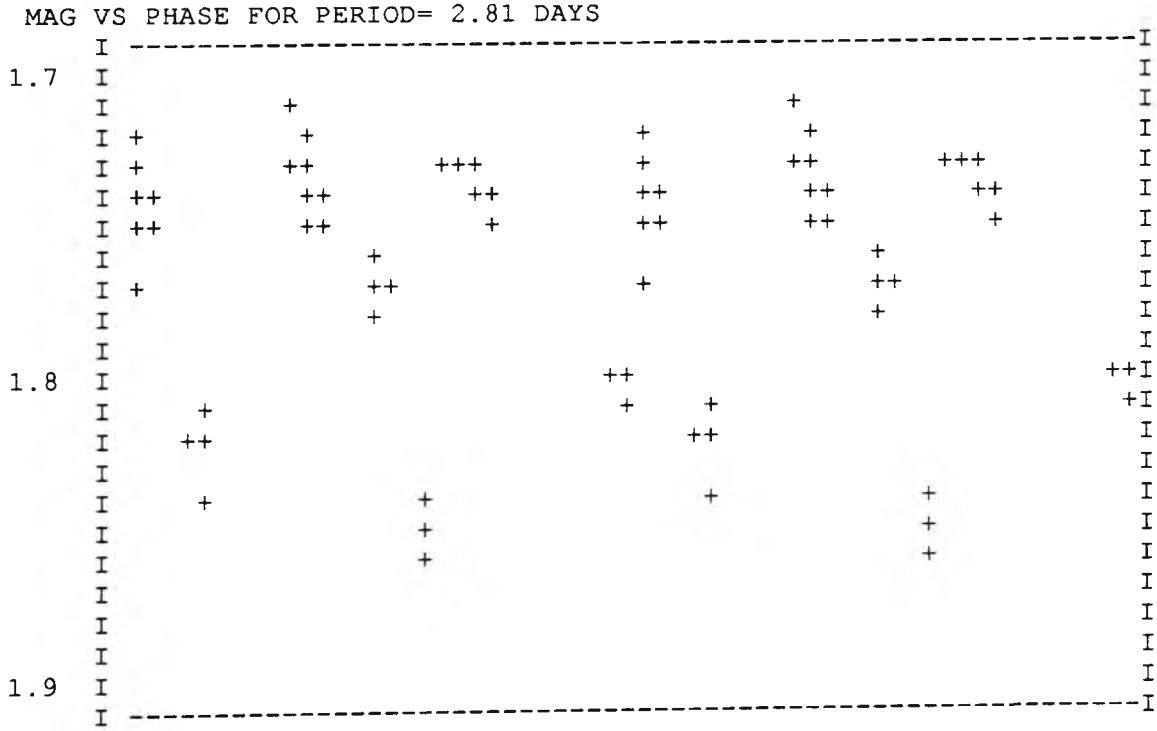

John. V Filter

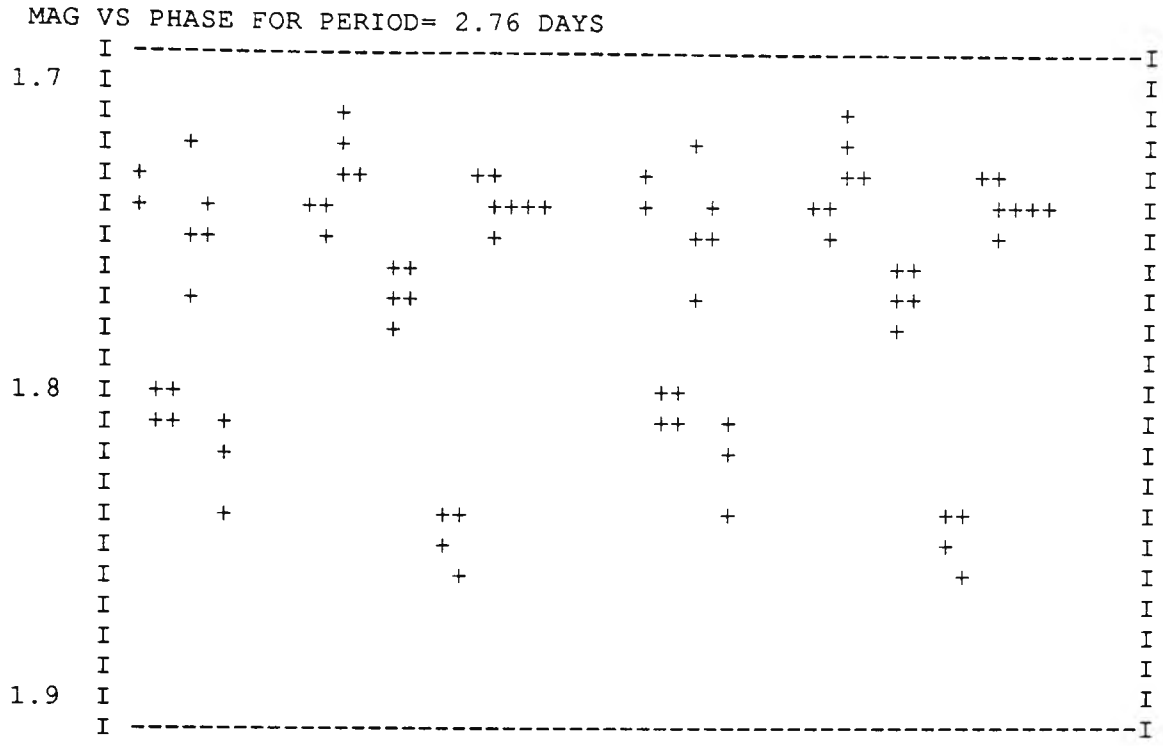

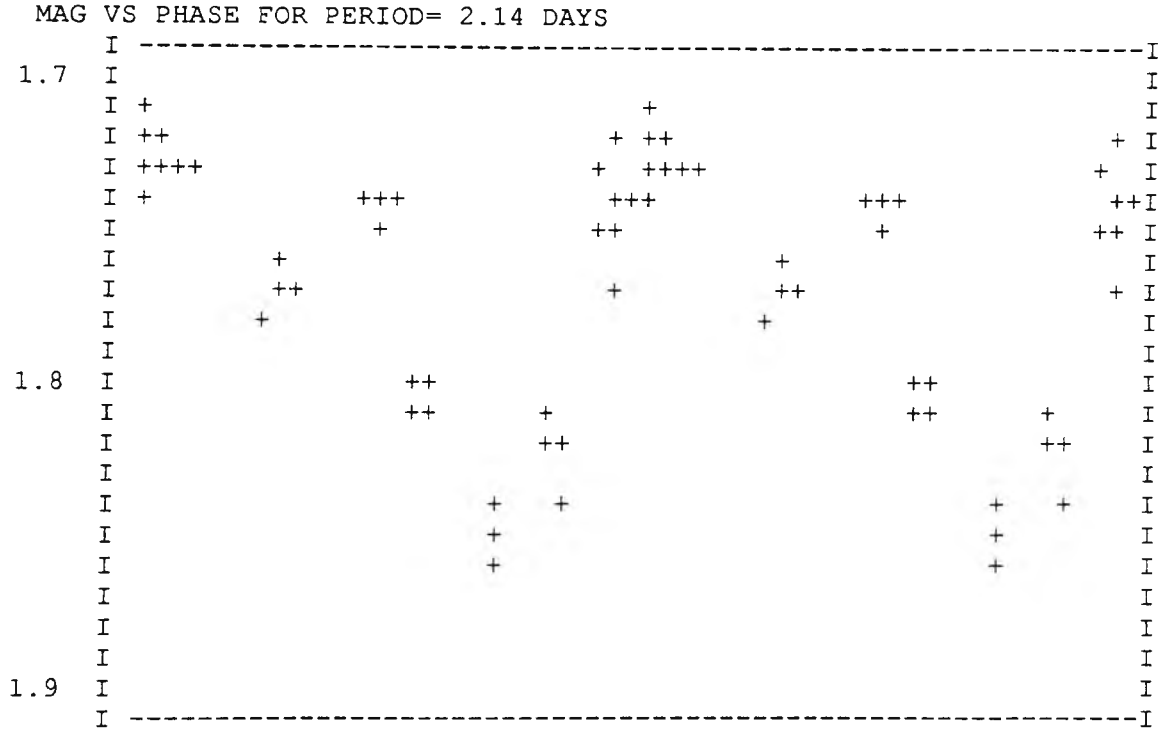

John. V Filter

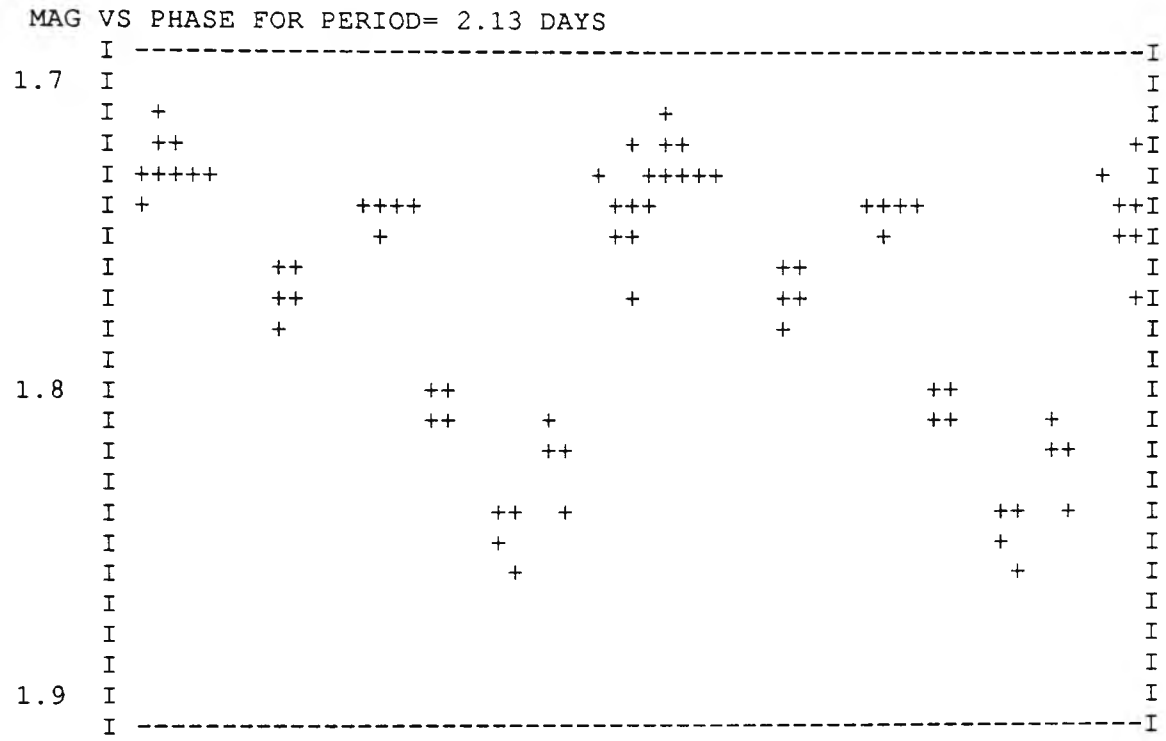

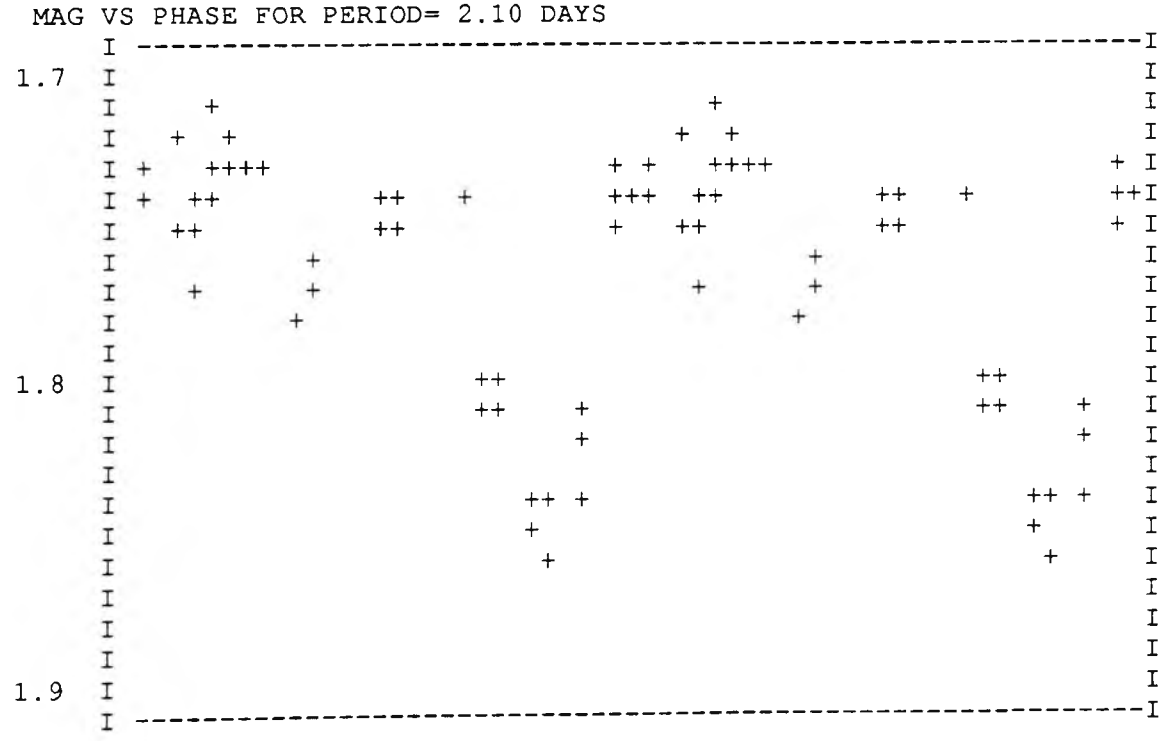

John. V Filter

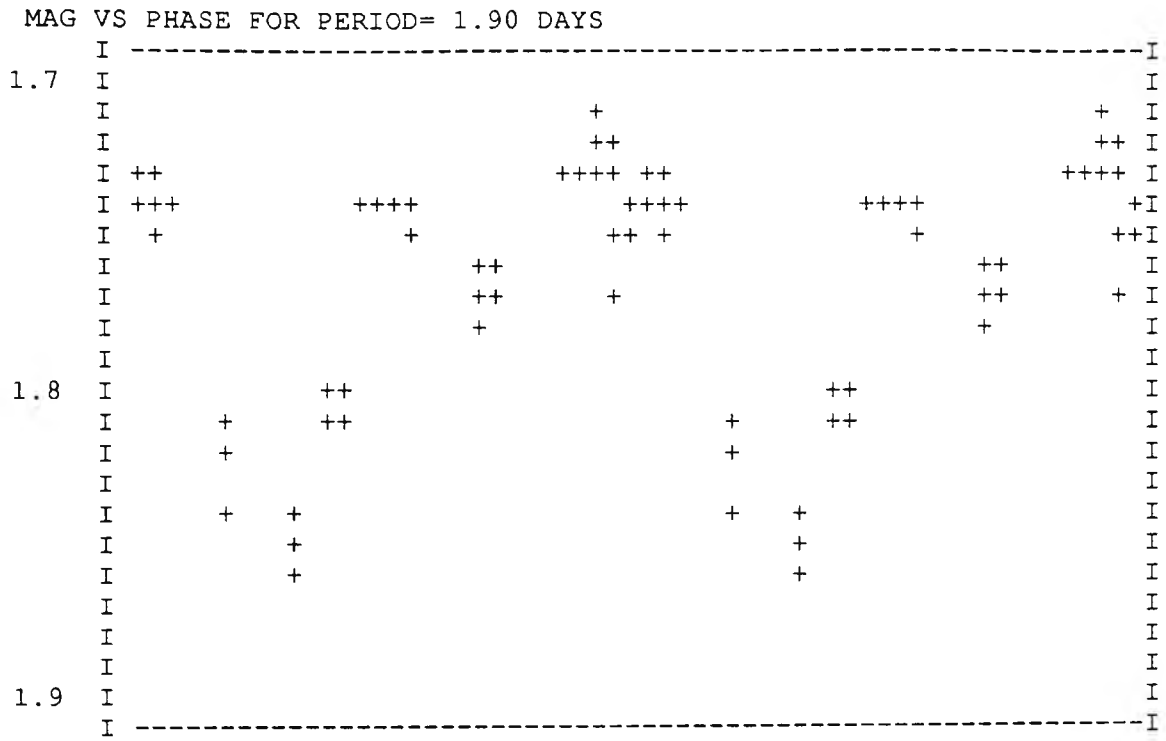

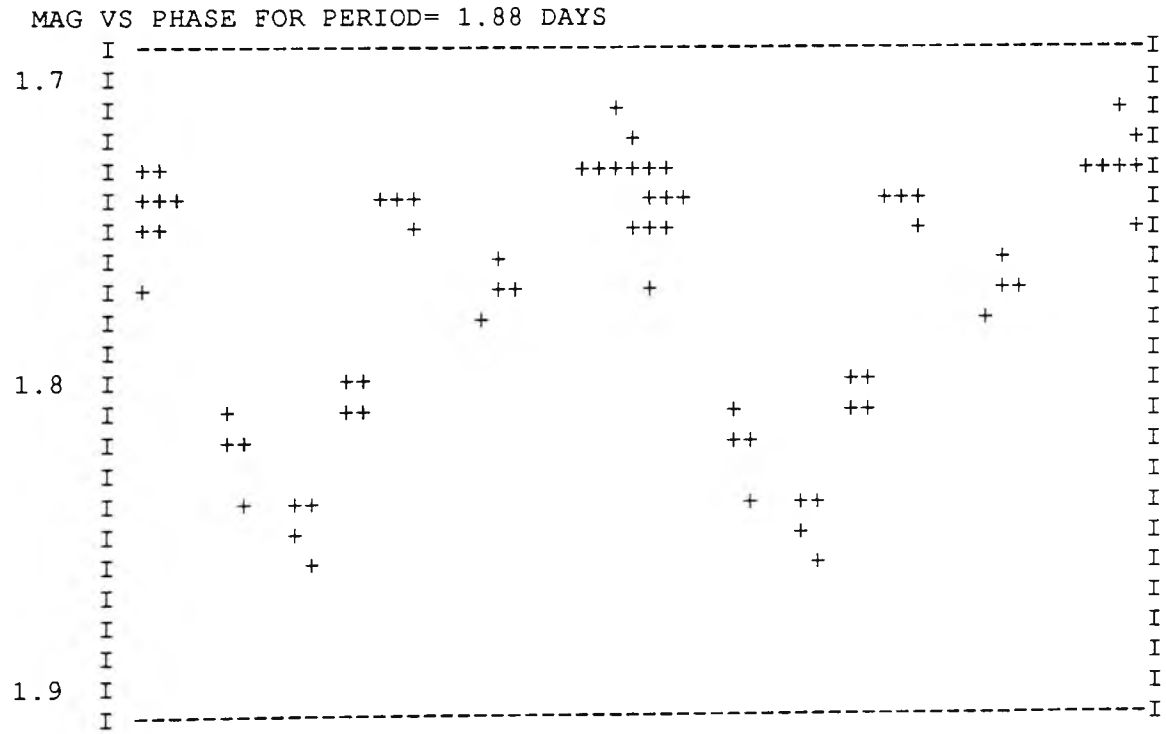

John. V Filter

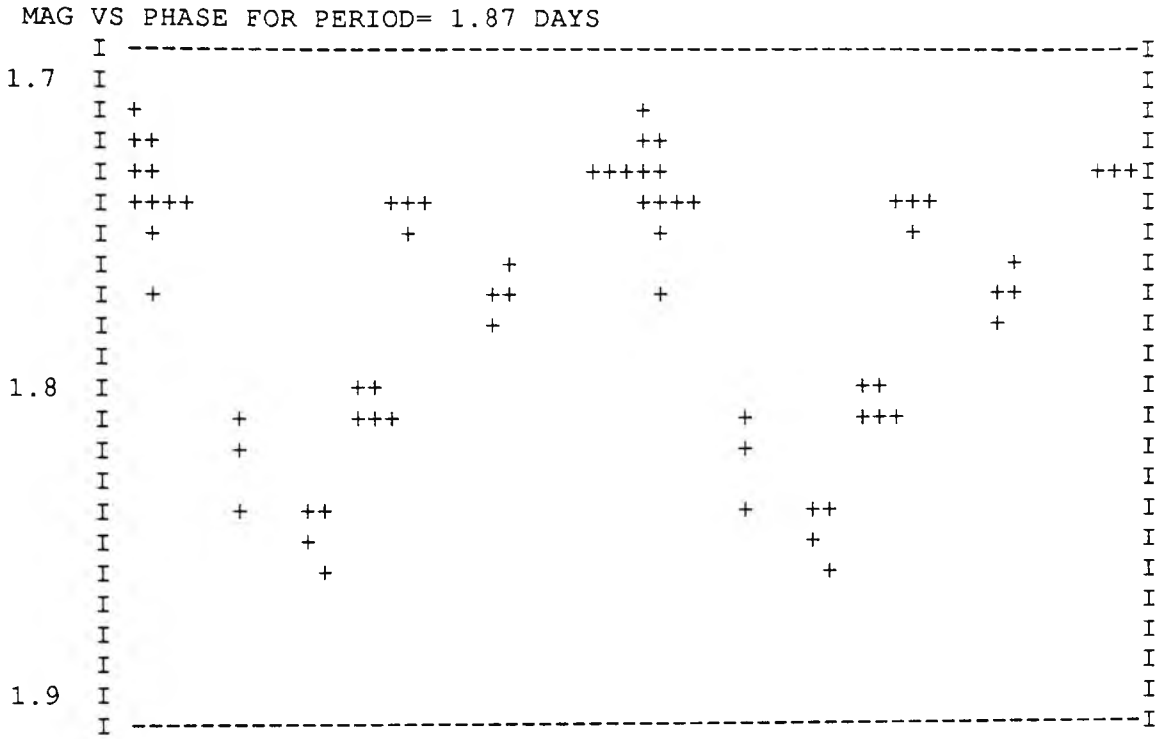

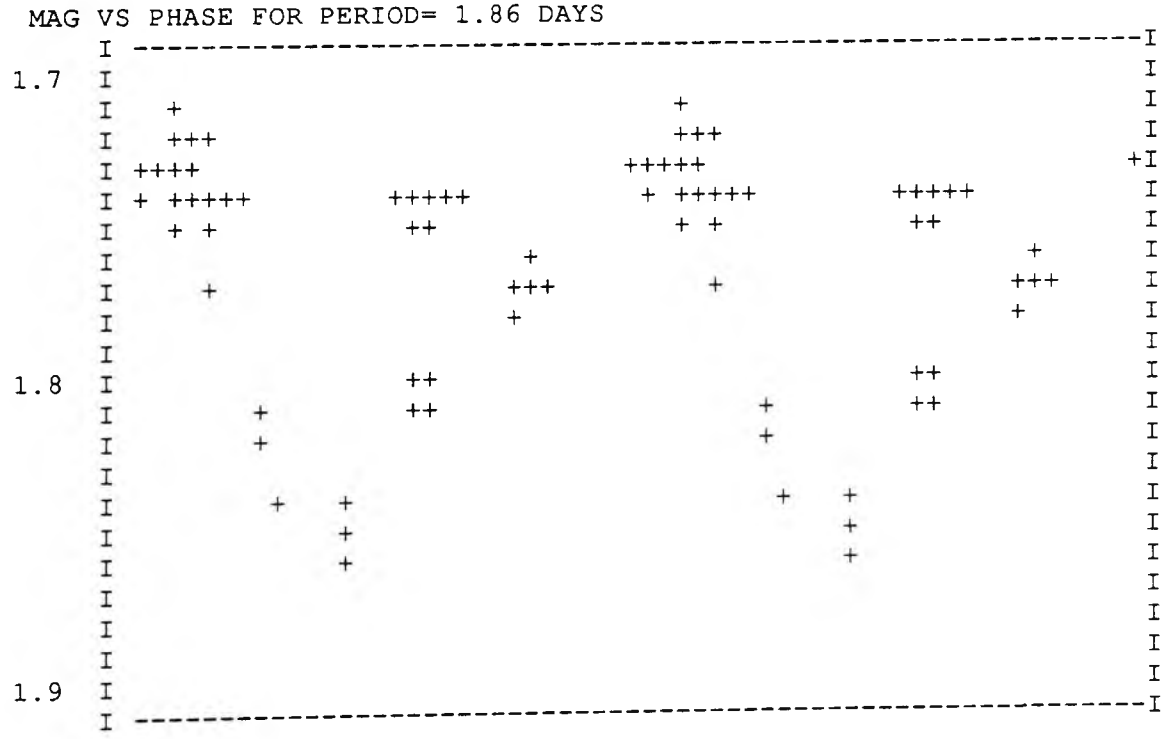

John. V Filter

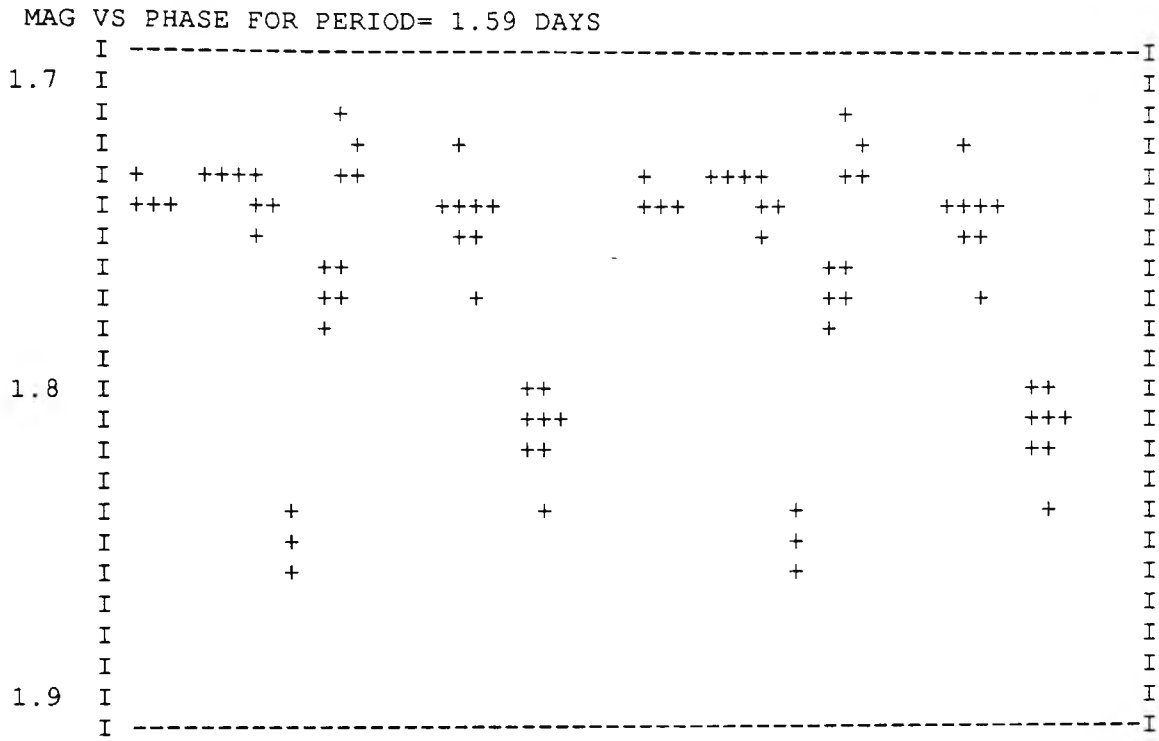

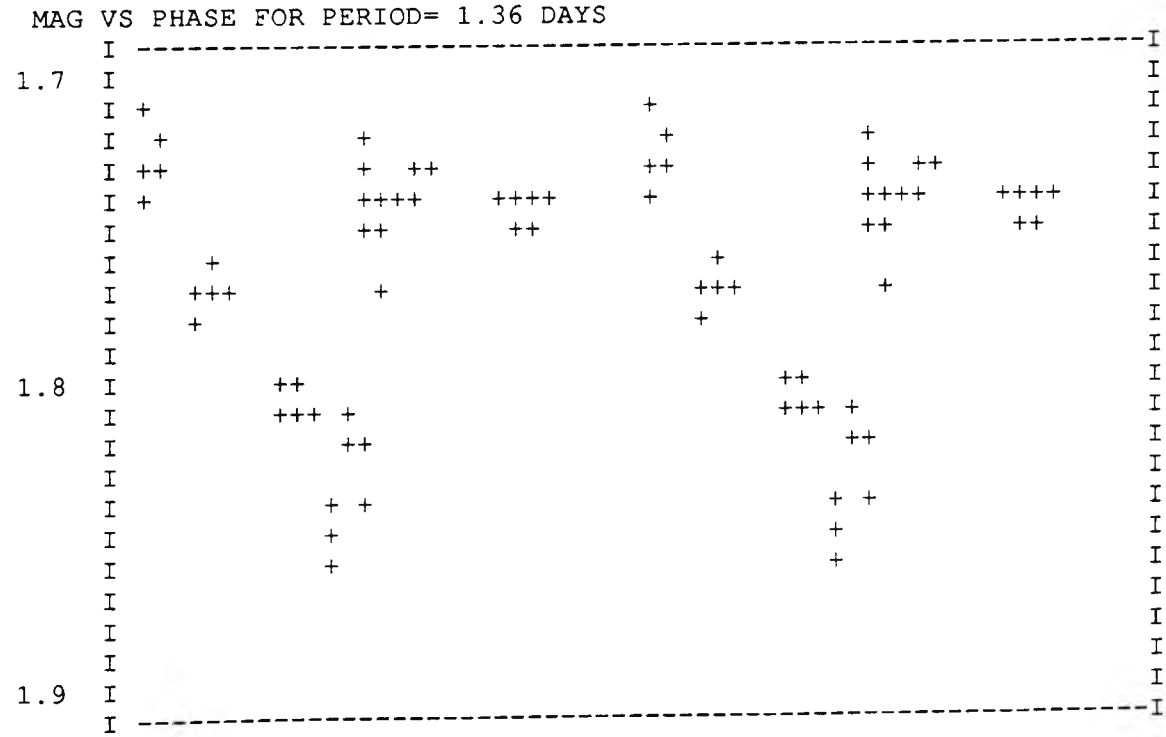

John. V Filter

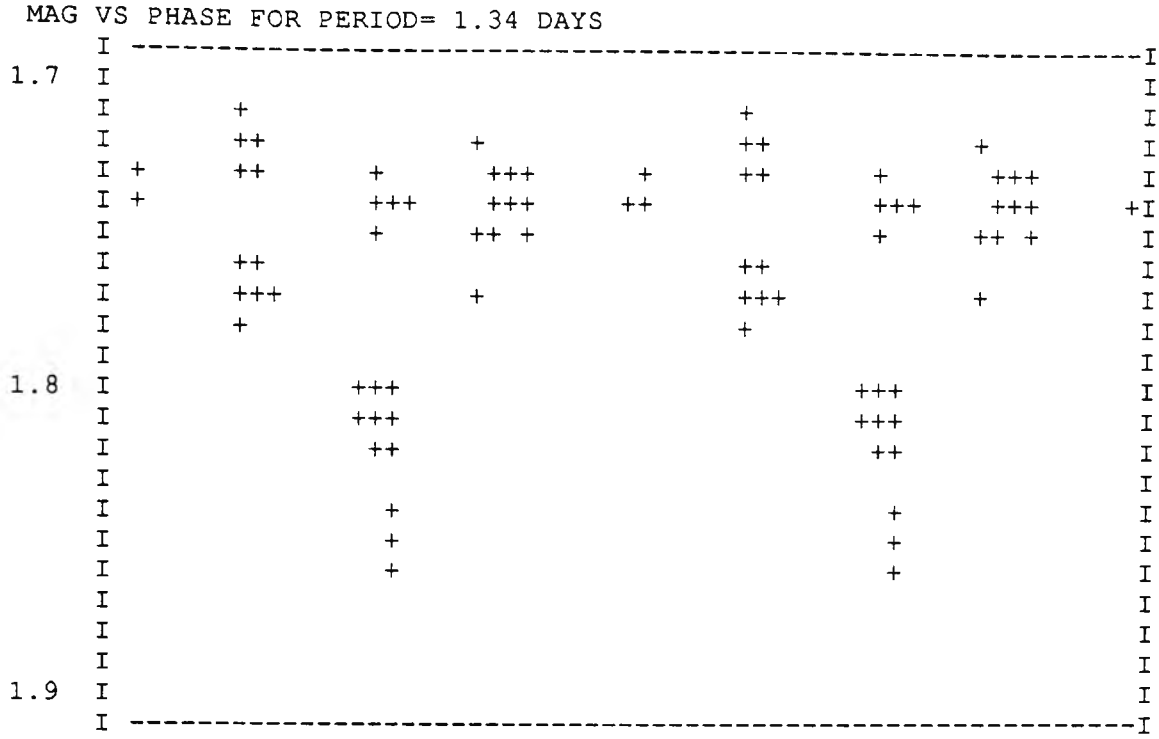

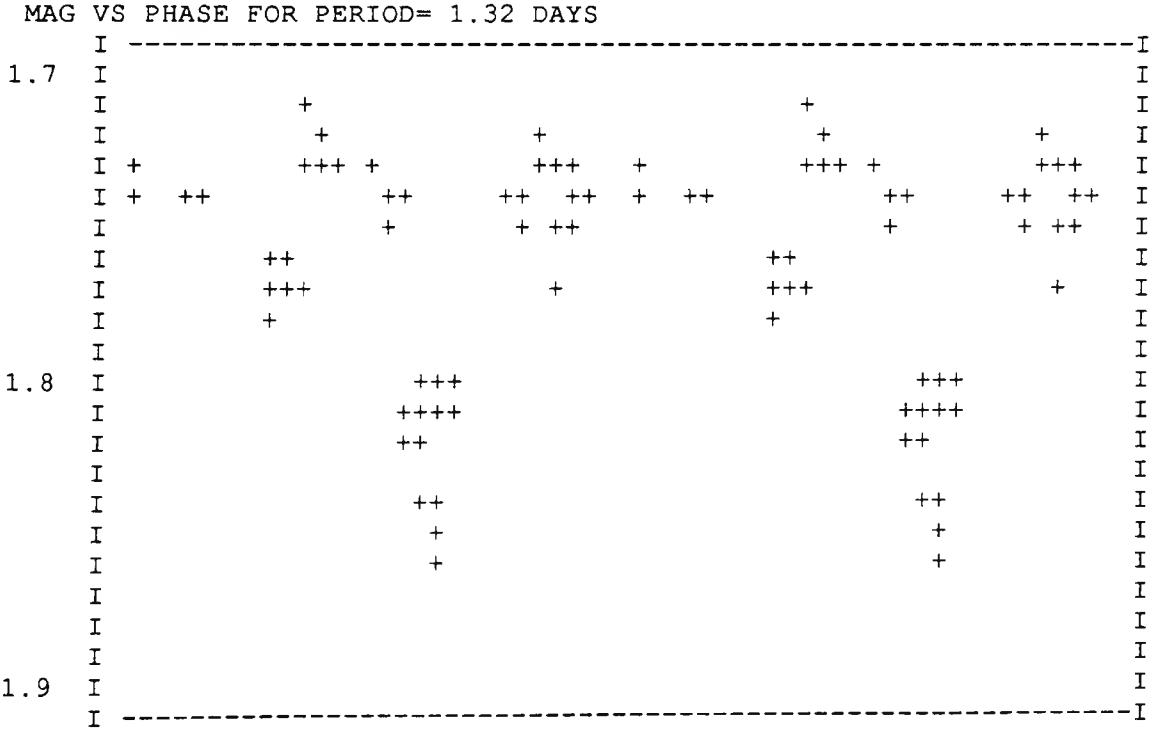

John. V Filter

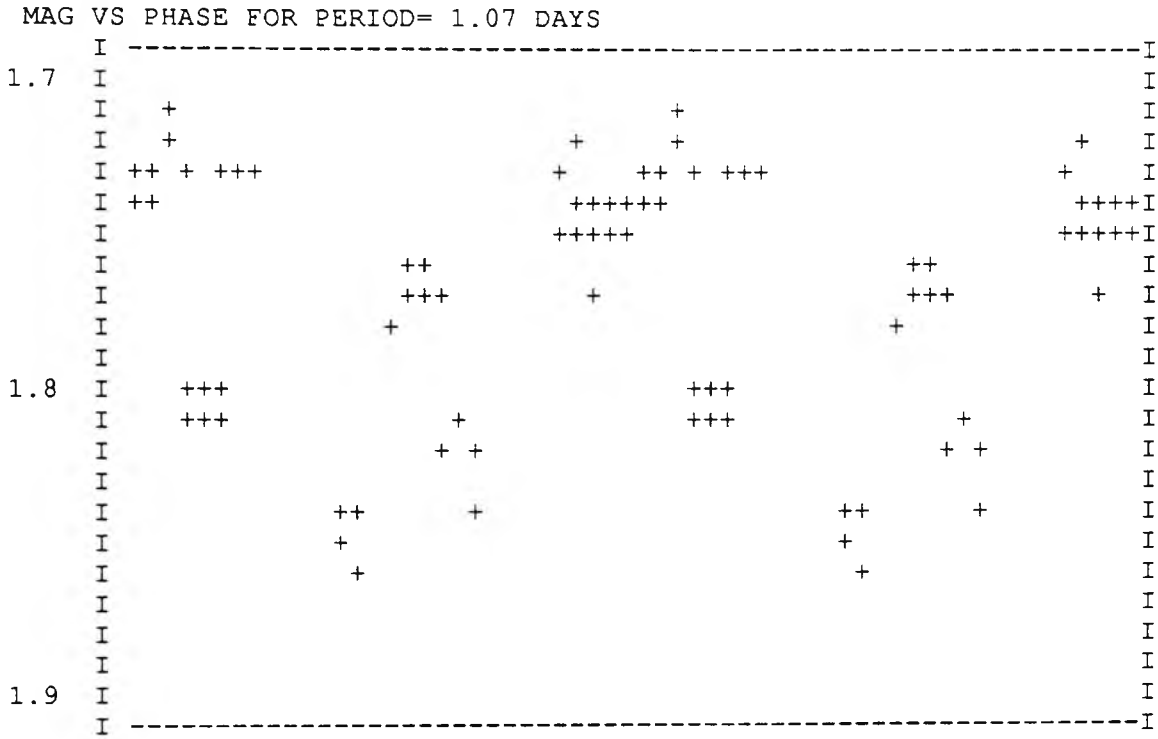

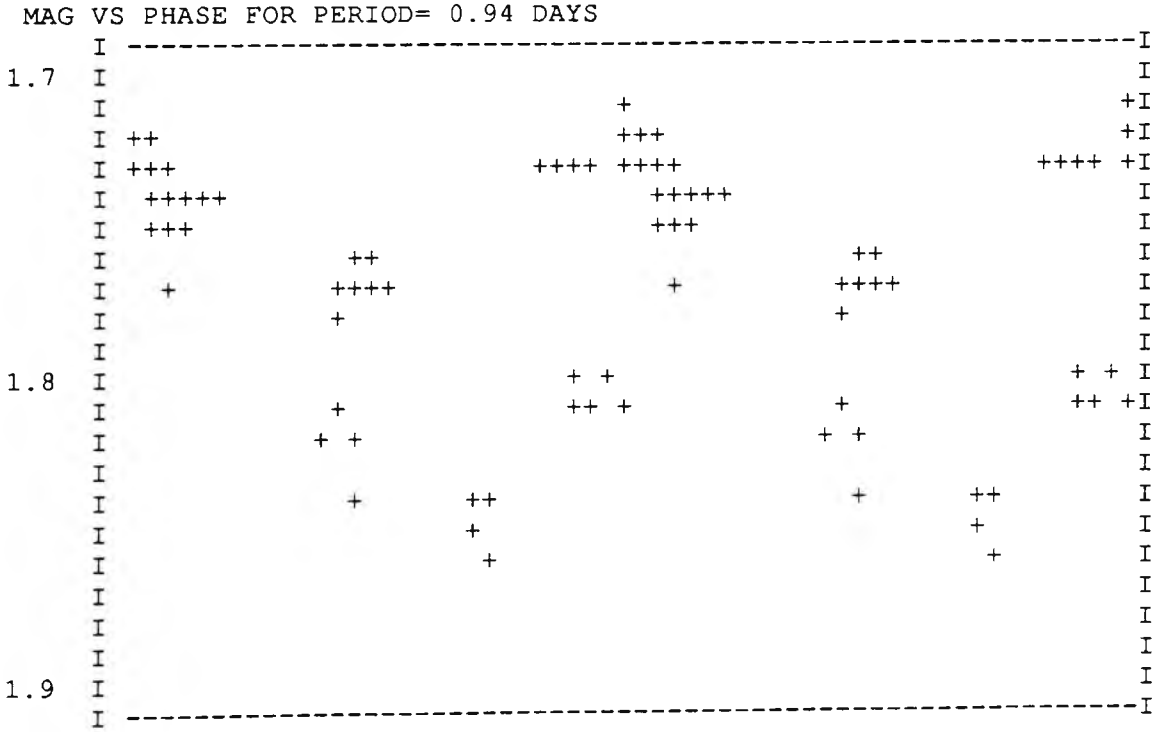

John. V Filter

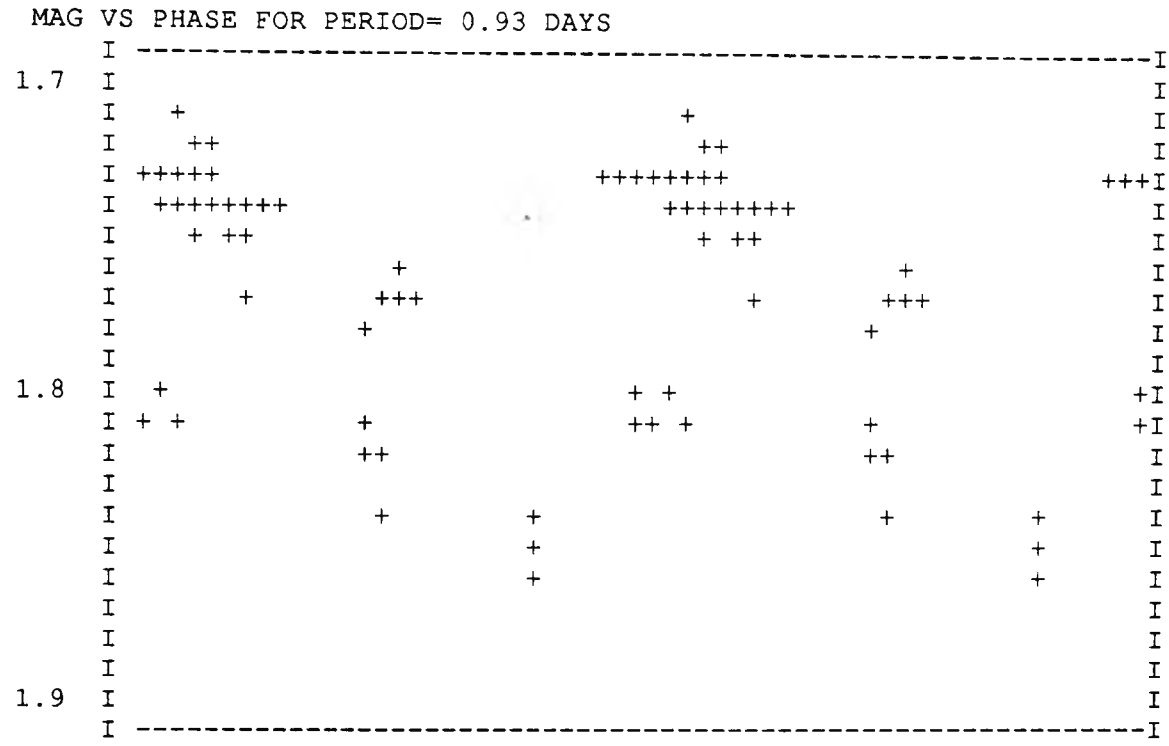

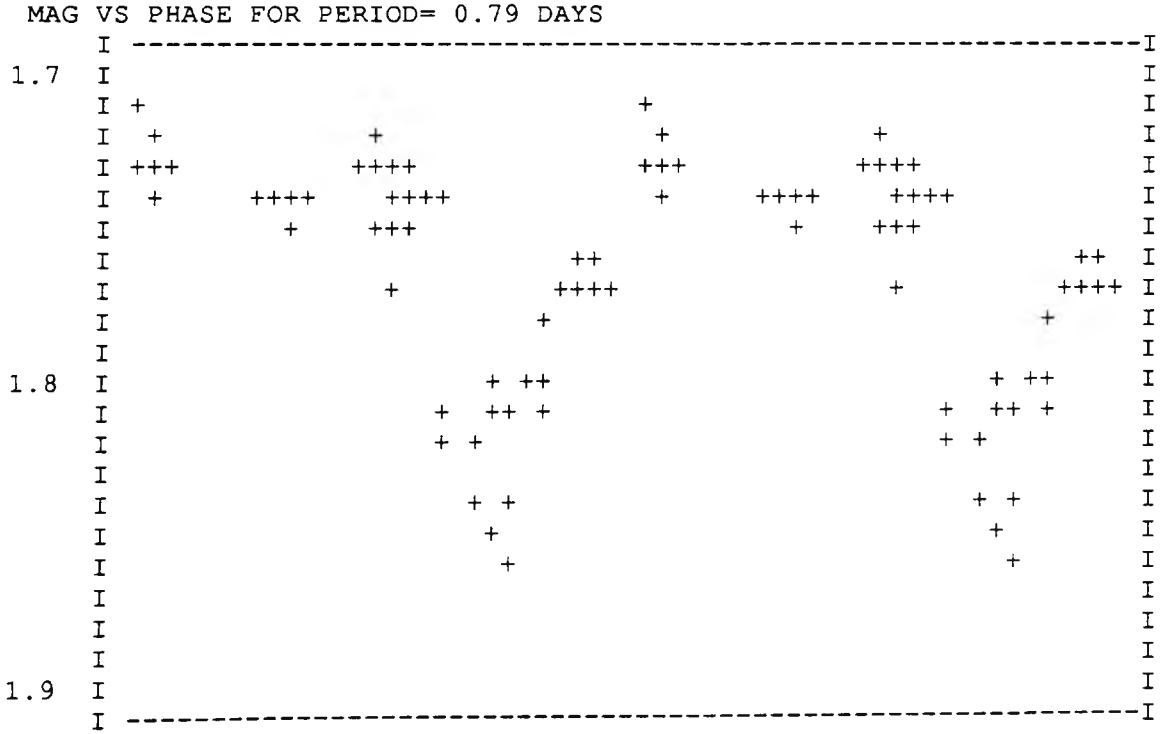

John. V Filter

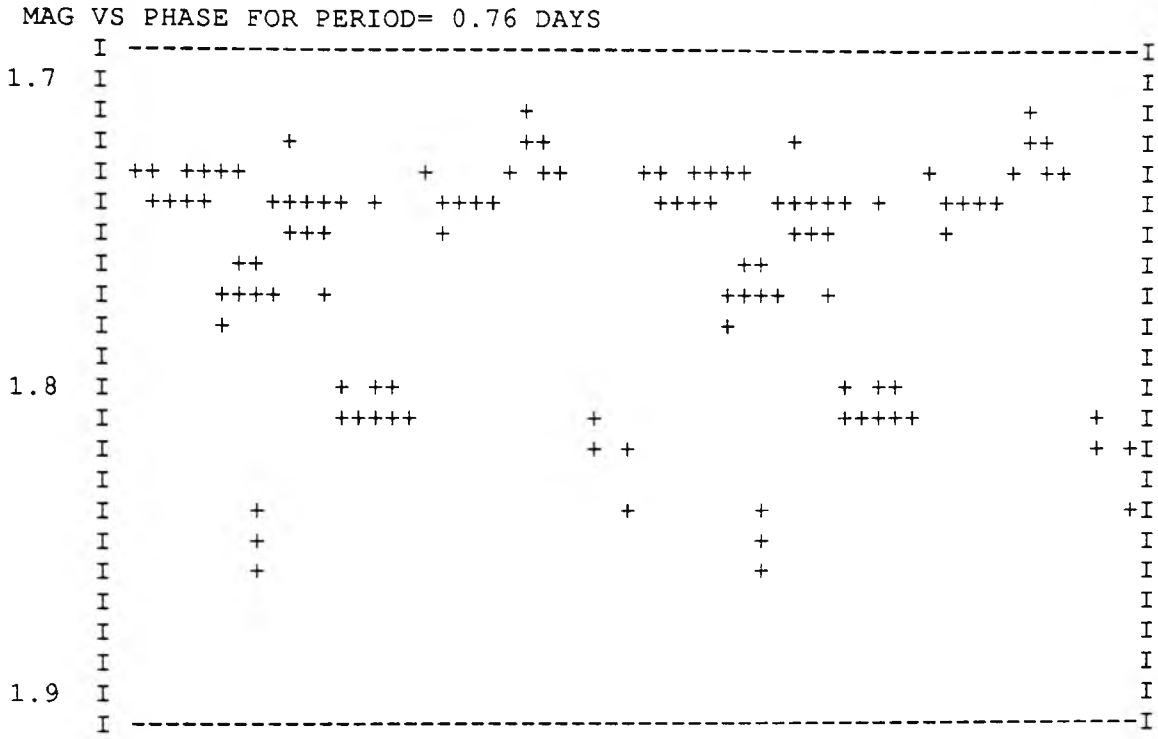

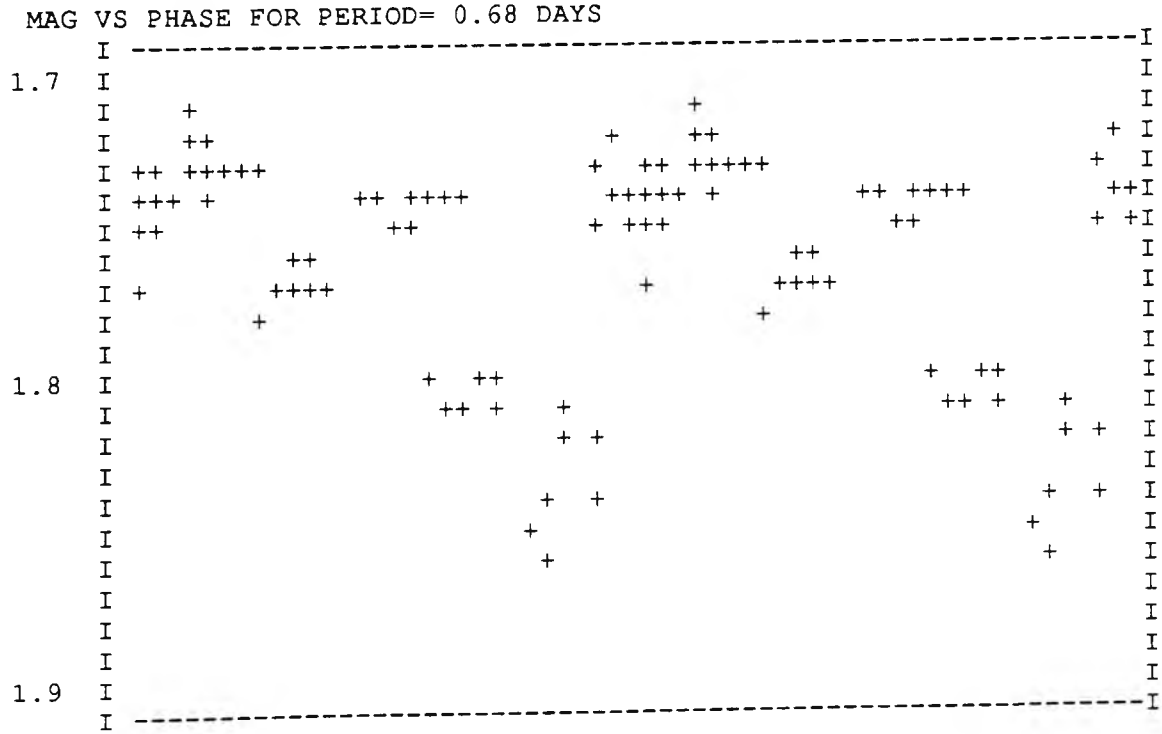

John. V Filter

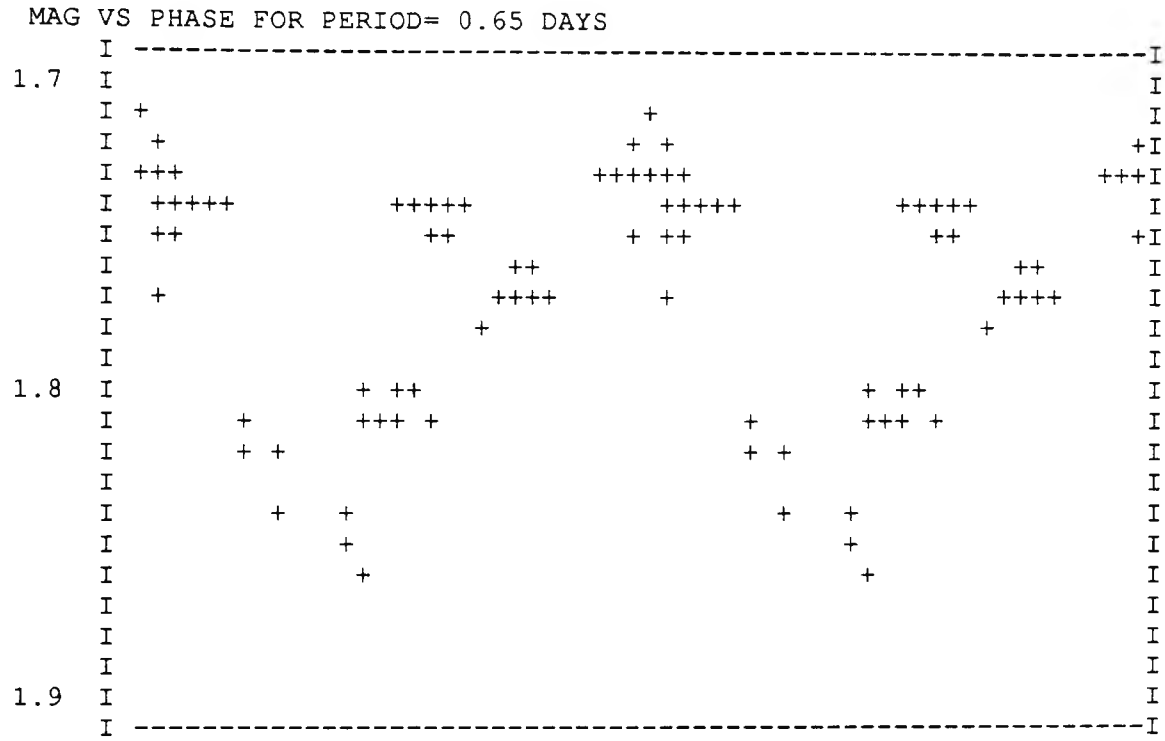

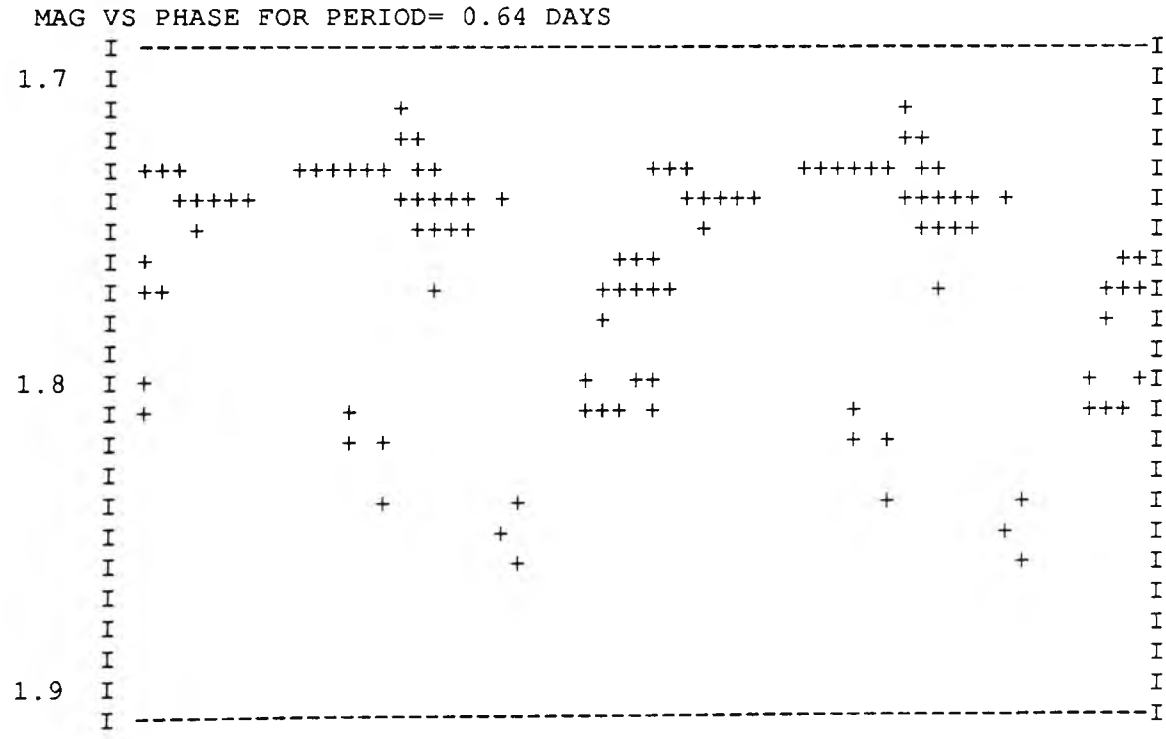

John. B Filter

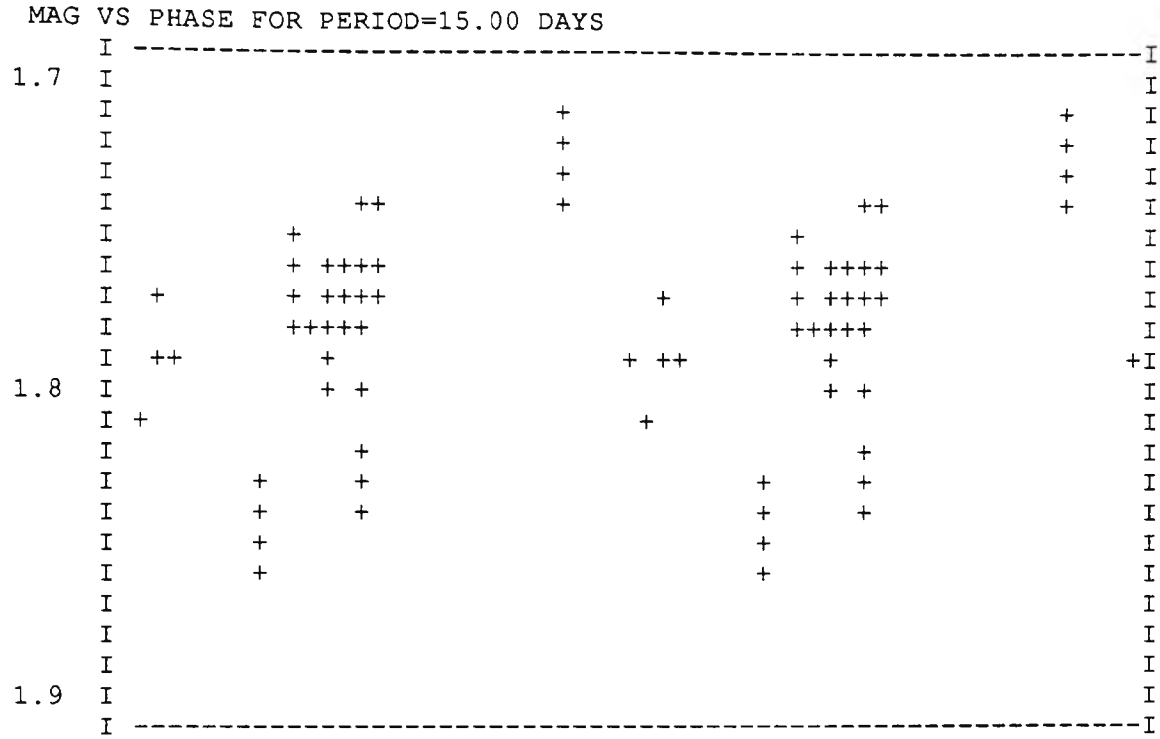

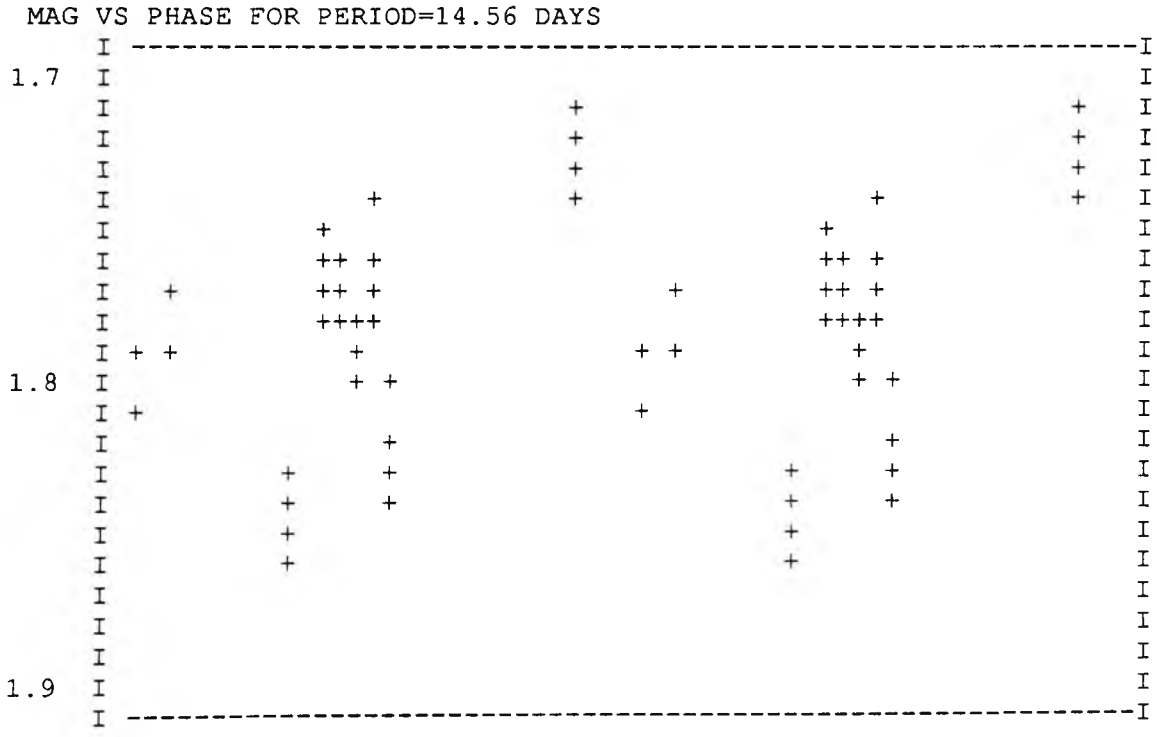

John. B Filter

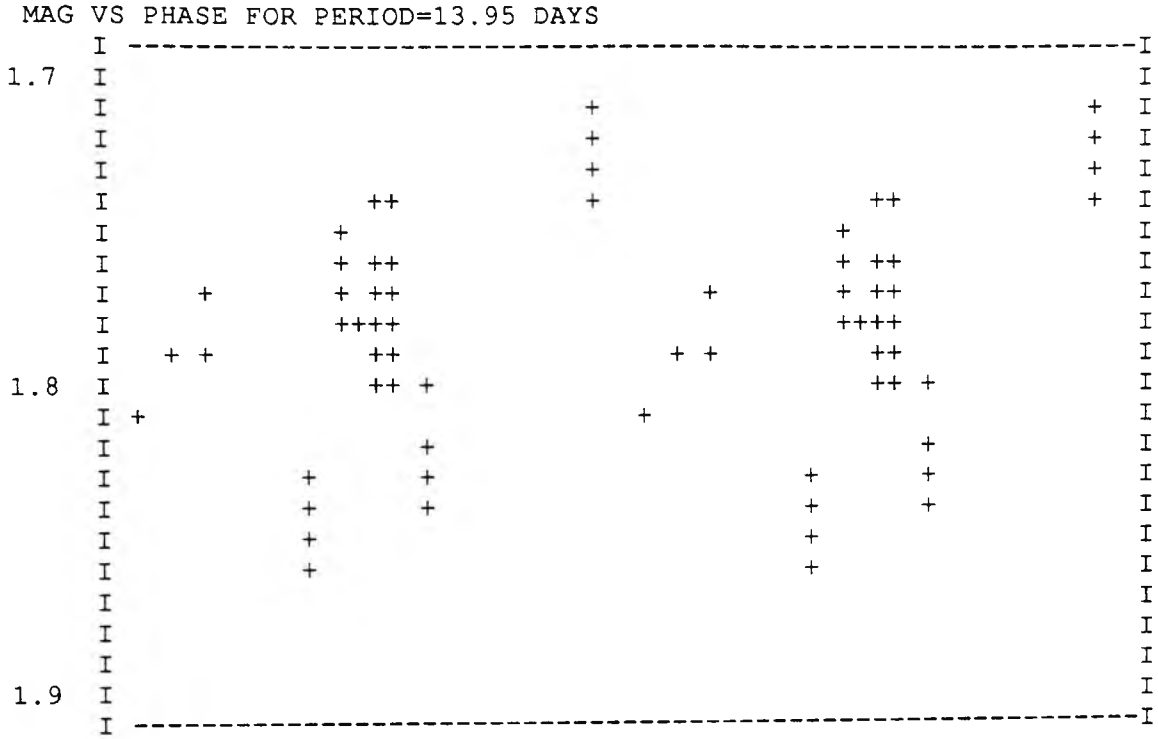

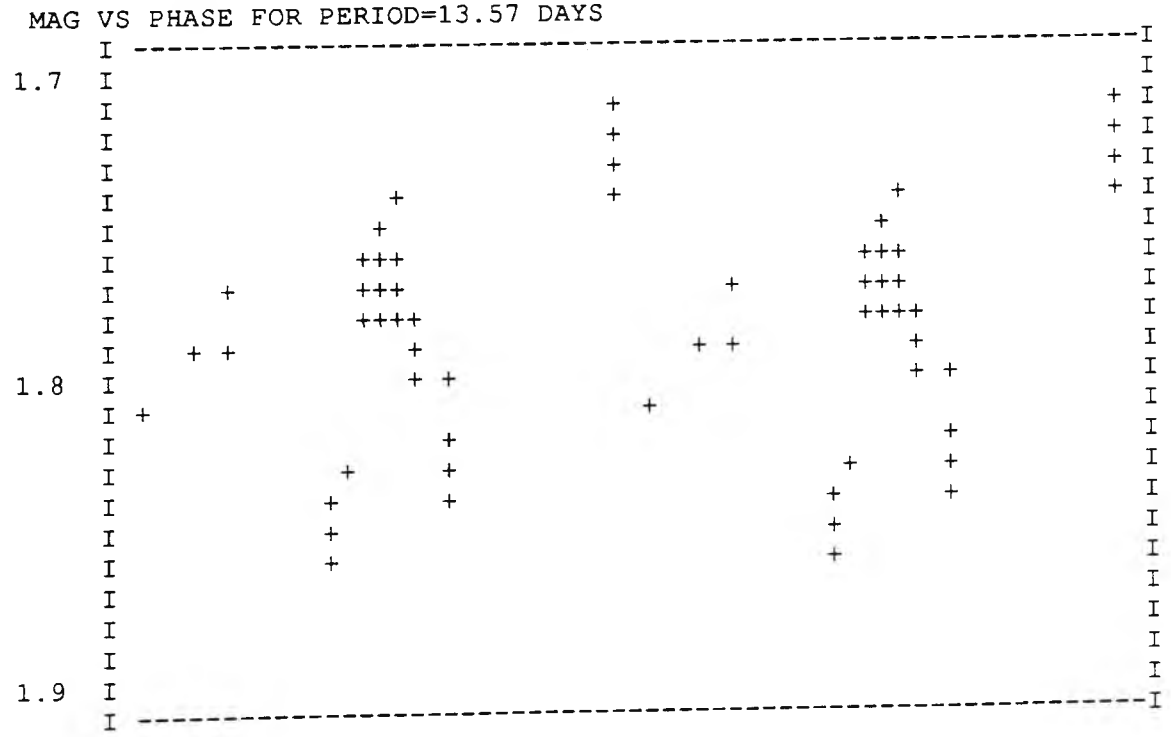

John. B Filter

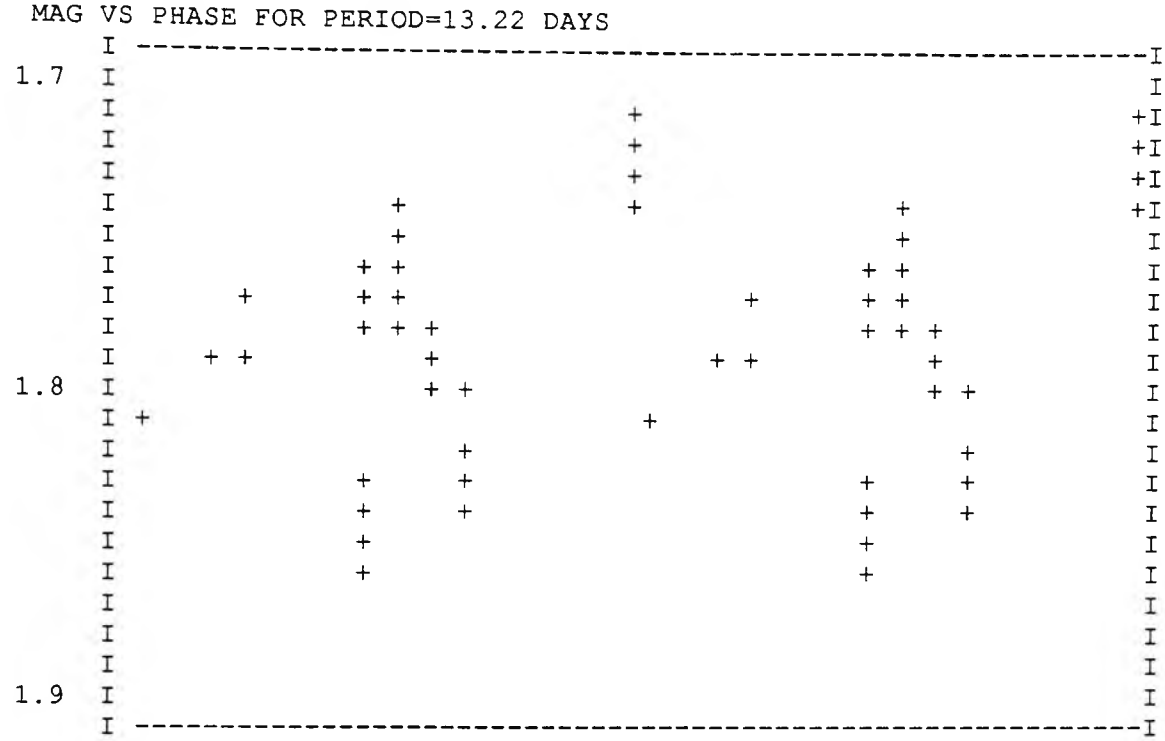

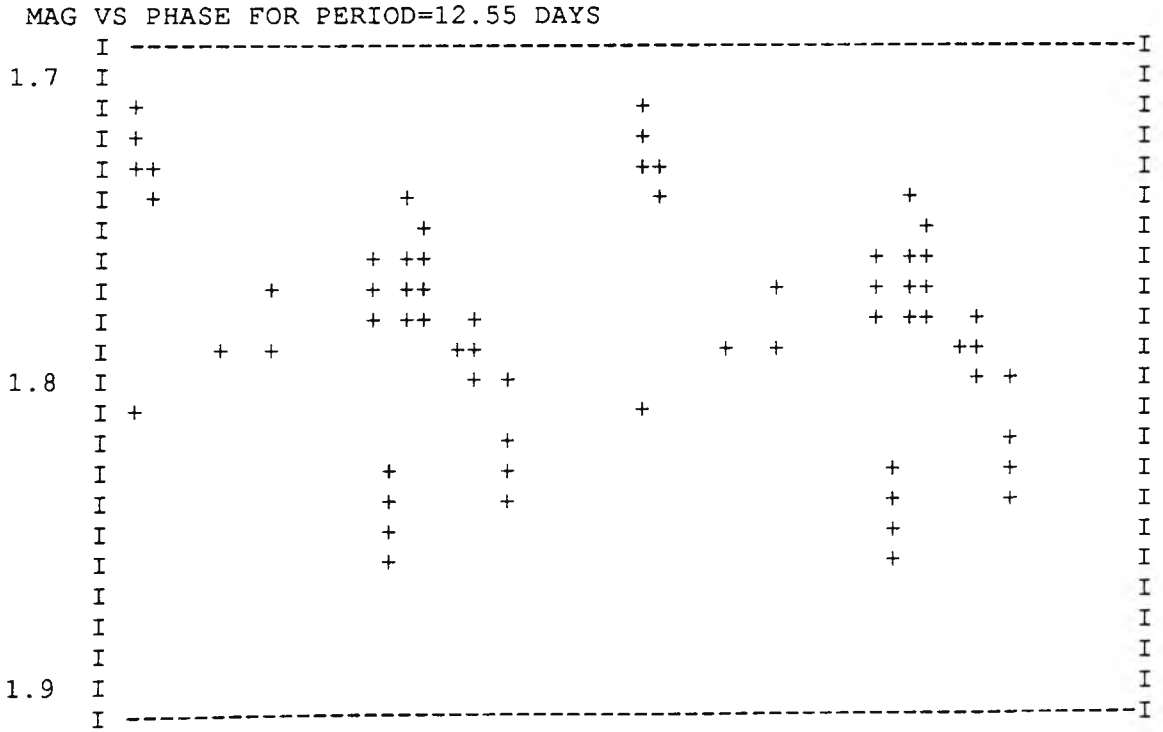

John. B Filter

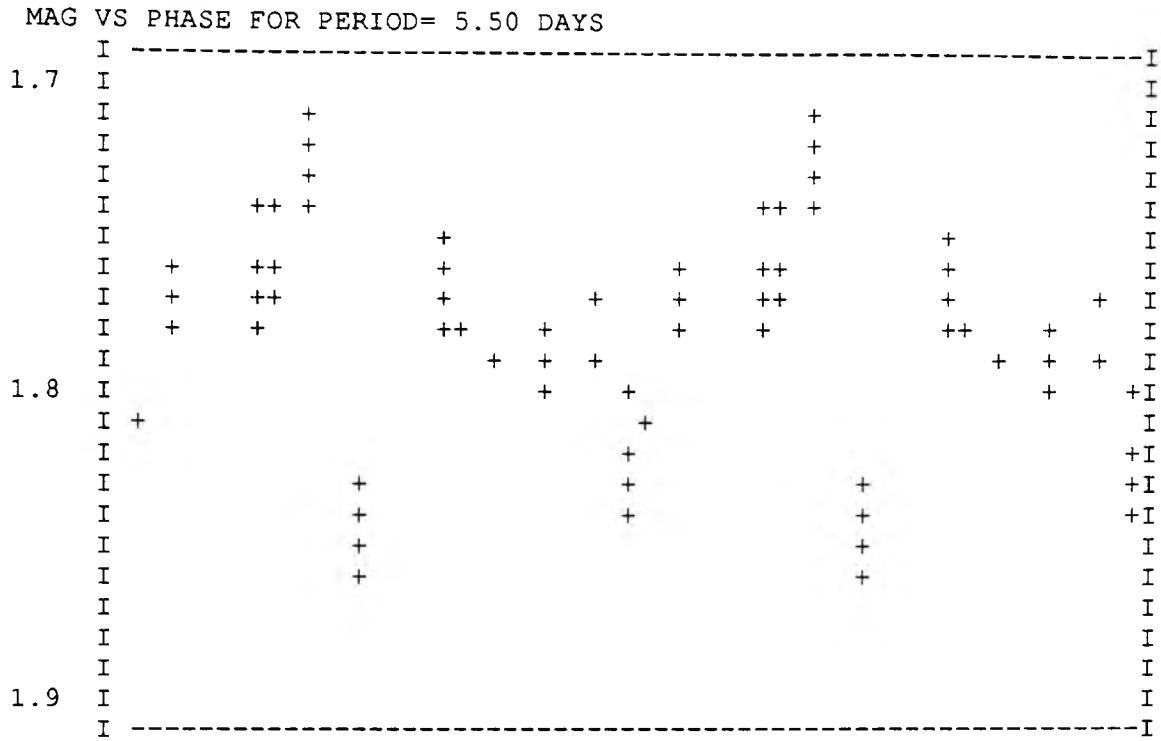

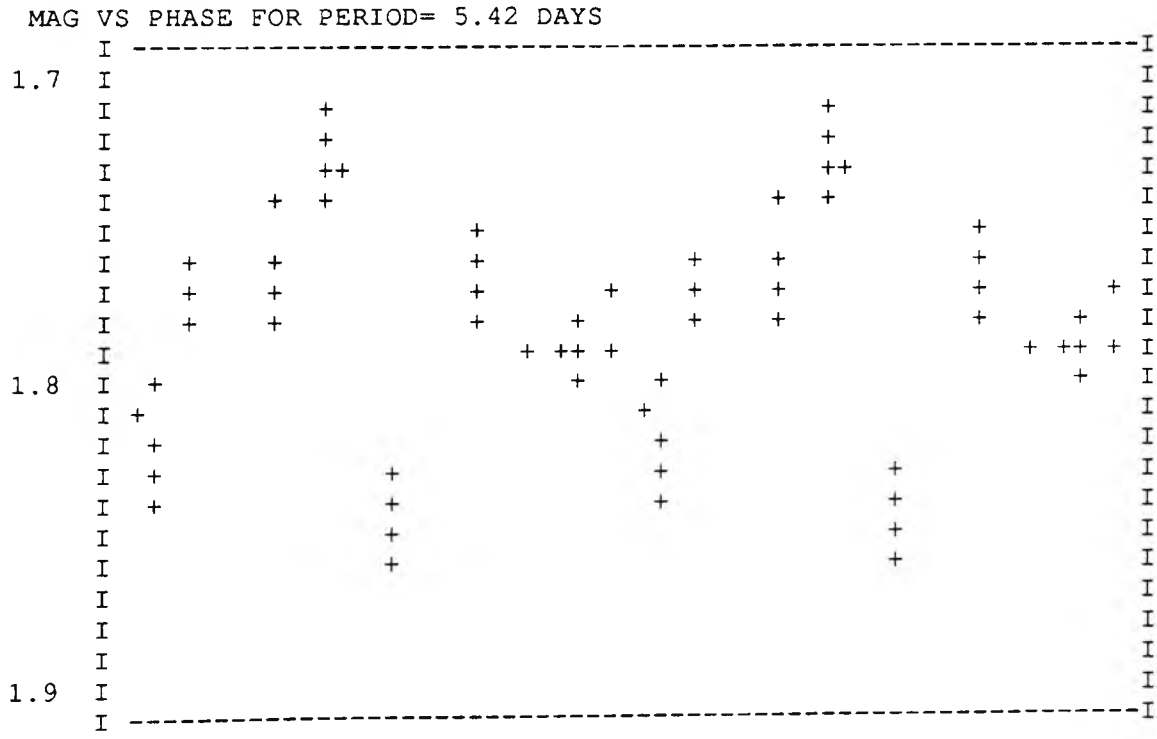

John. B Filter

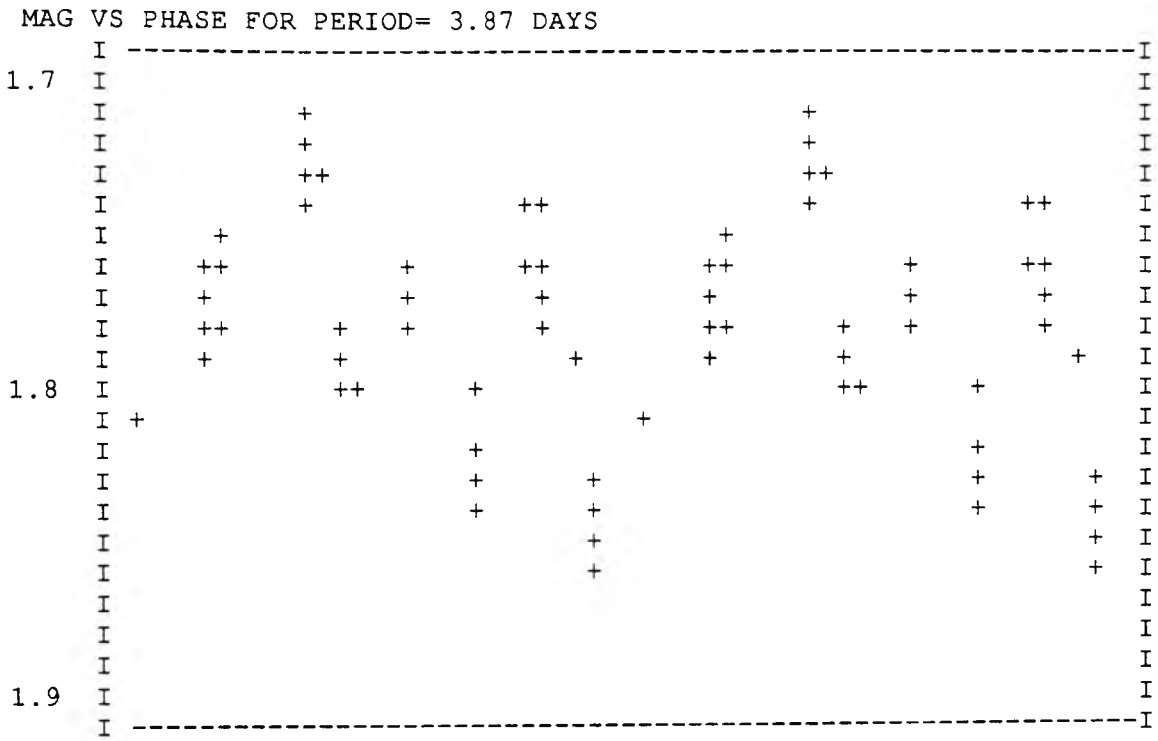

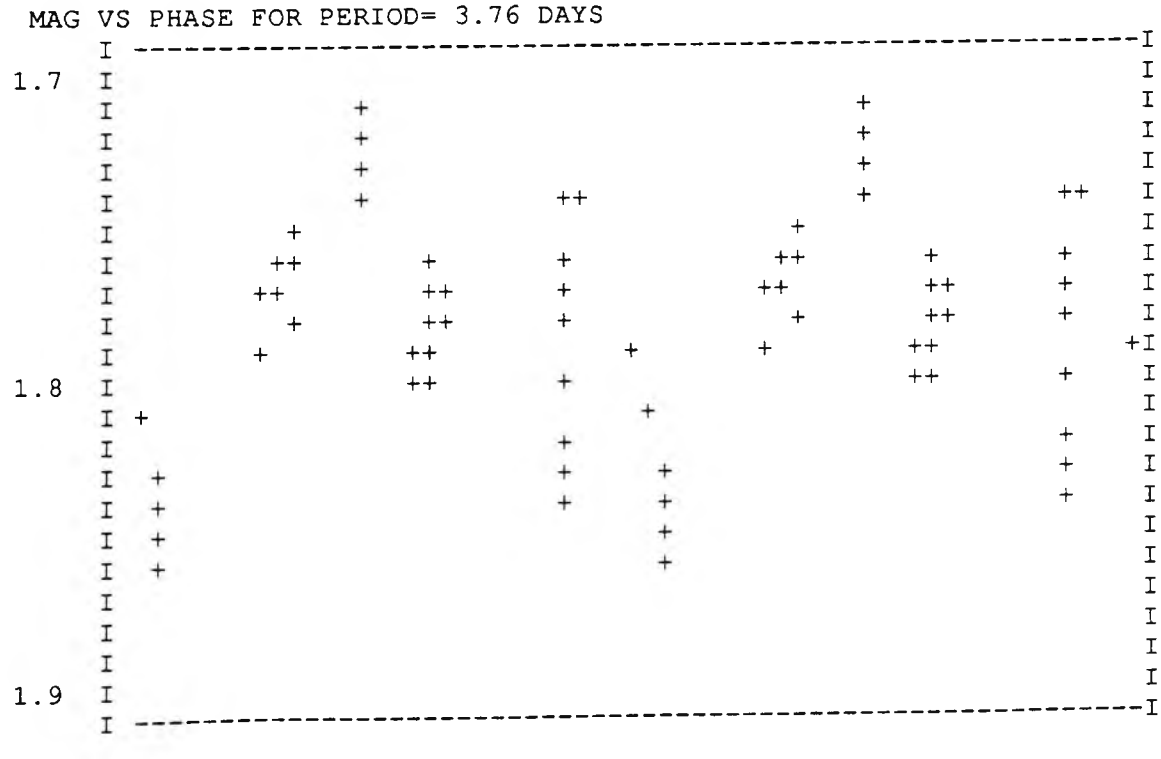

John. B Filter

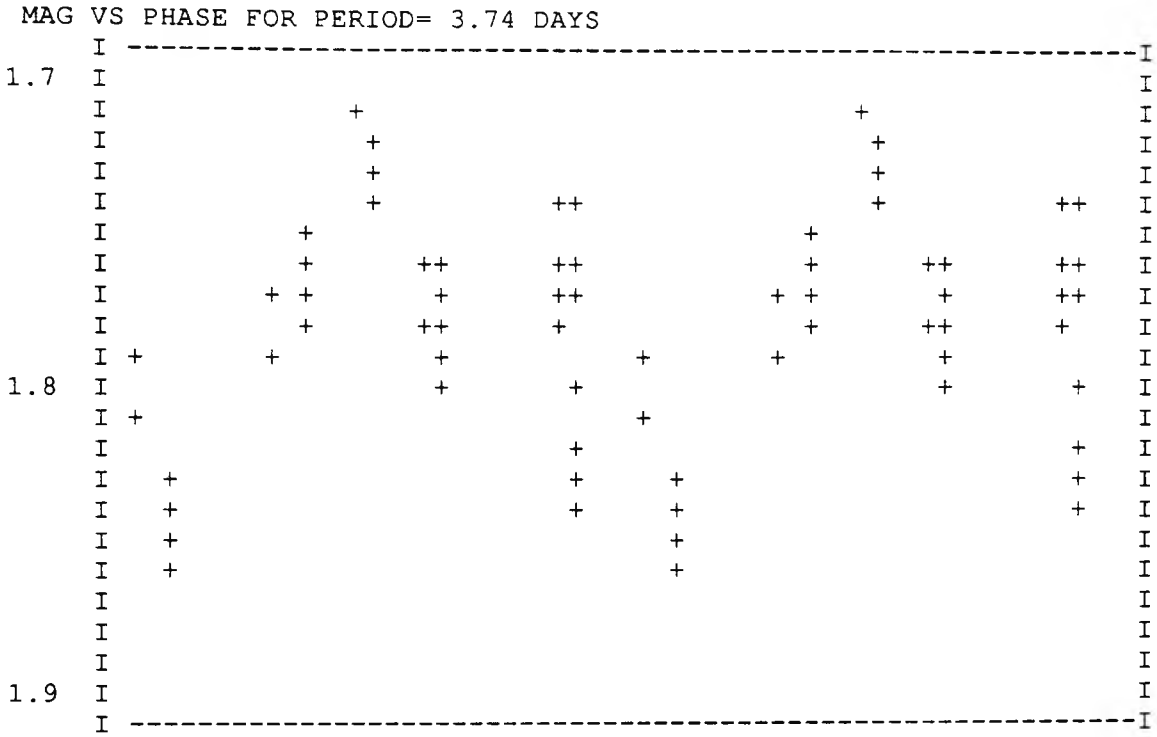

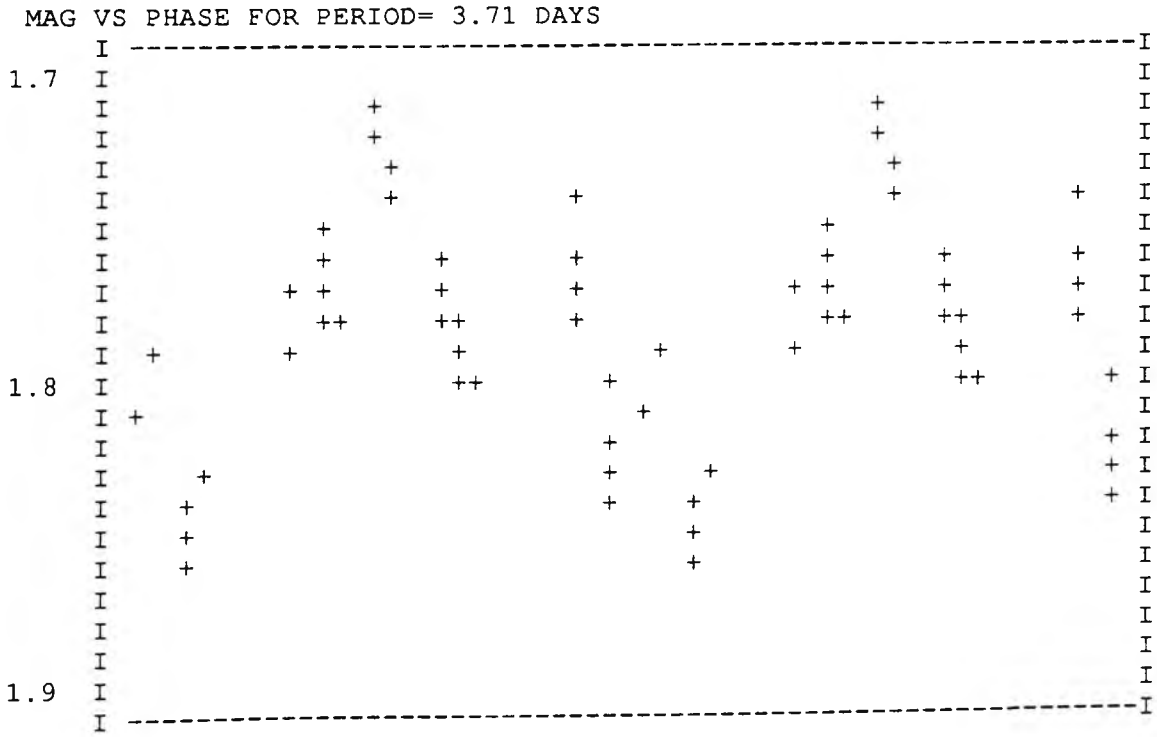

John. B Filter

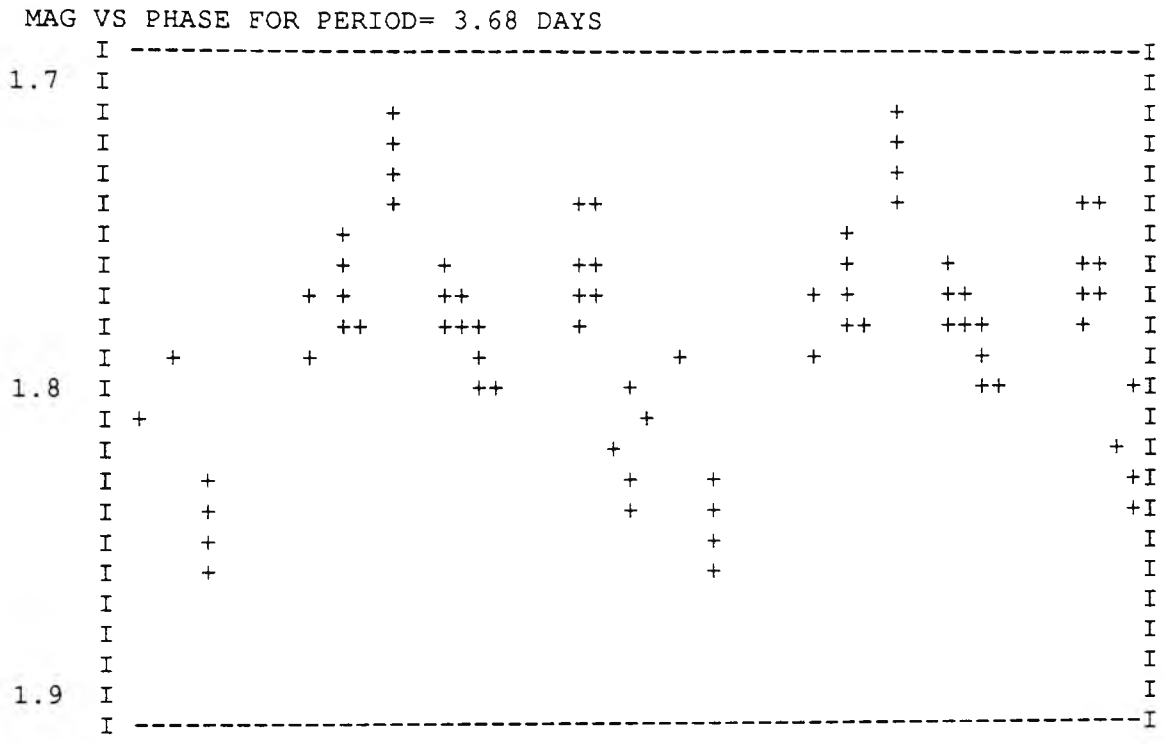

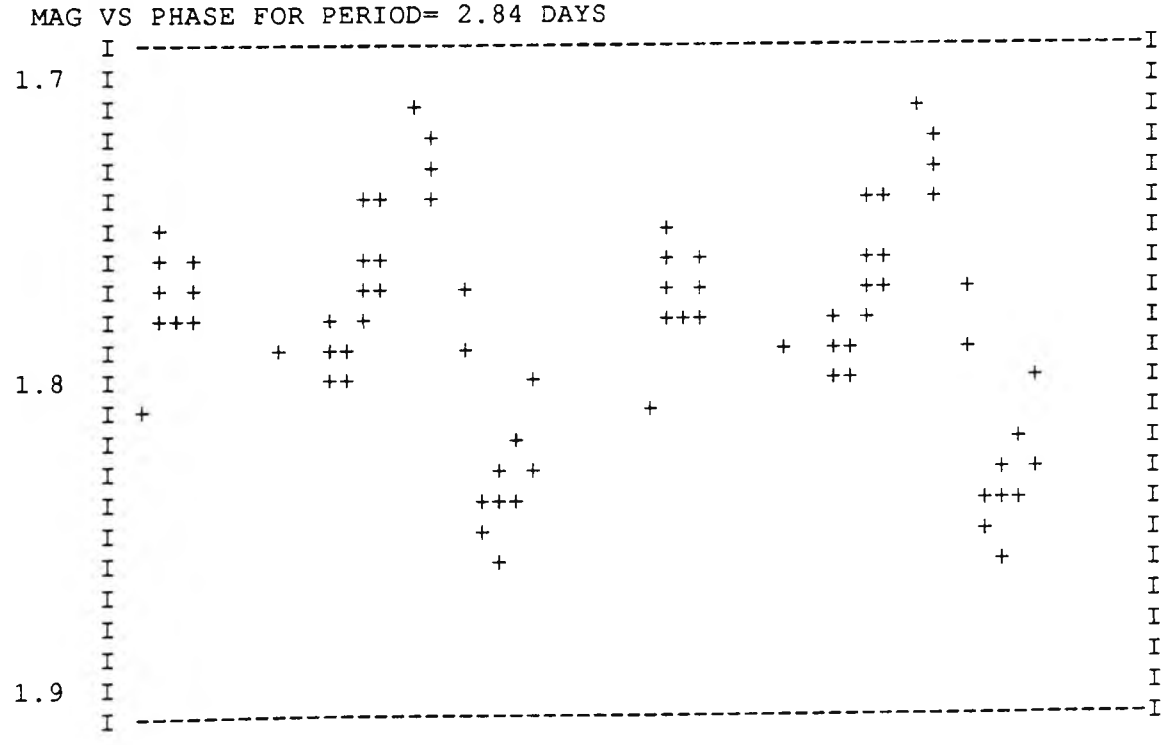

John. B Filter

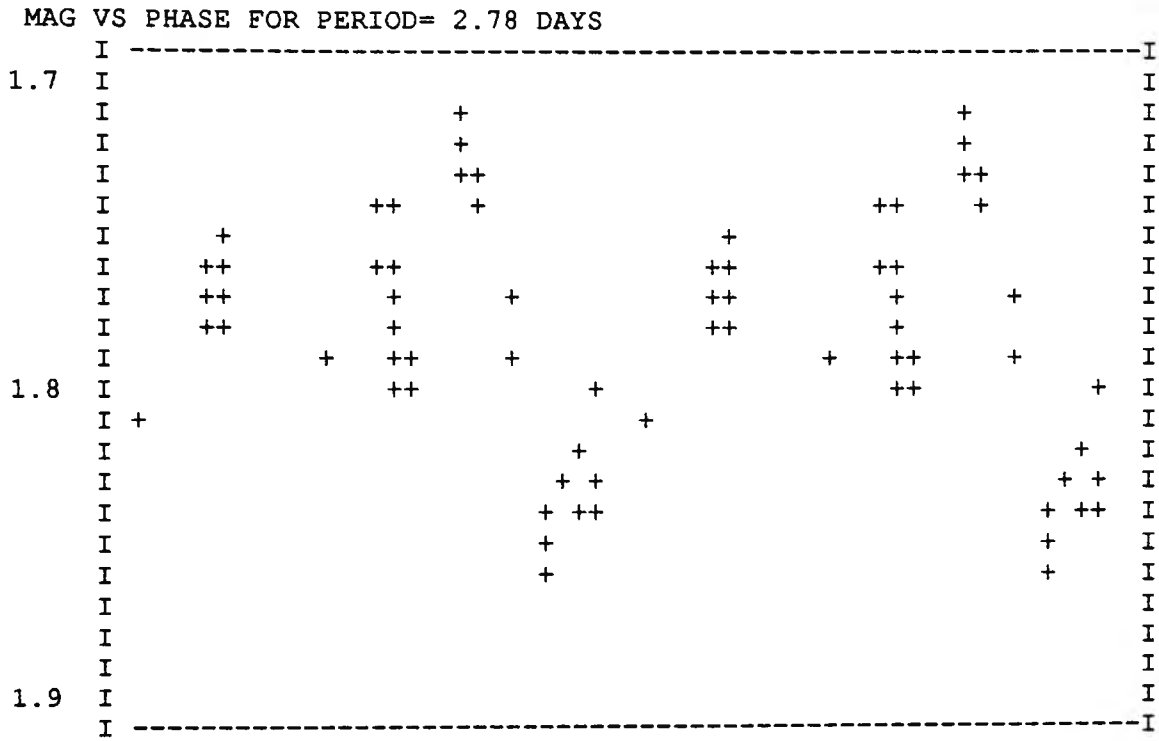

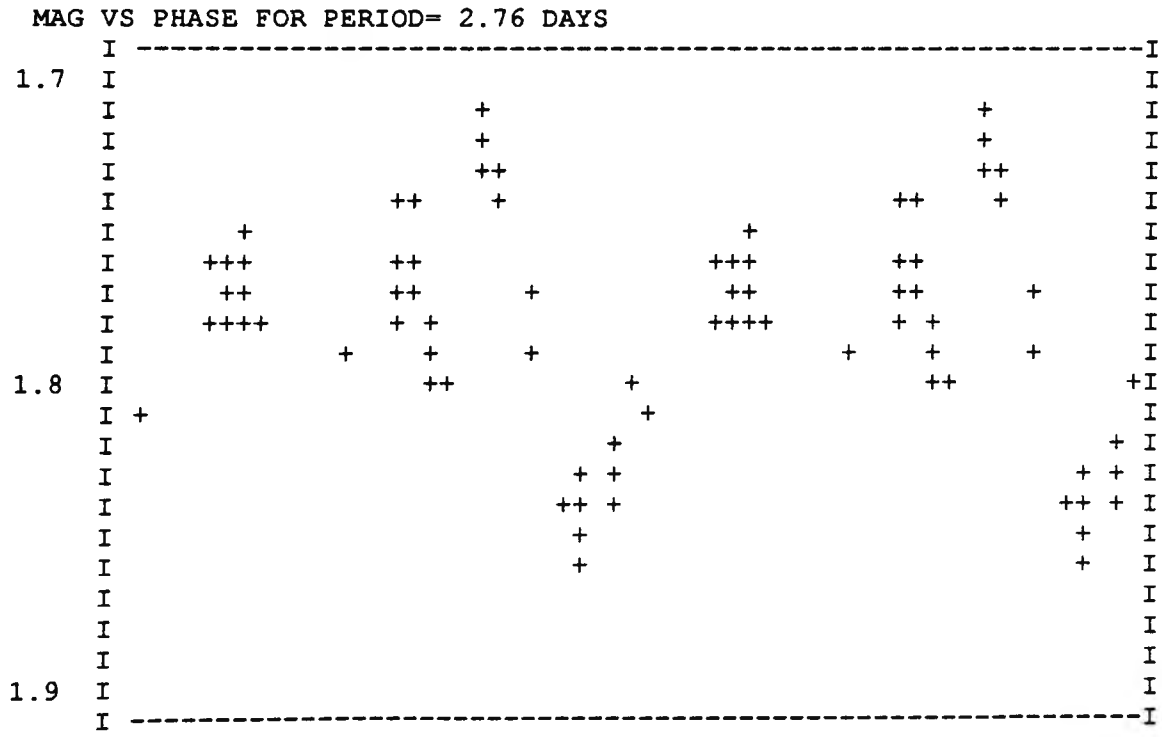

John. B Filter

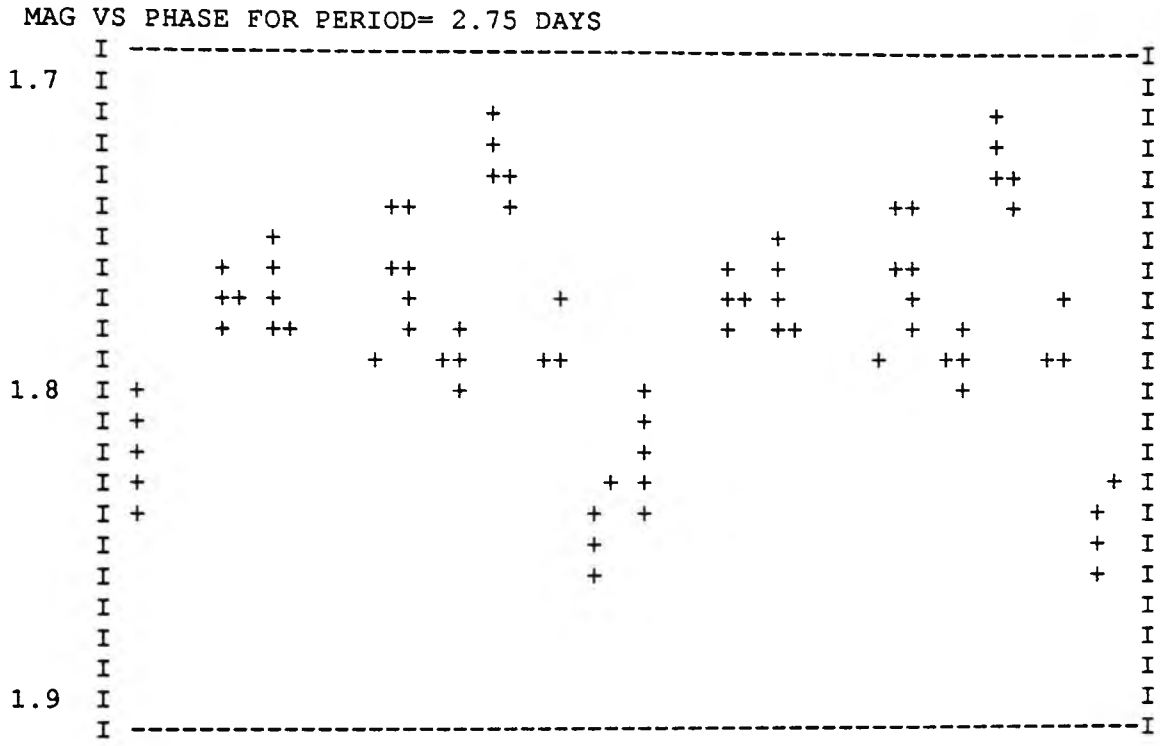

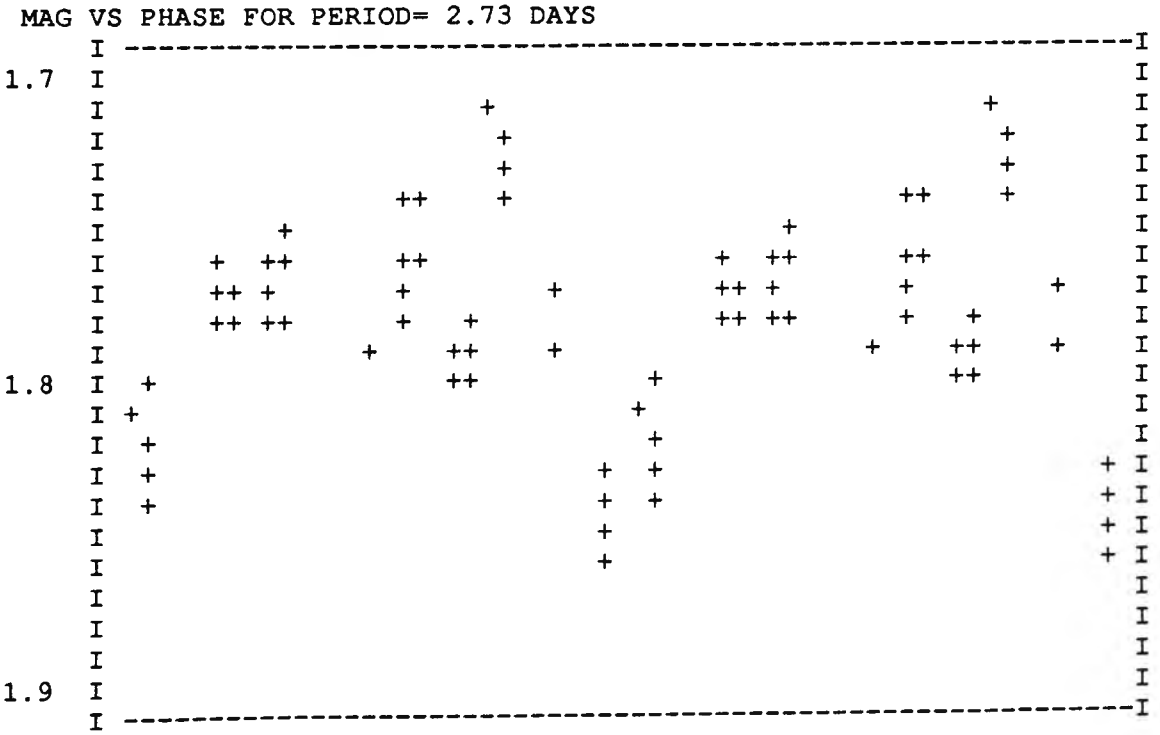

John. B Filter

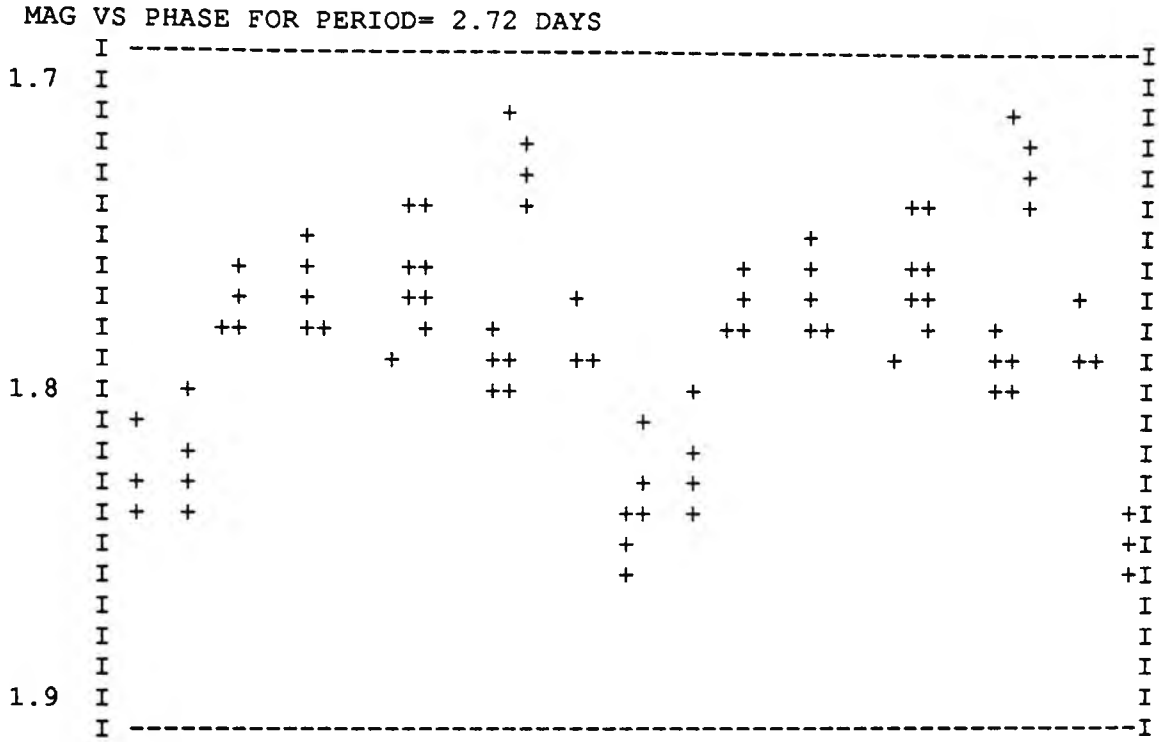

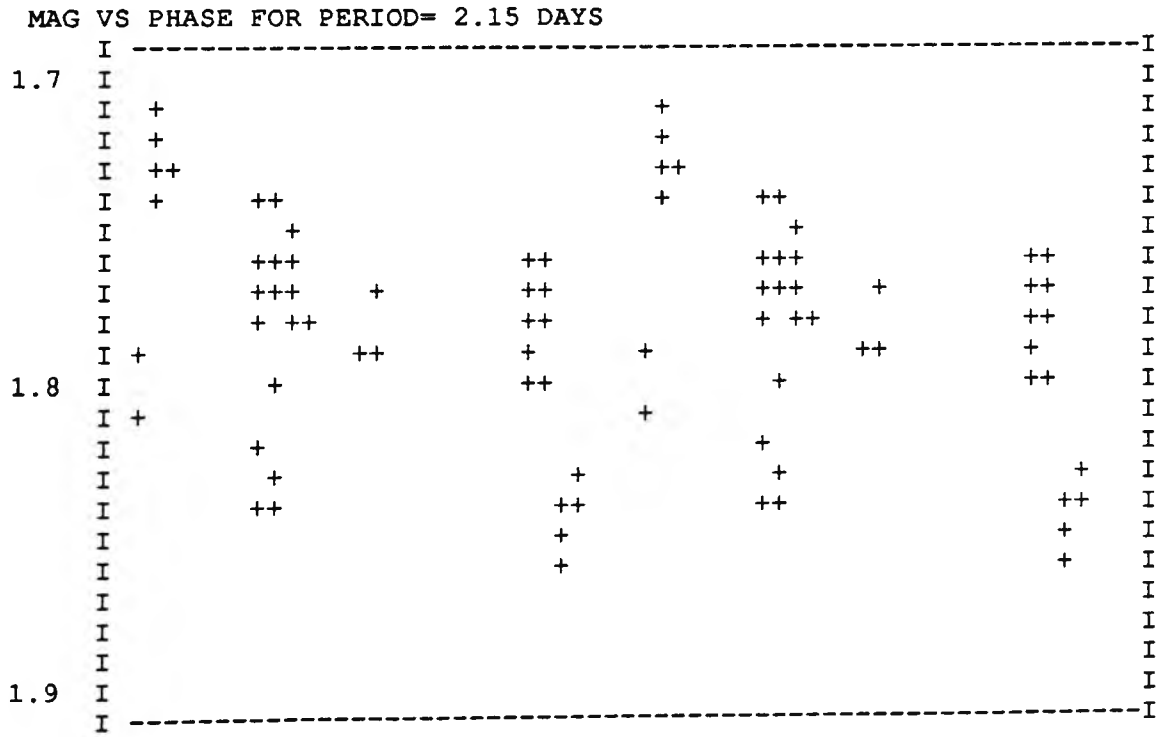

John. B Filter

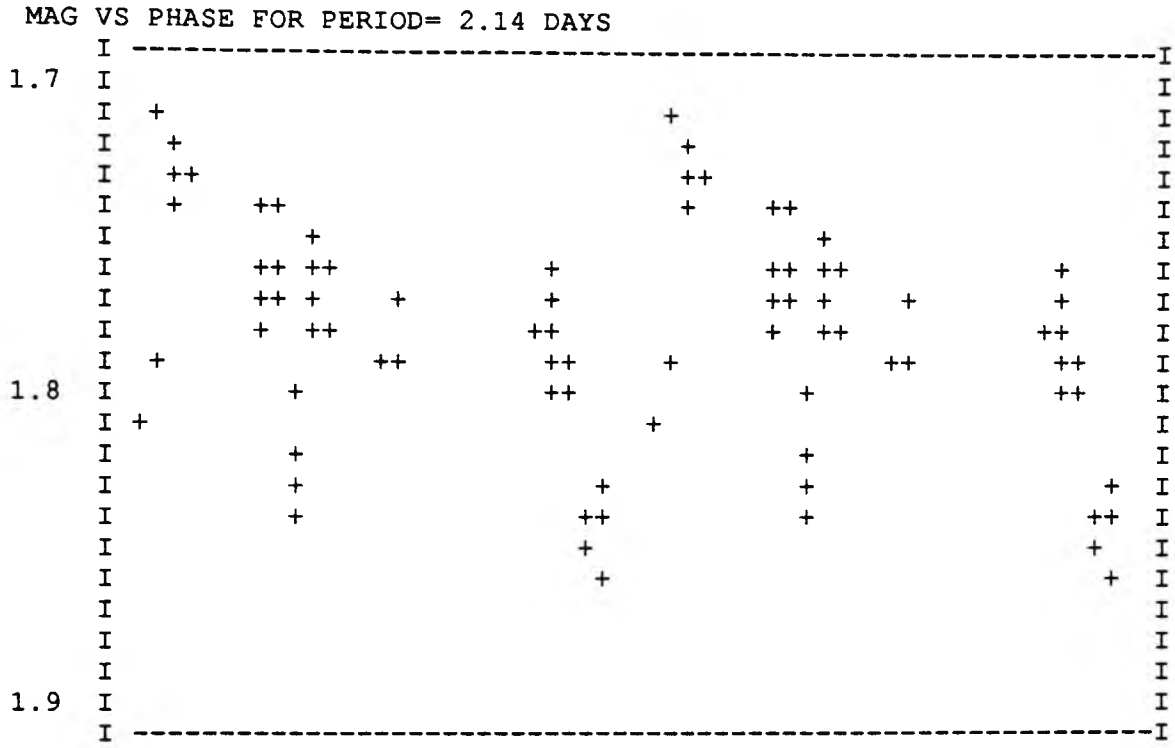

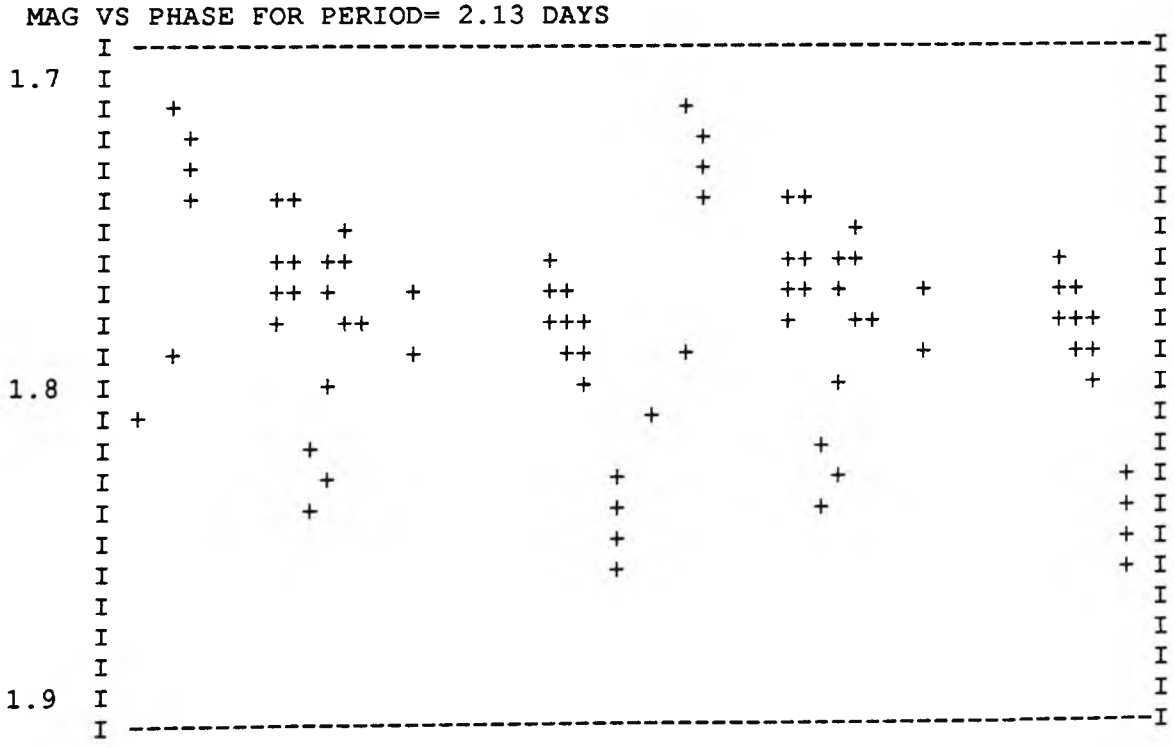

John. B Filter

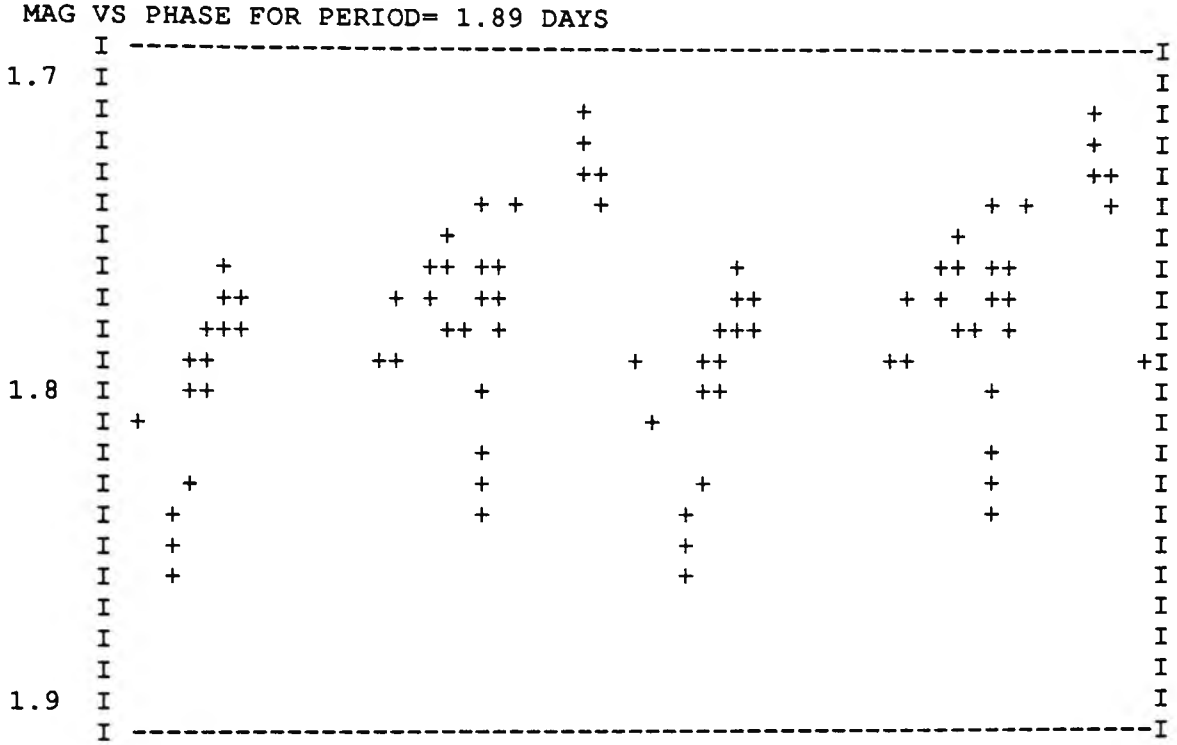

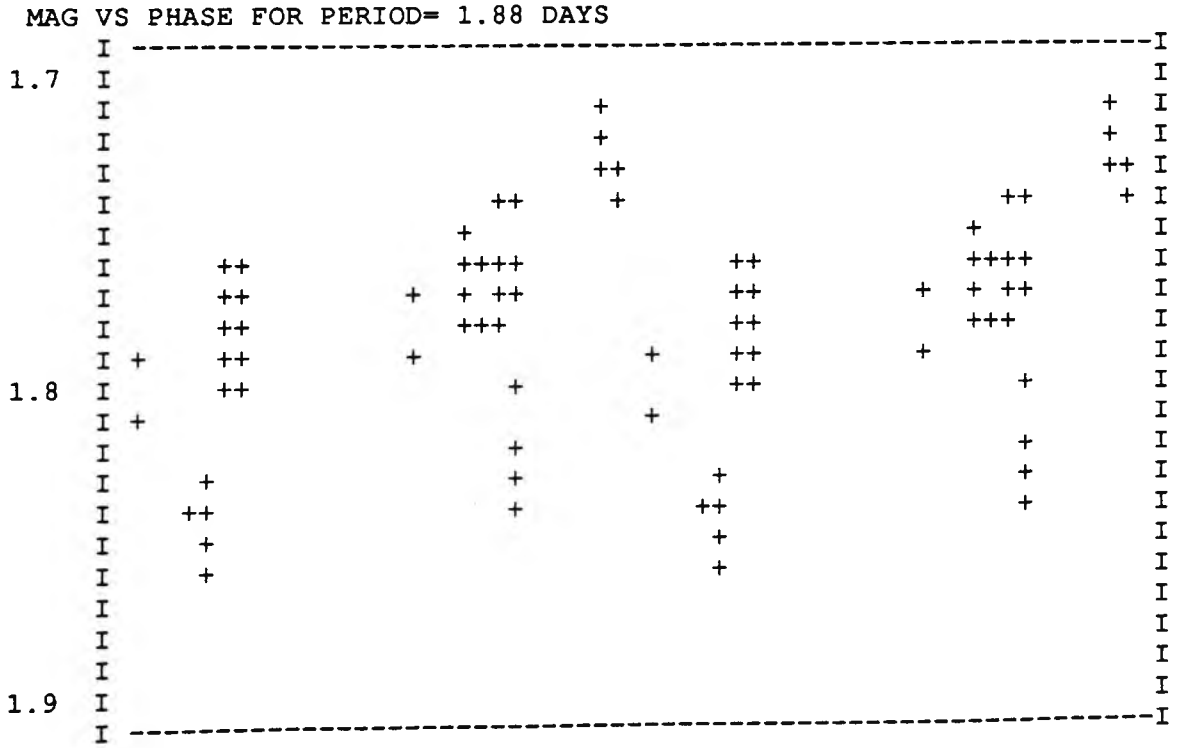

John. B Filter

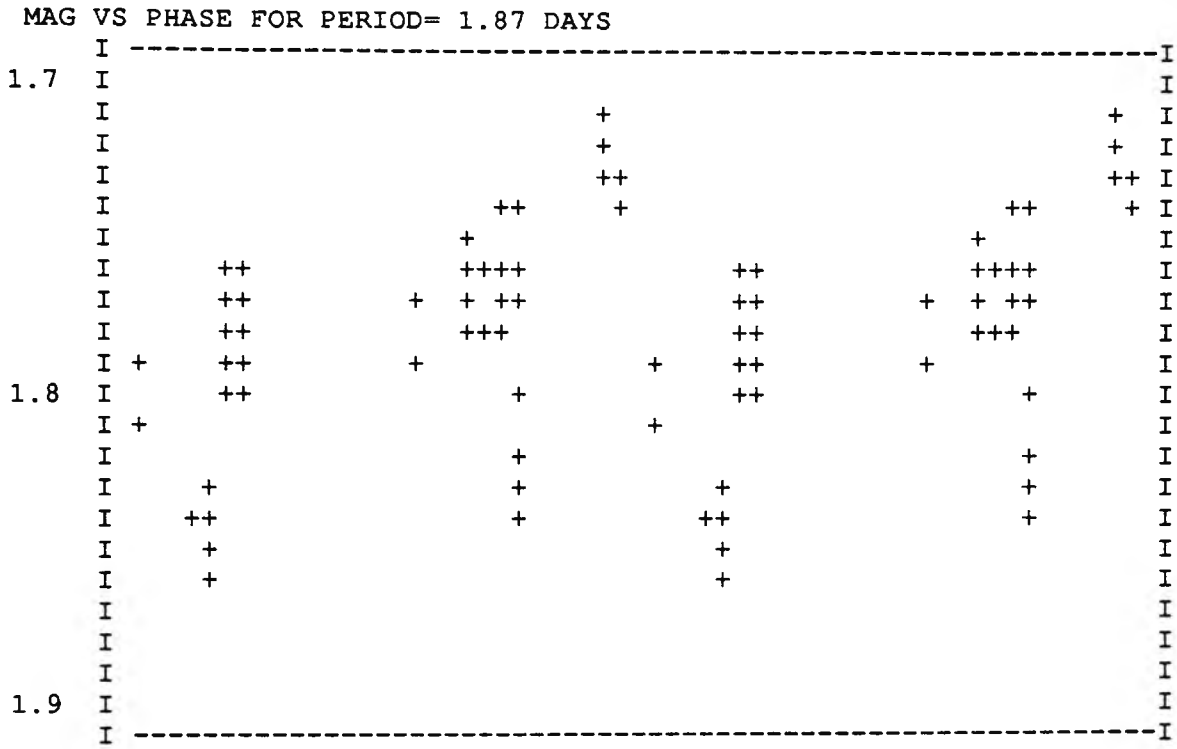

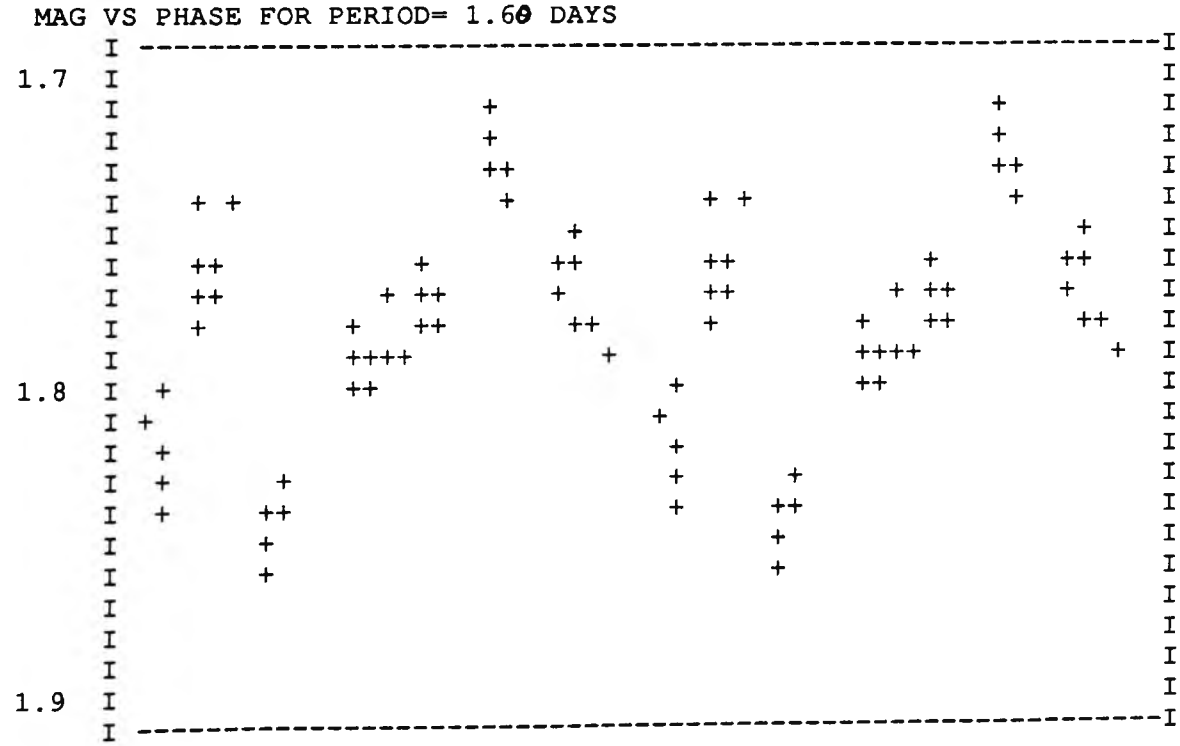

John. B Filter

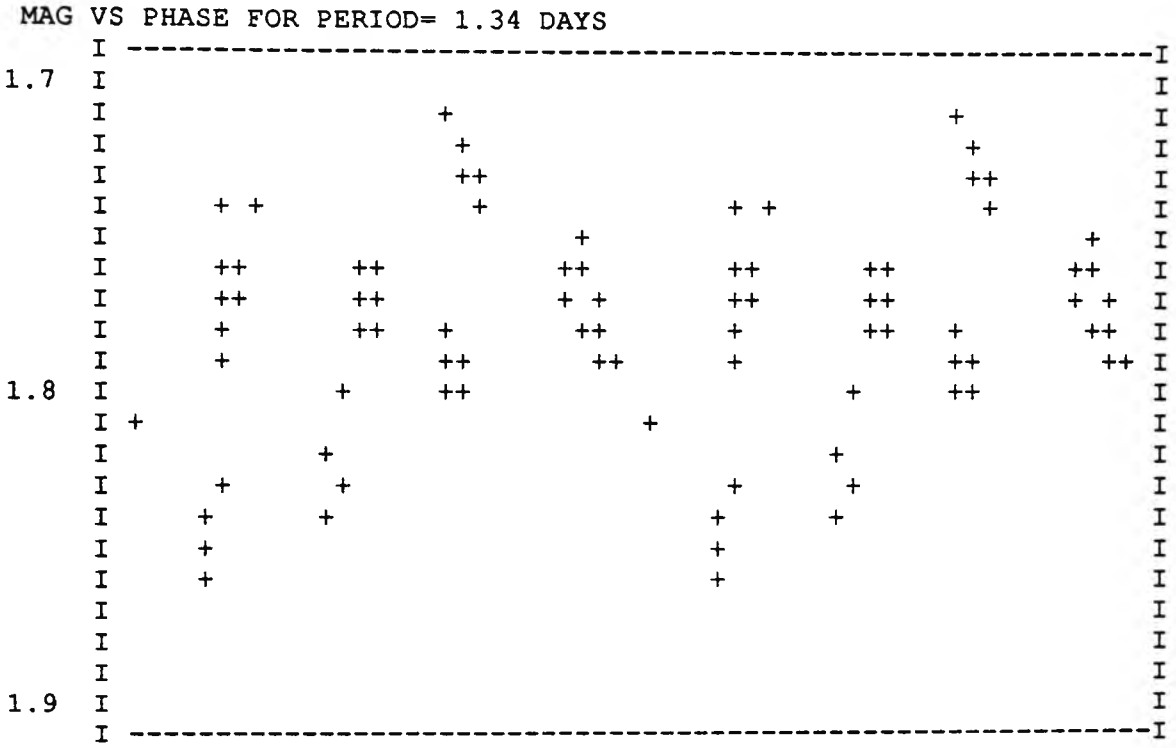

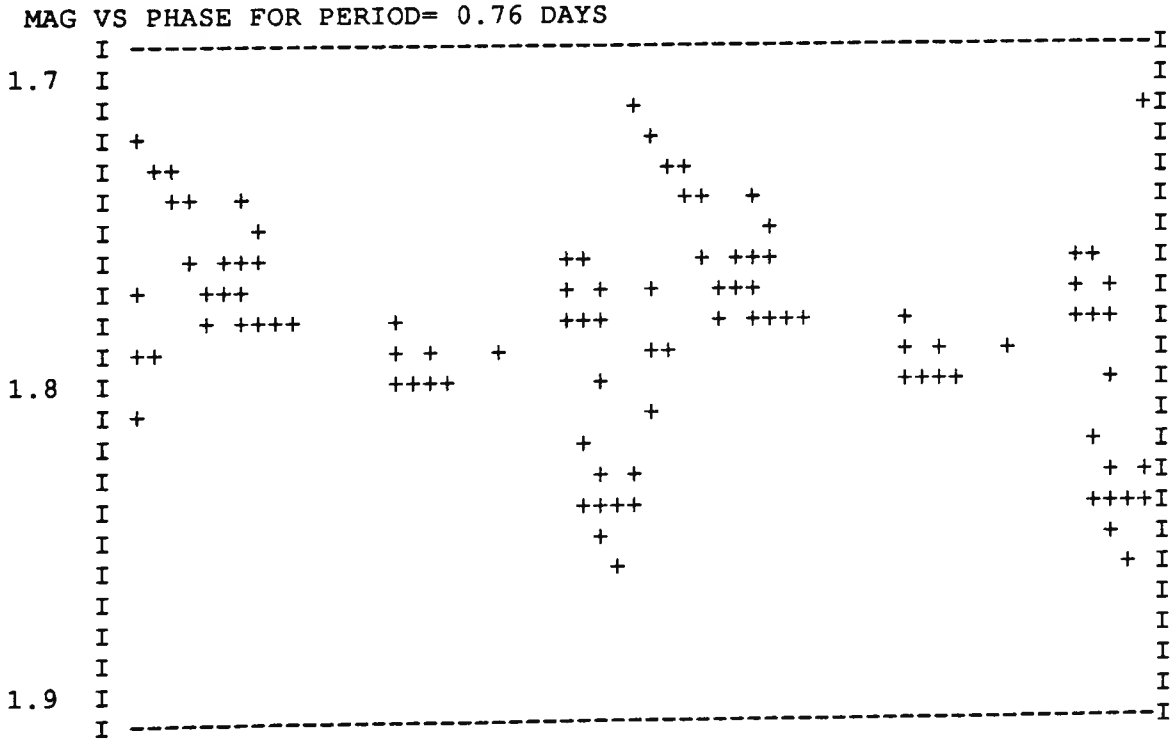

John. B Filter

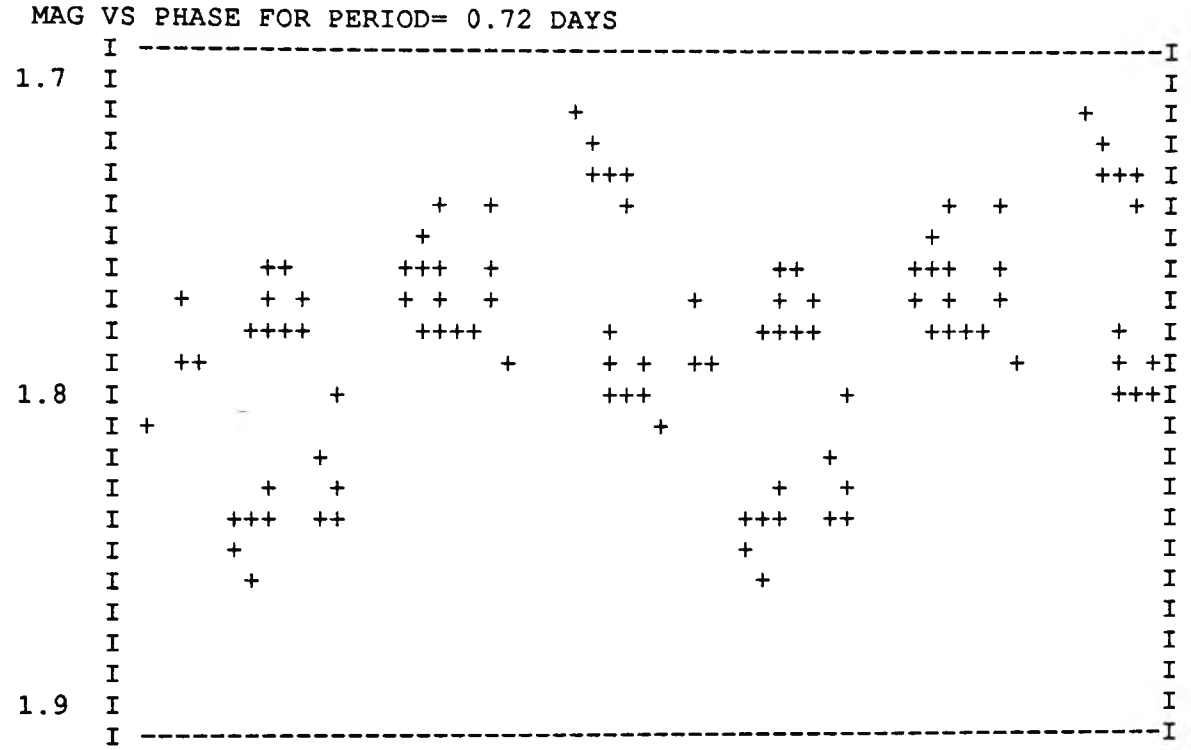

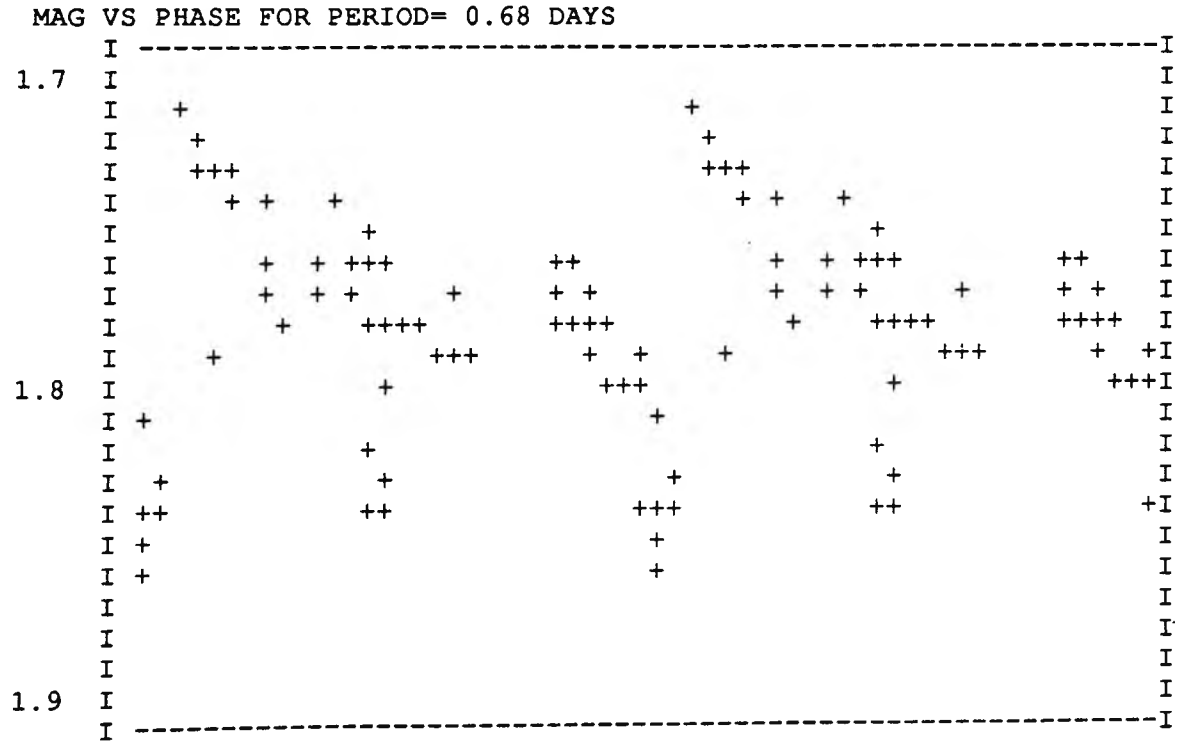

John. B Filter

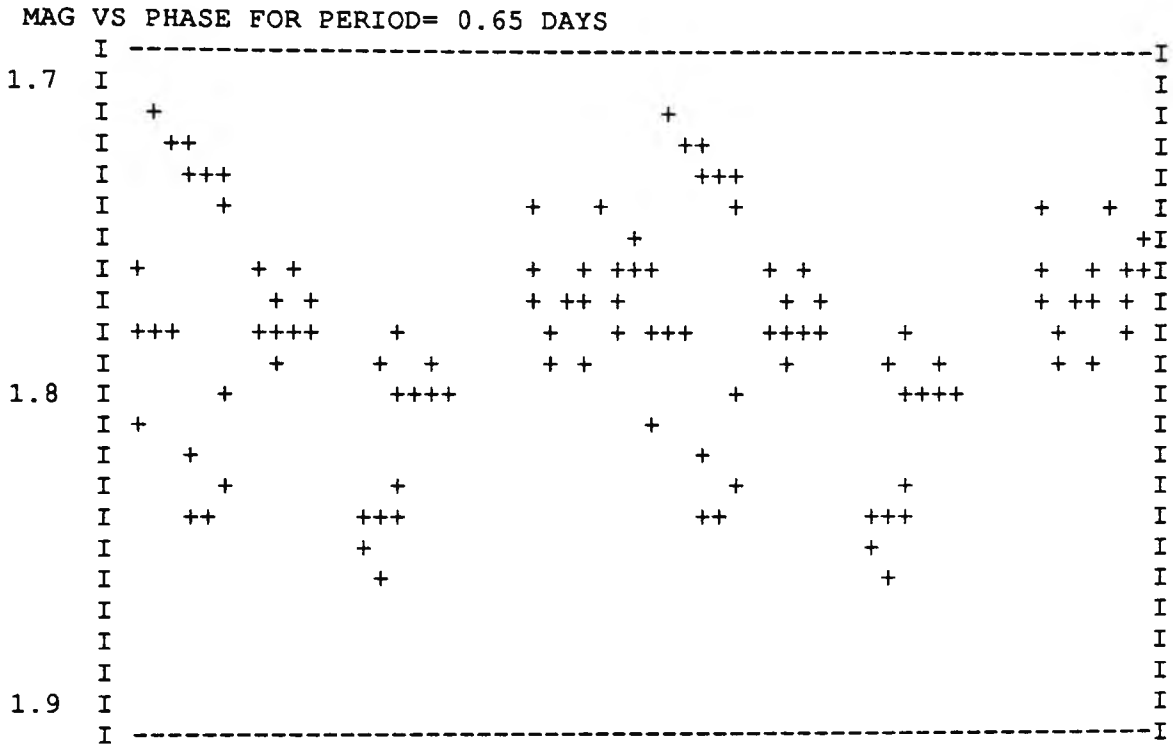

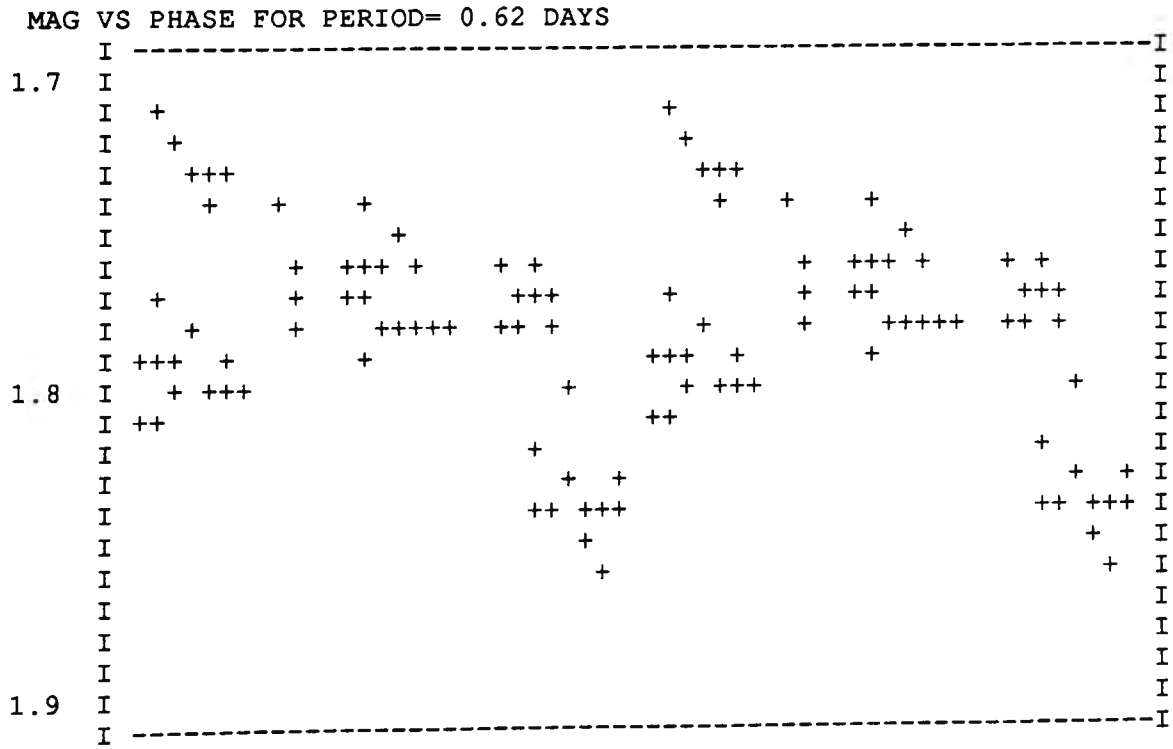

Strom. b Filter

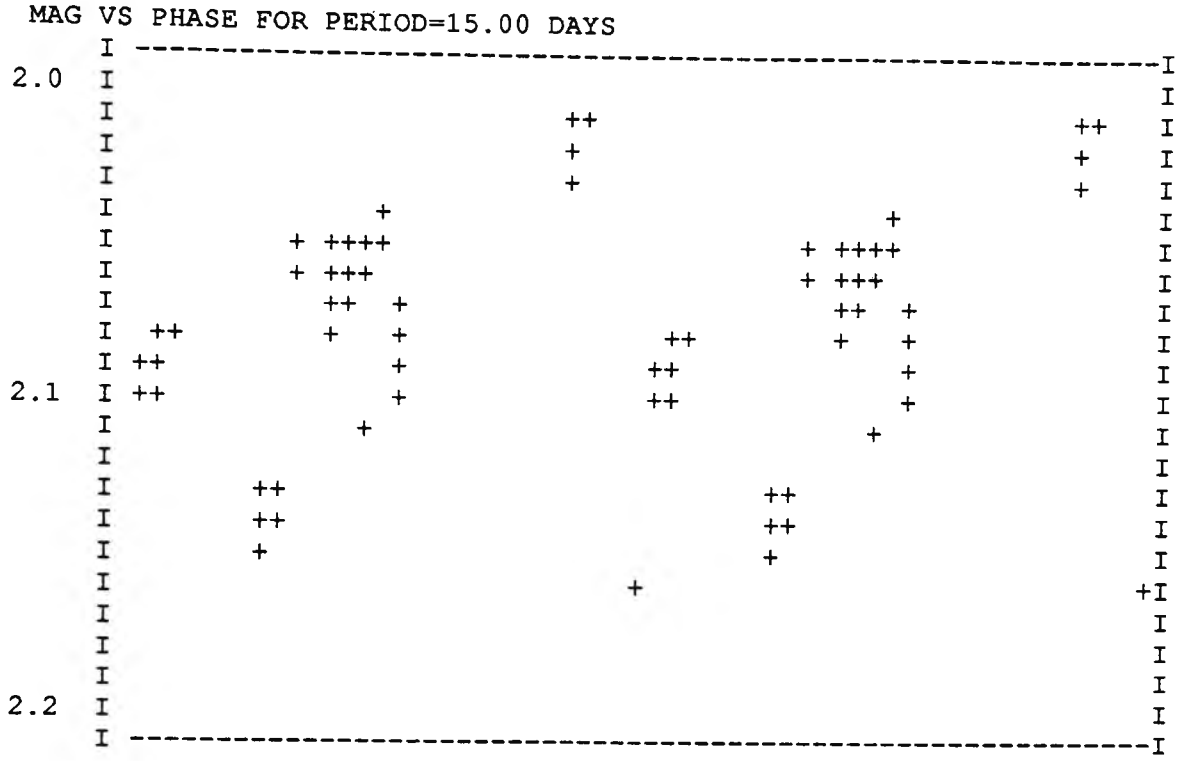

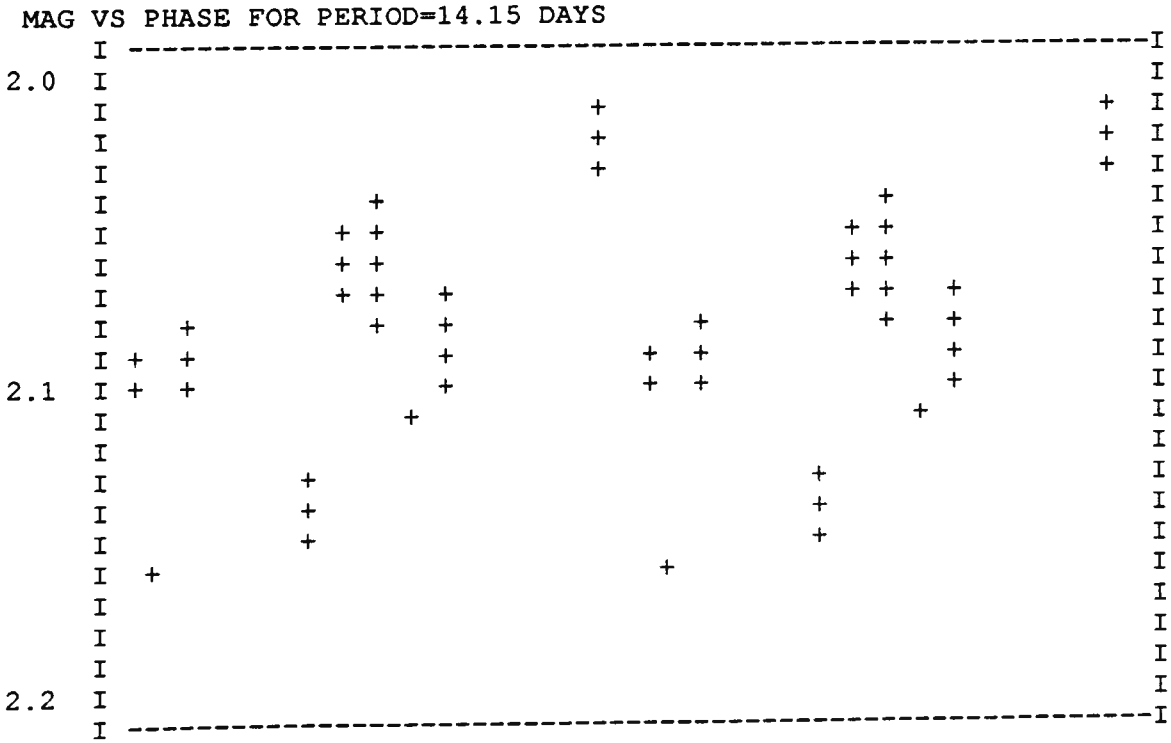

Strom. b Filter

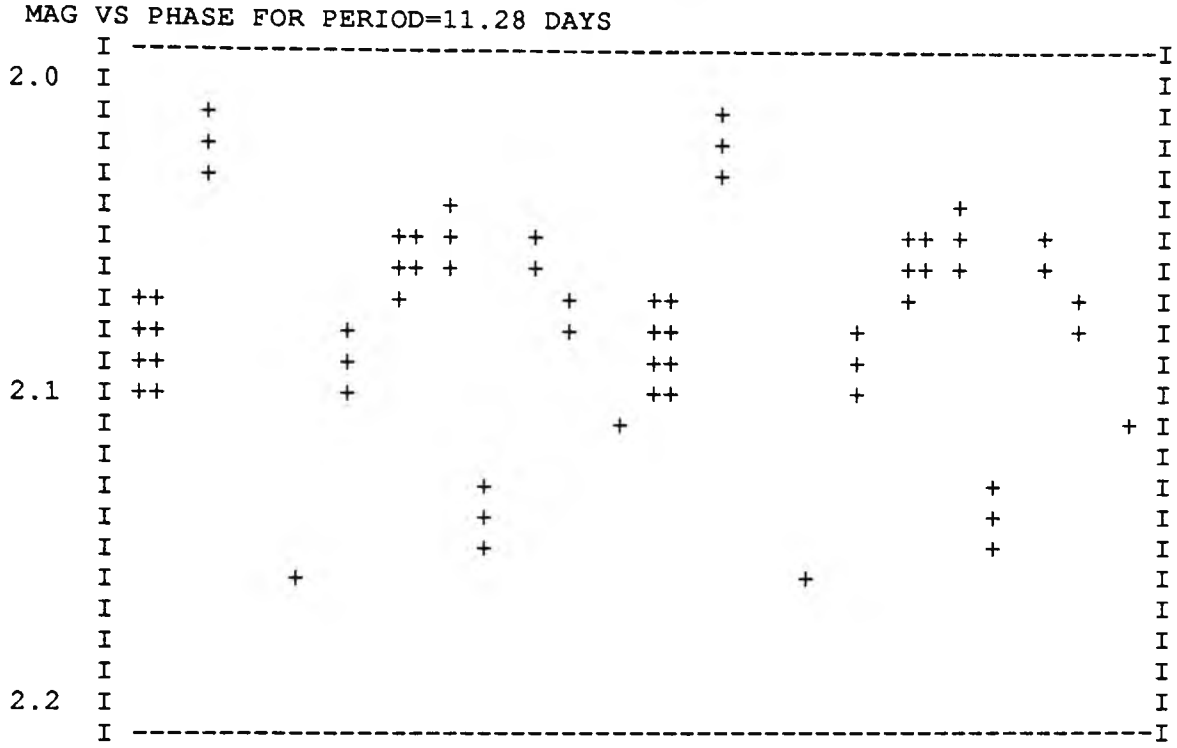

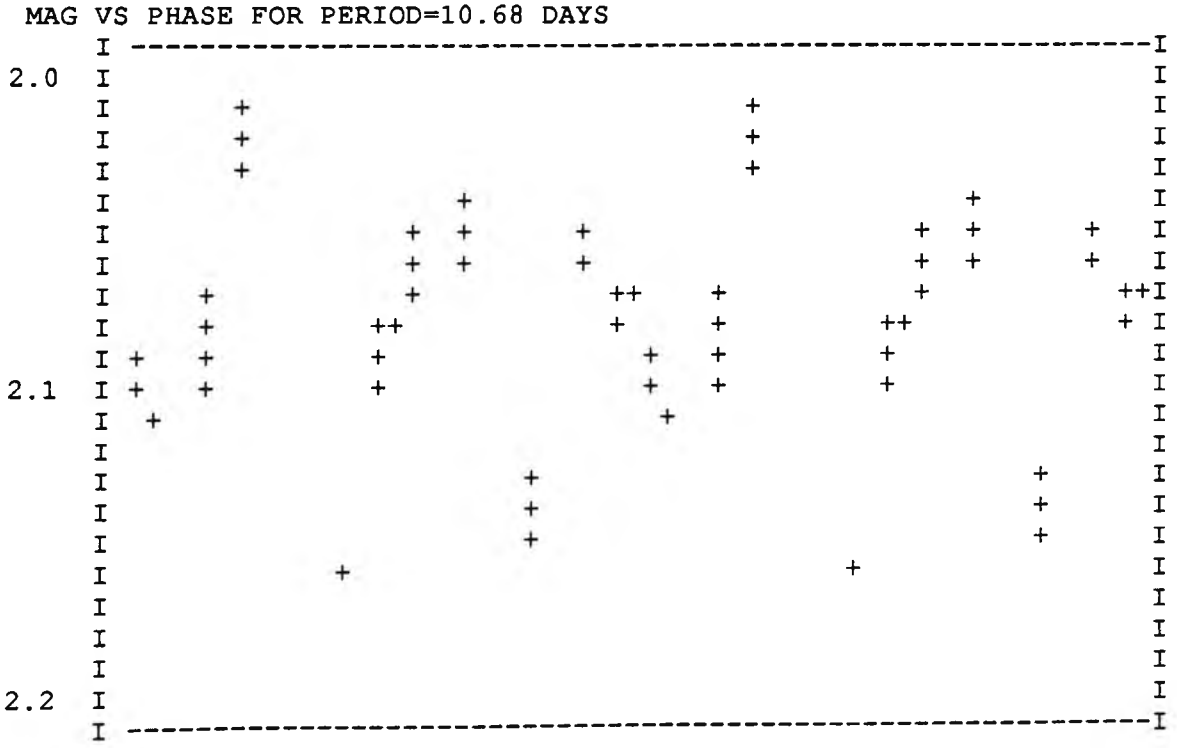

Strom. b Filter

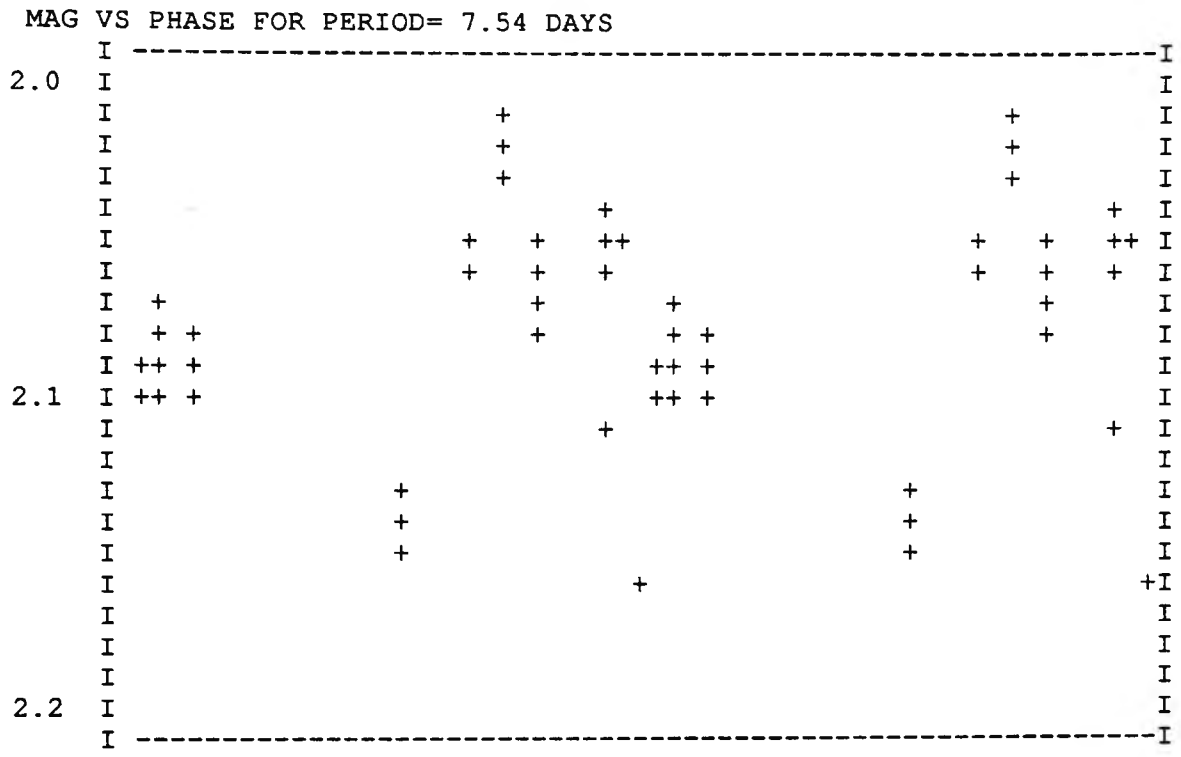

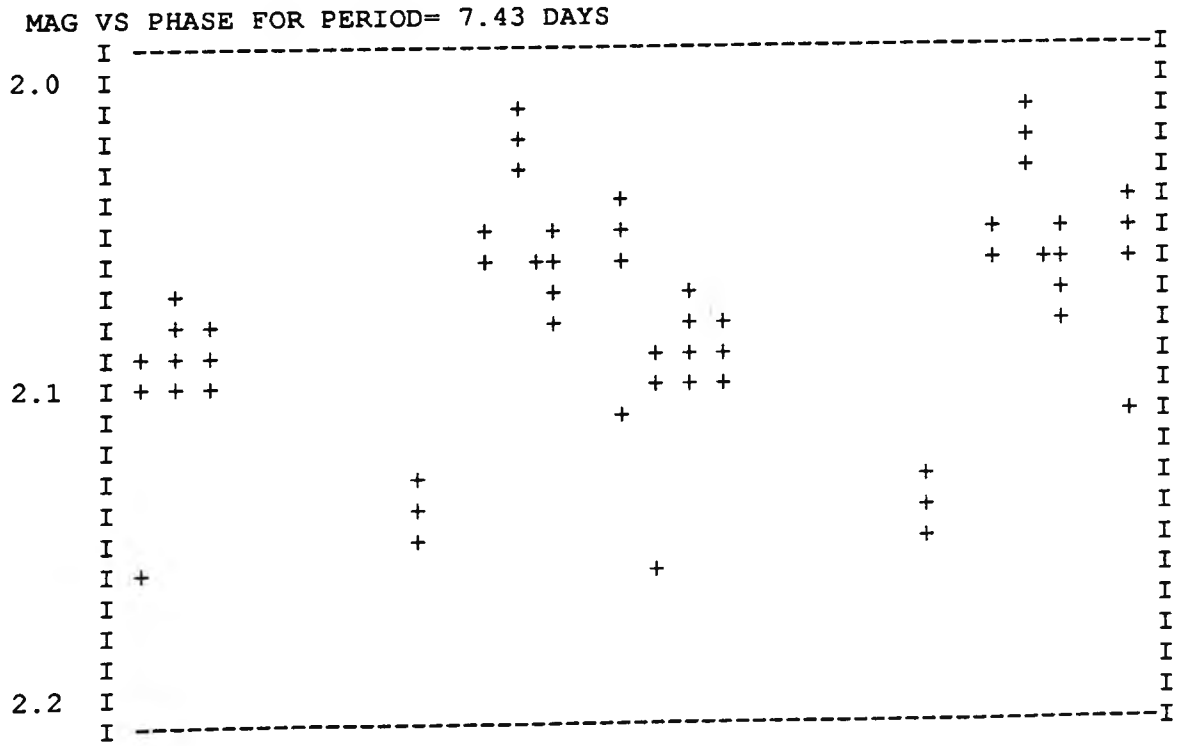

Strom. b Filter

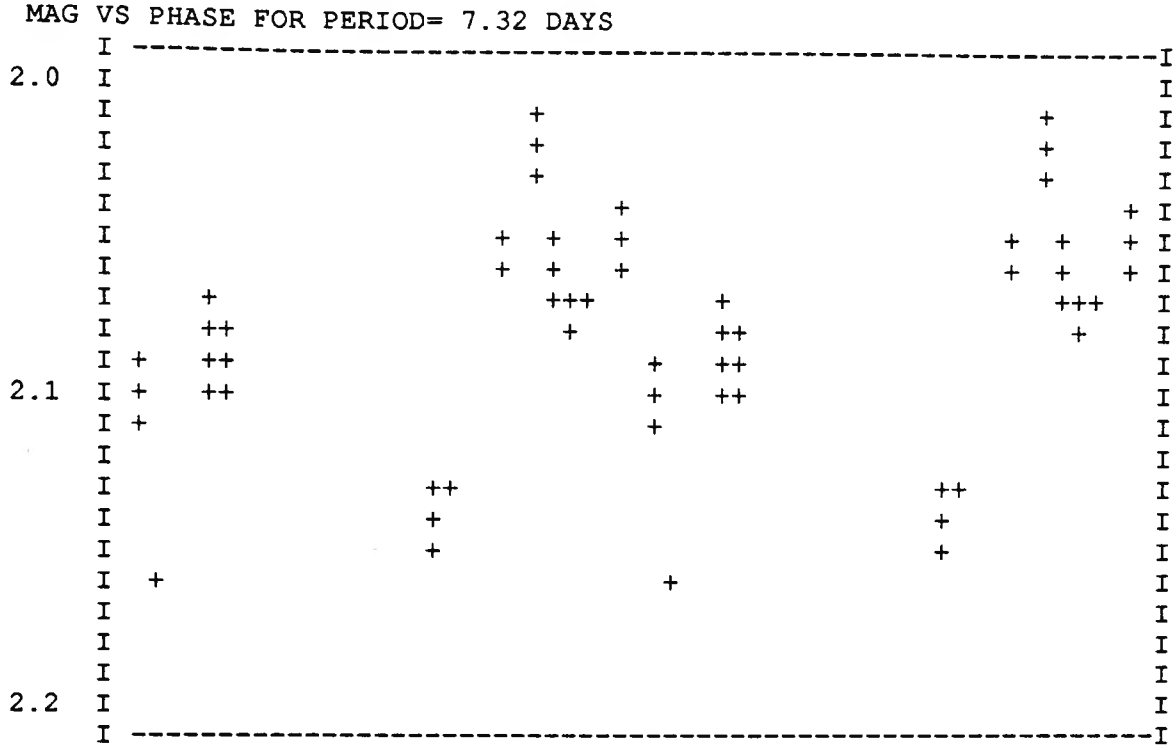

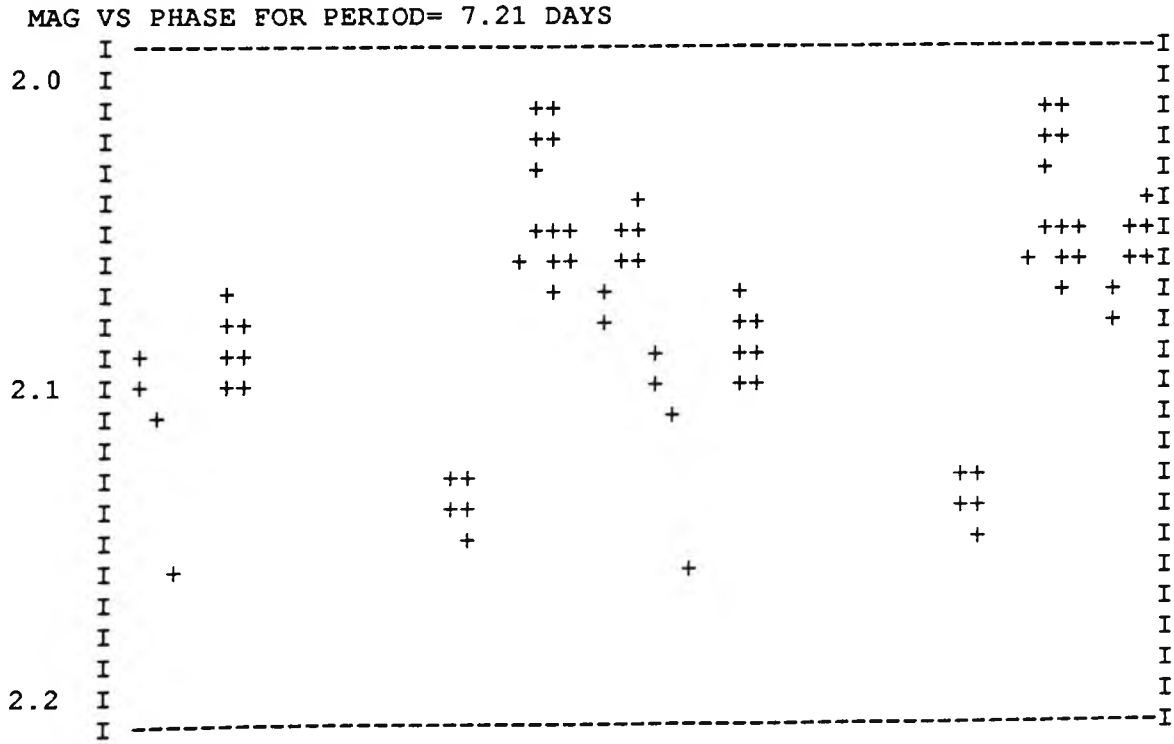

Strom. b Filter

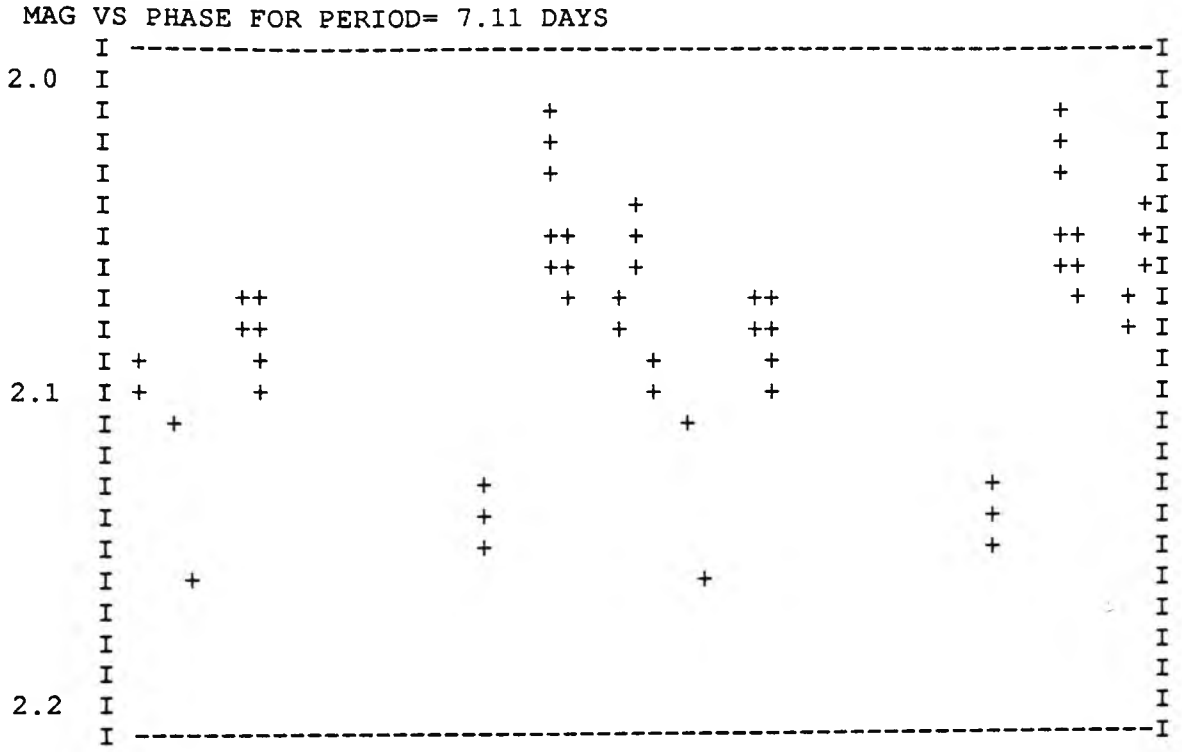

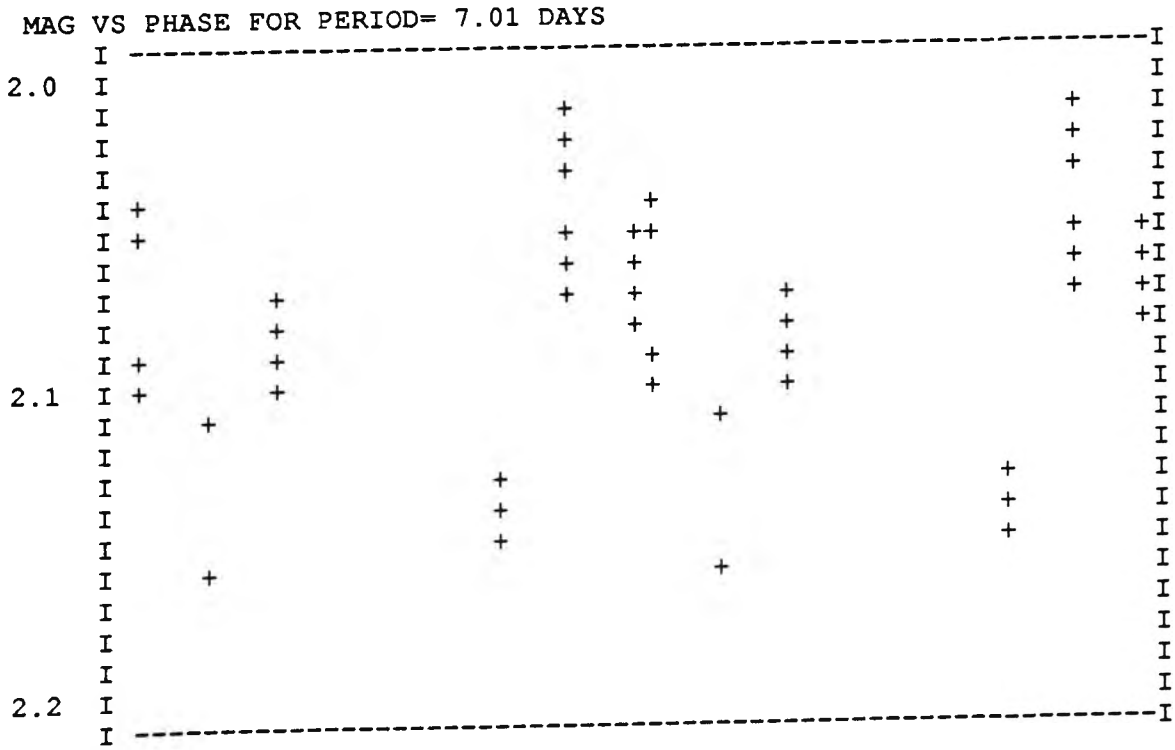

Strom. b Filter

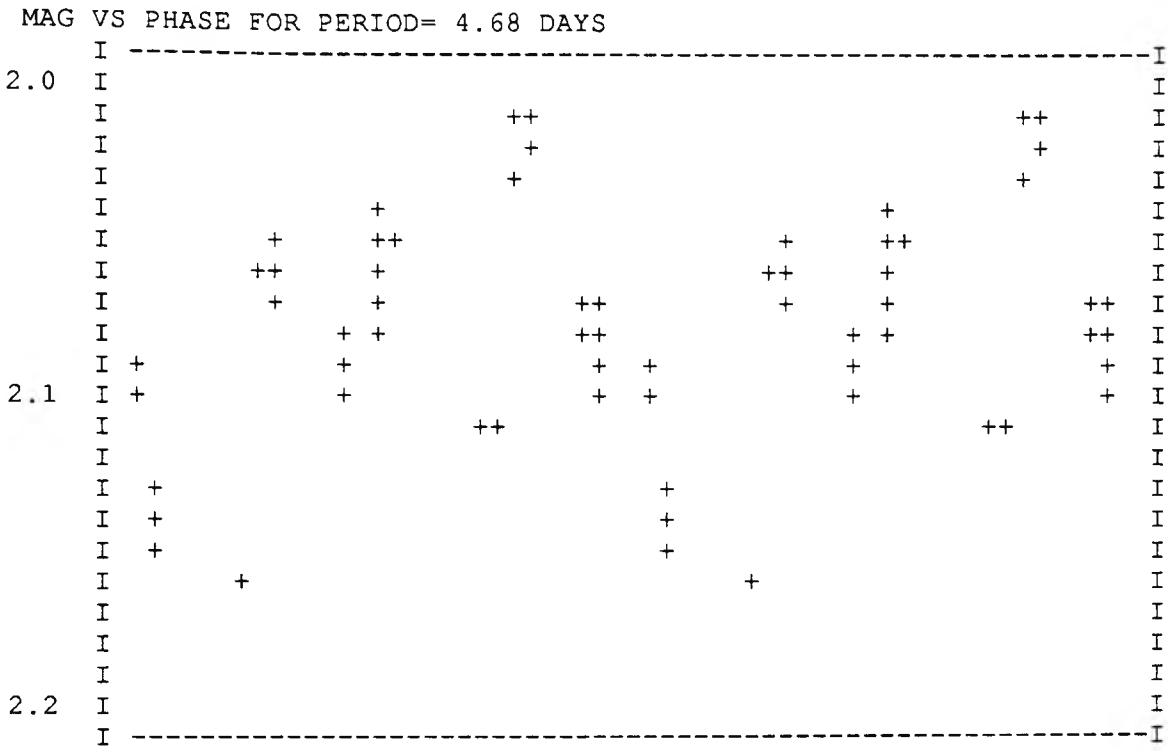

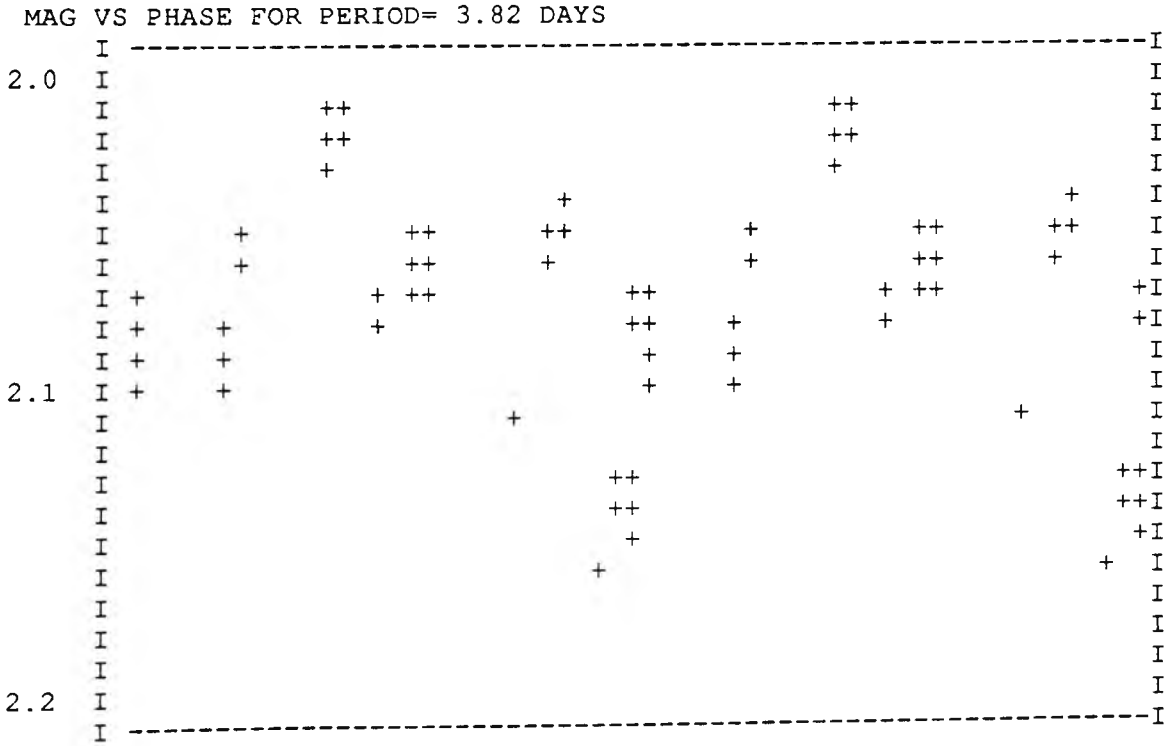

Strom. b Filter

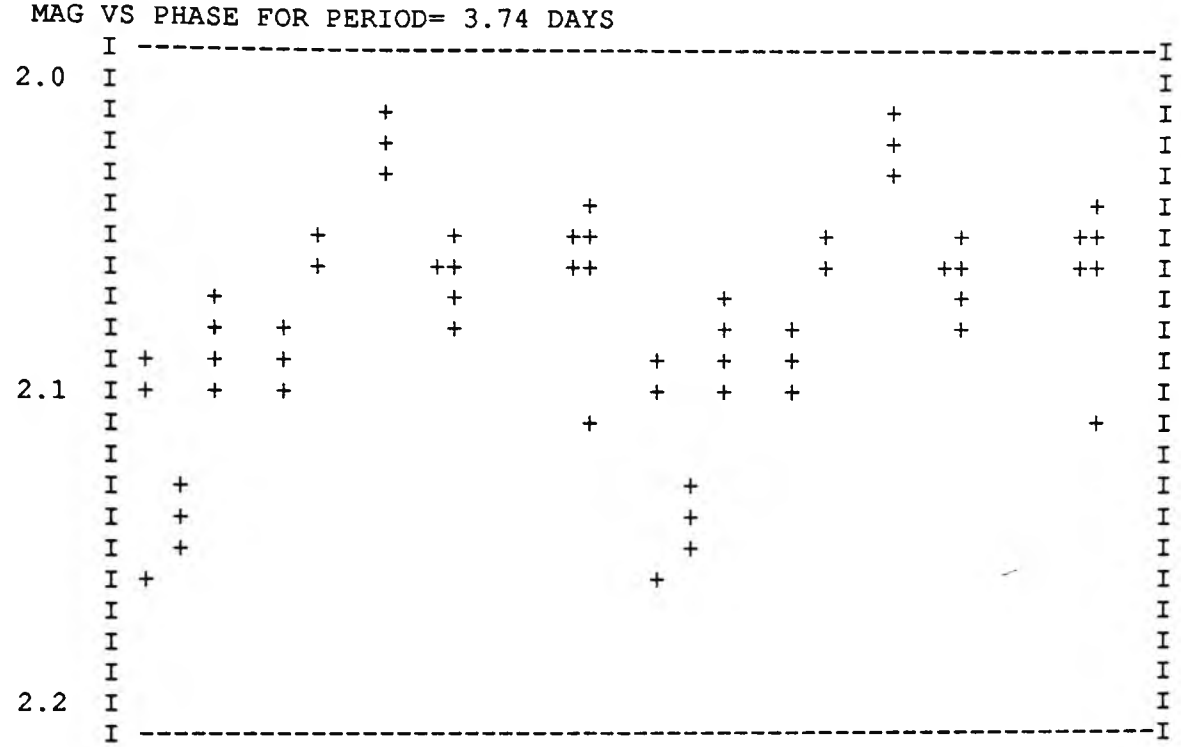

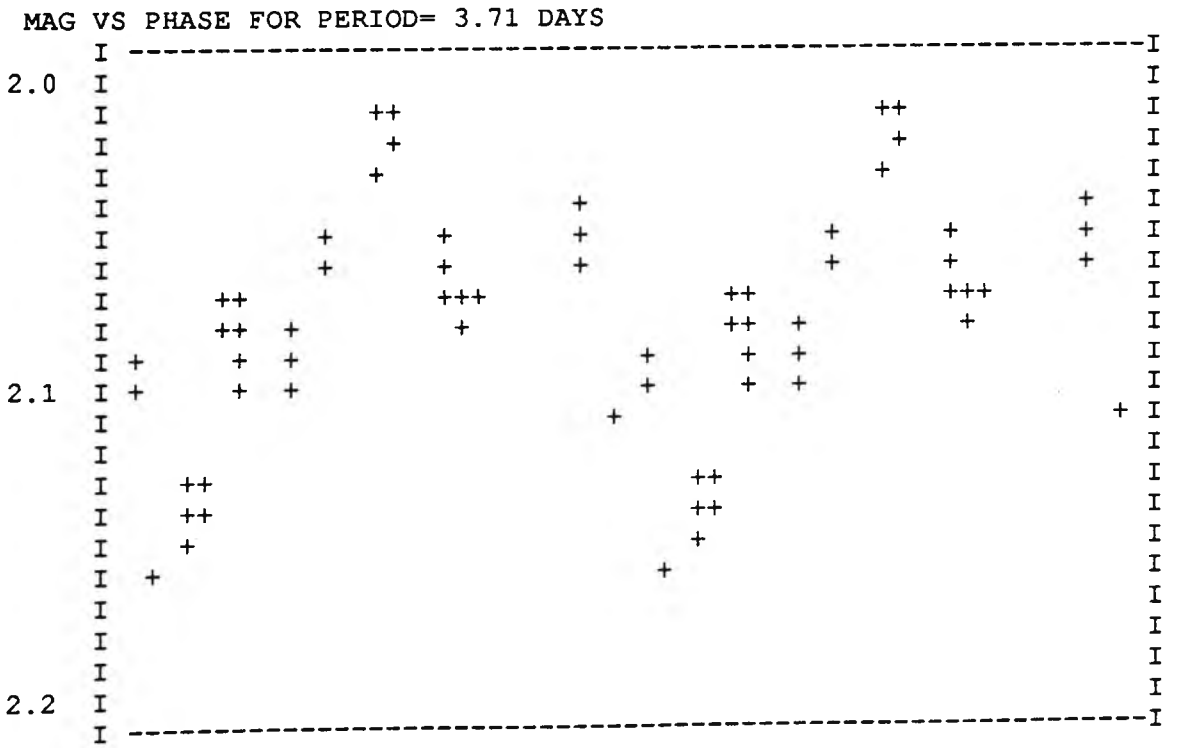

Strom. b Filter

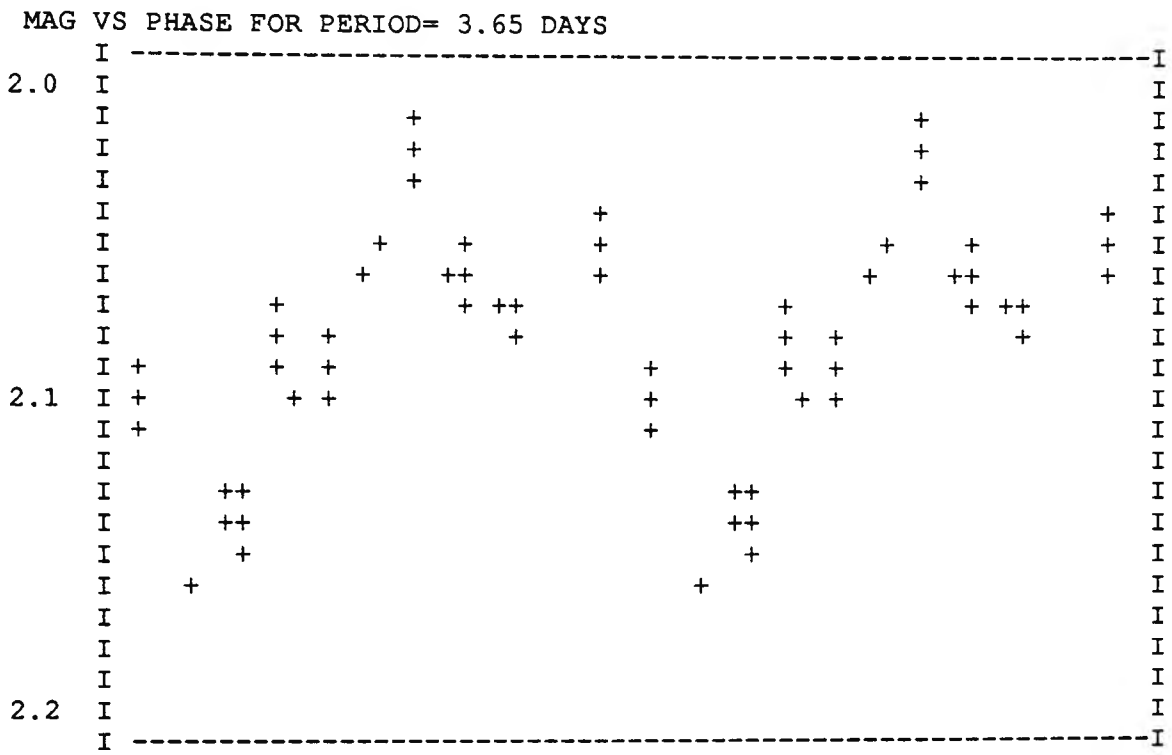

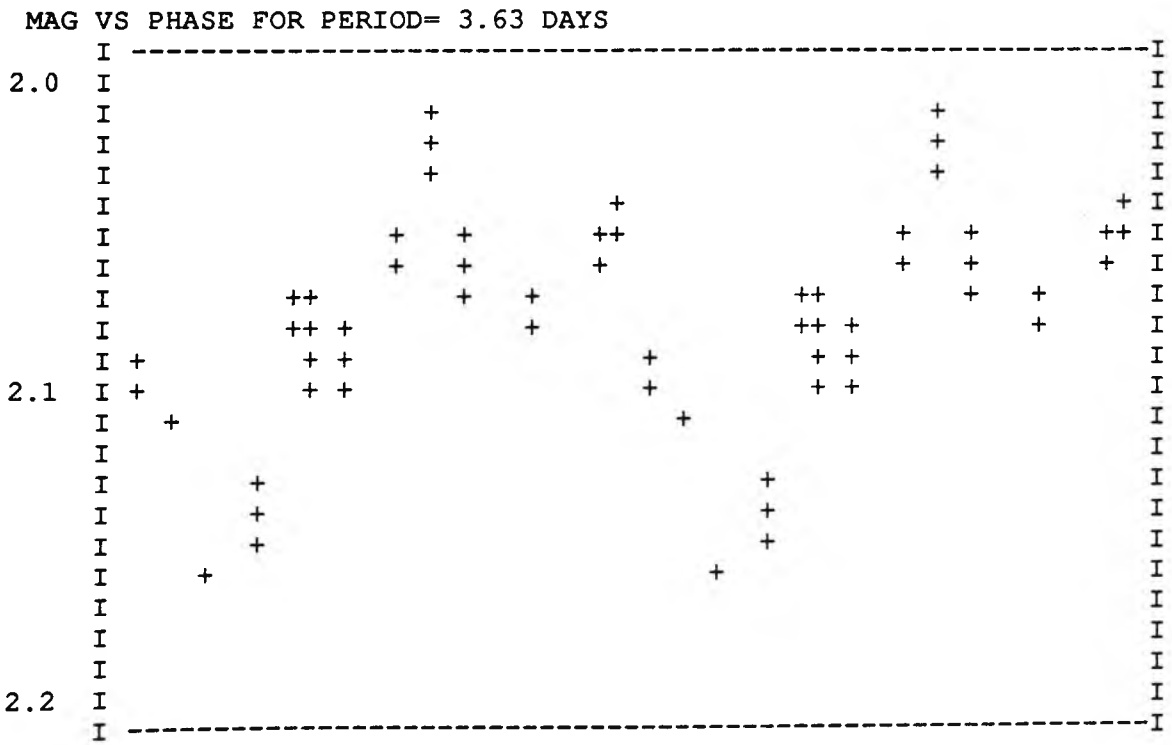

Strom. b Filter

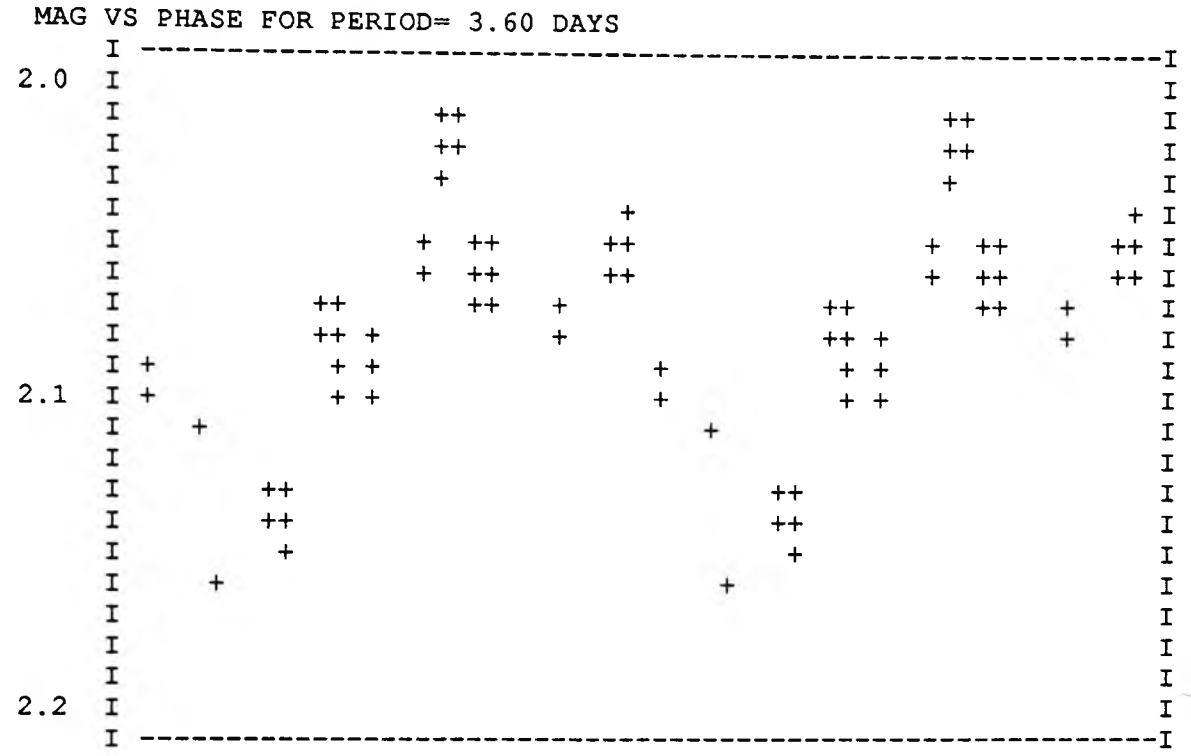

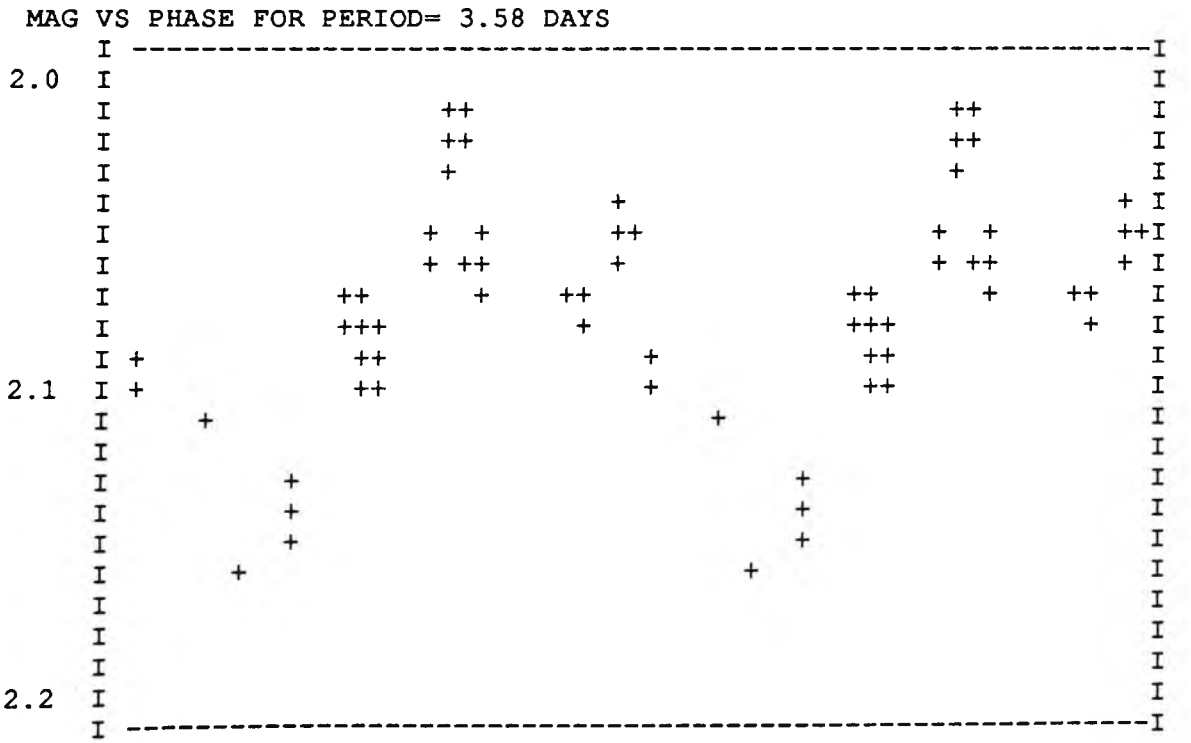

Strom. b Filter

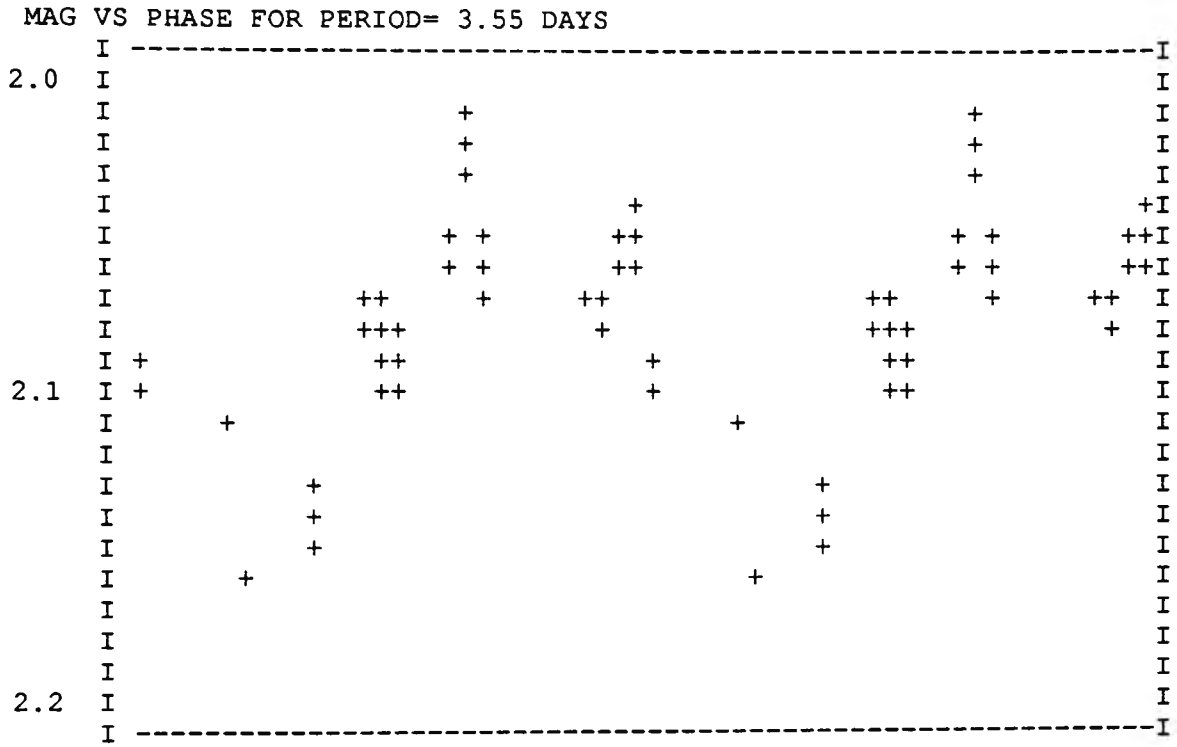

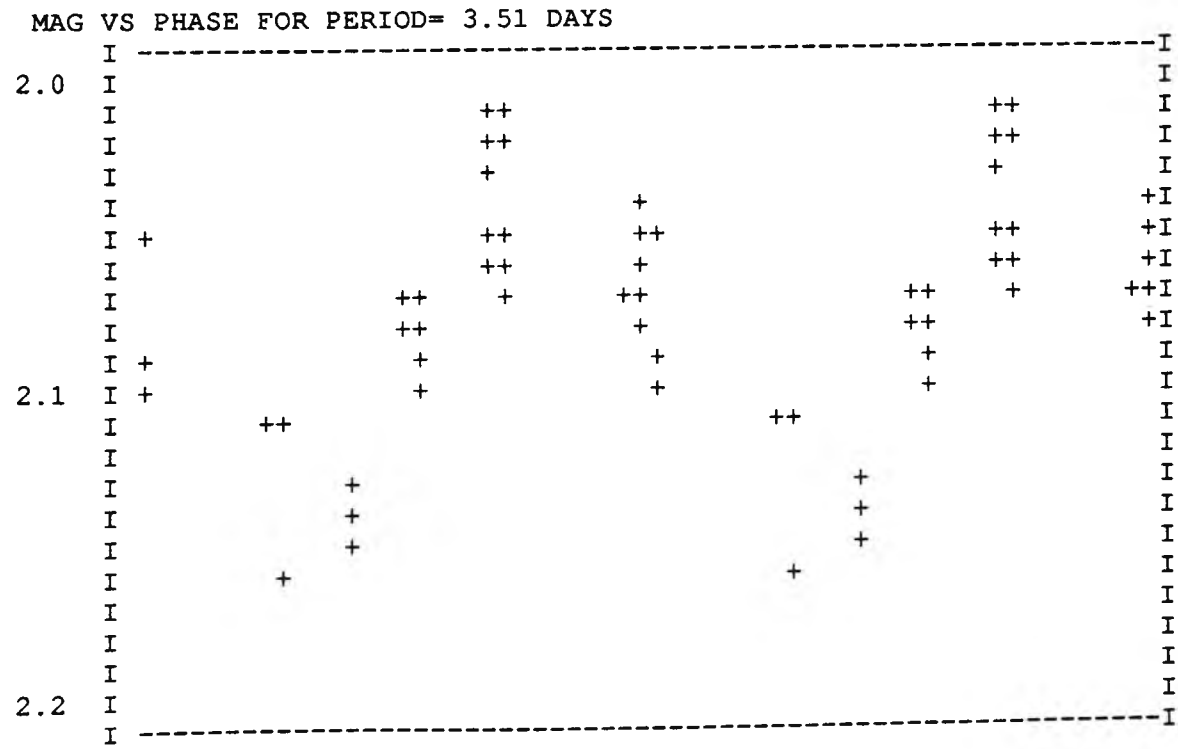

Strom. b Filter

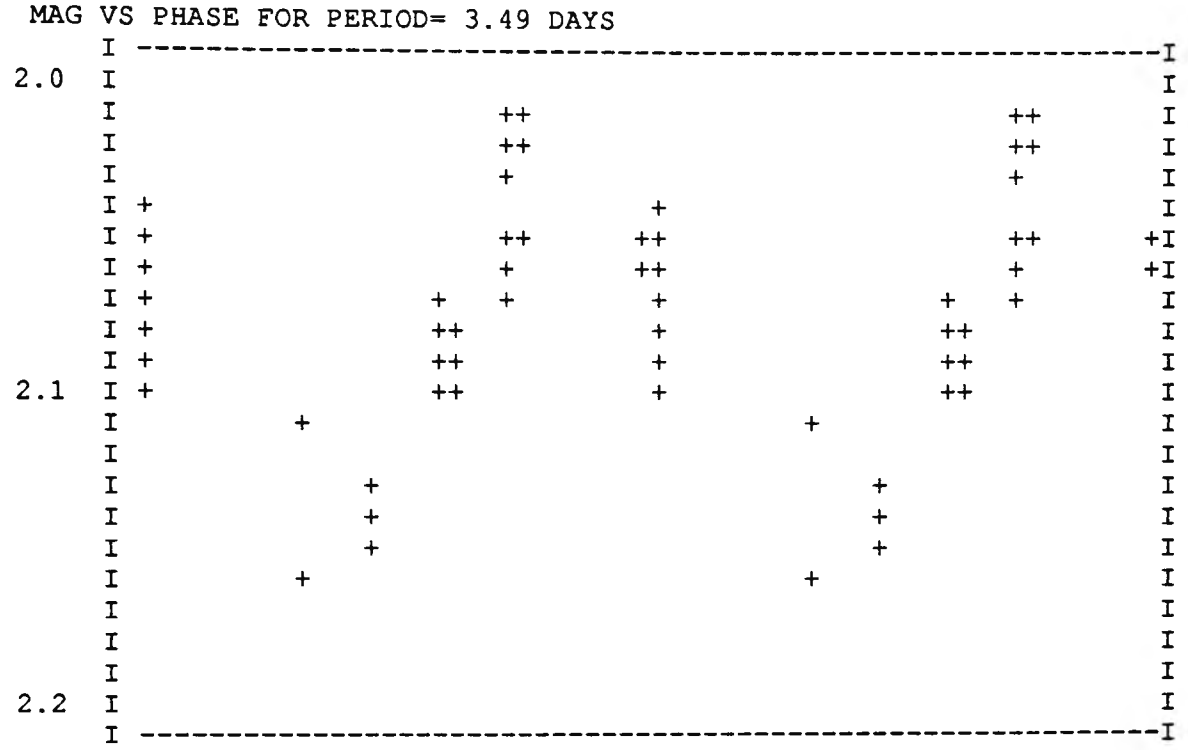

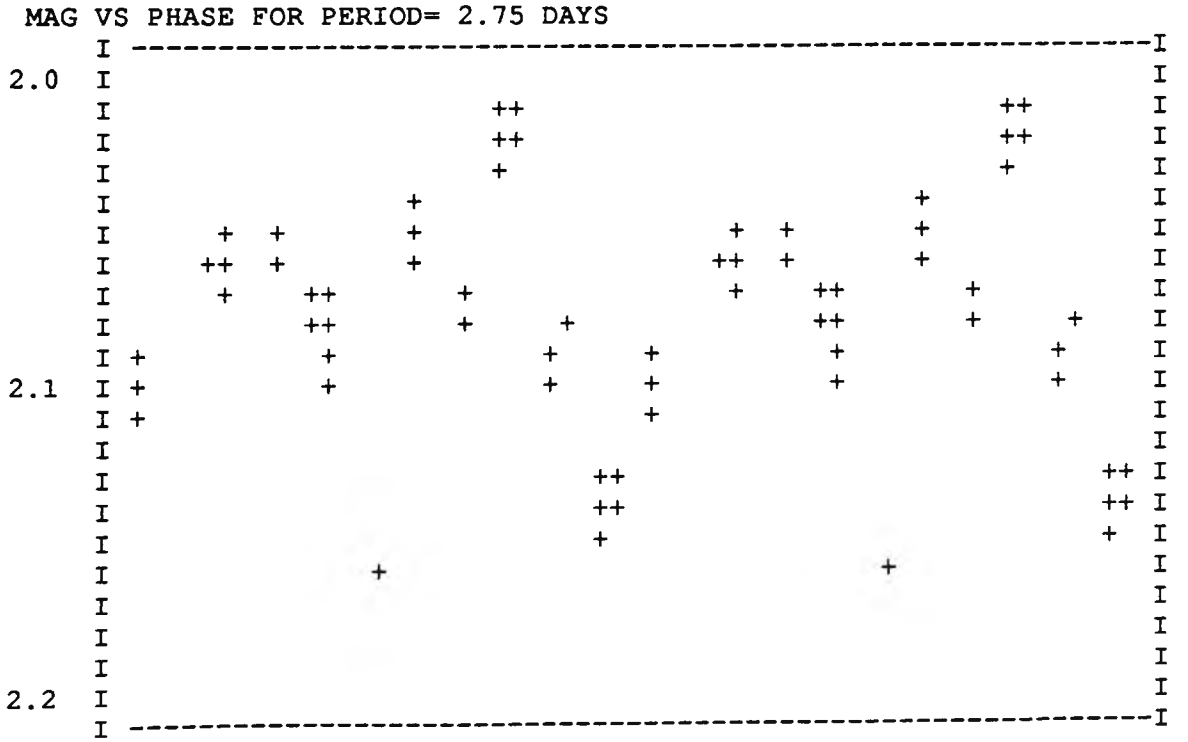

Strom. b Filter

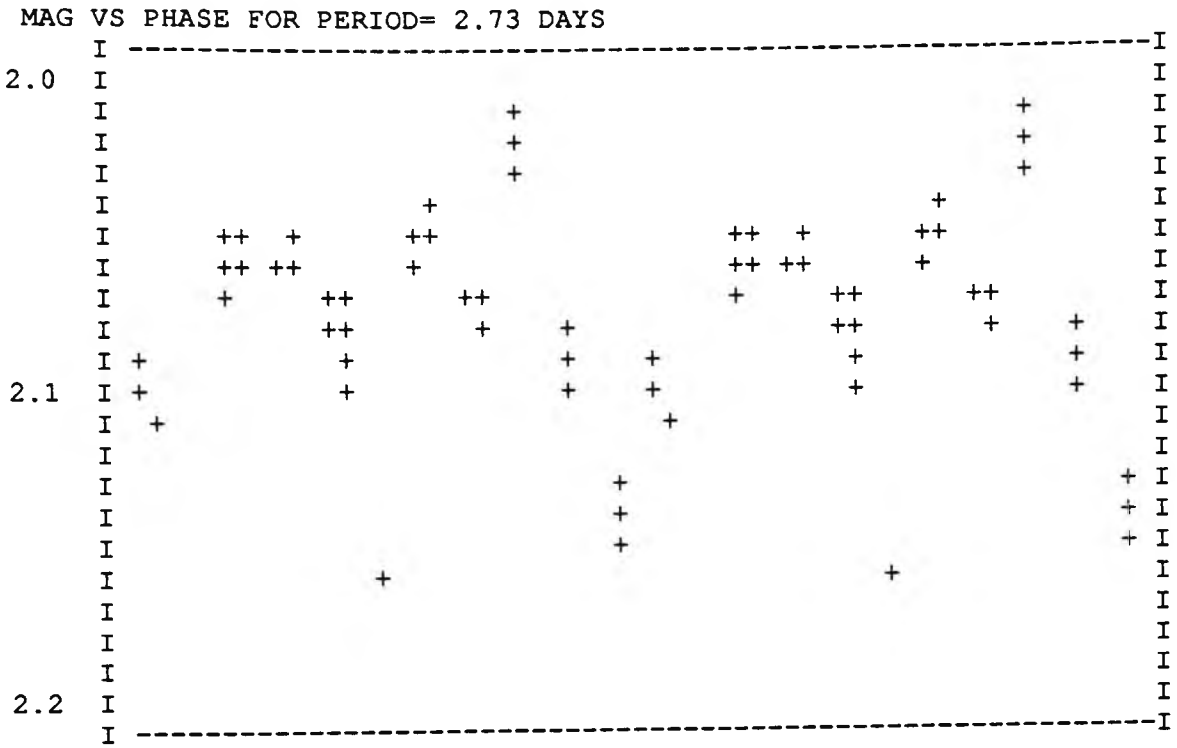

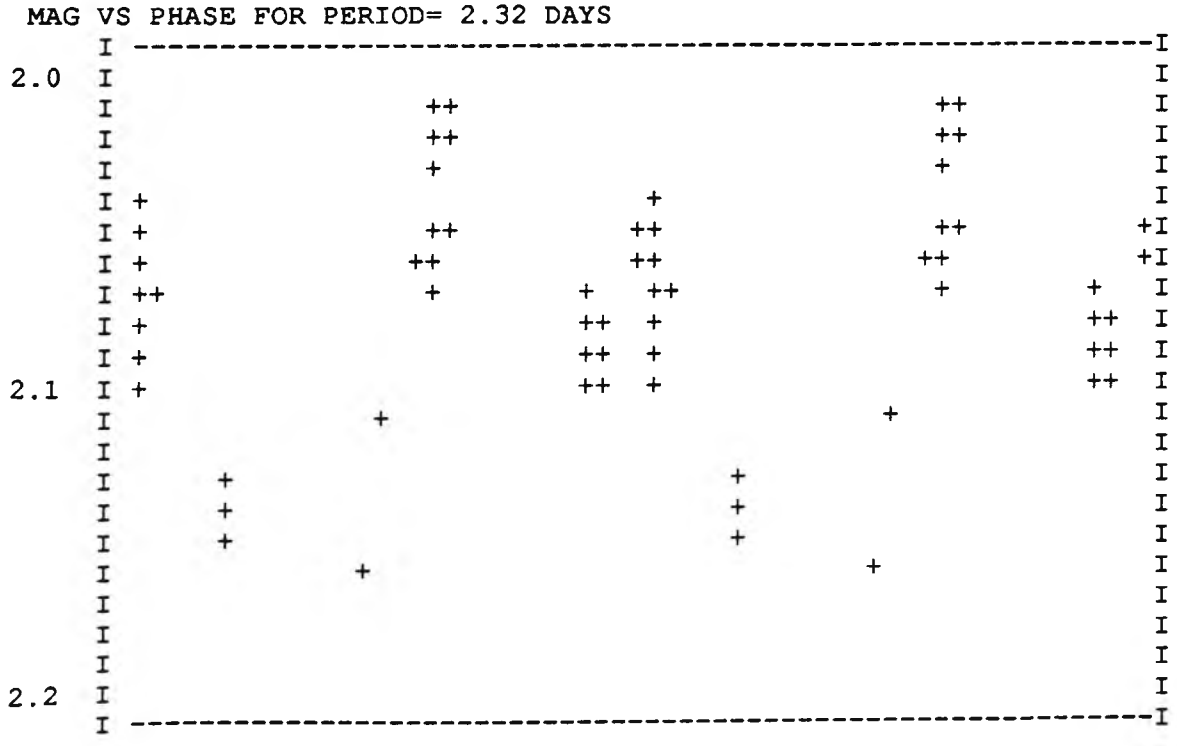

Strom. b Filter

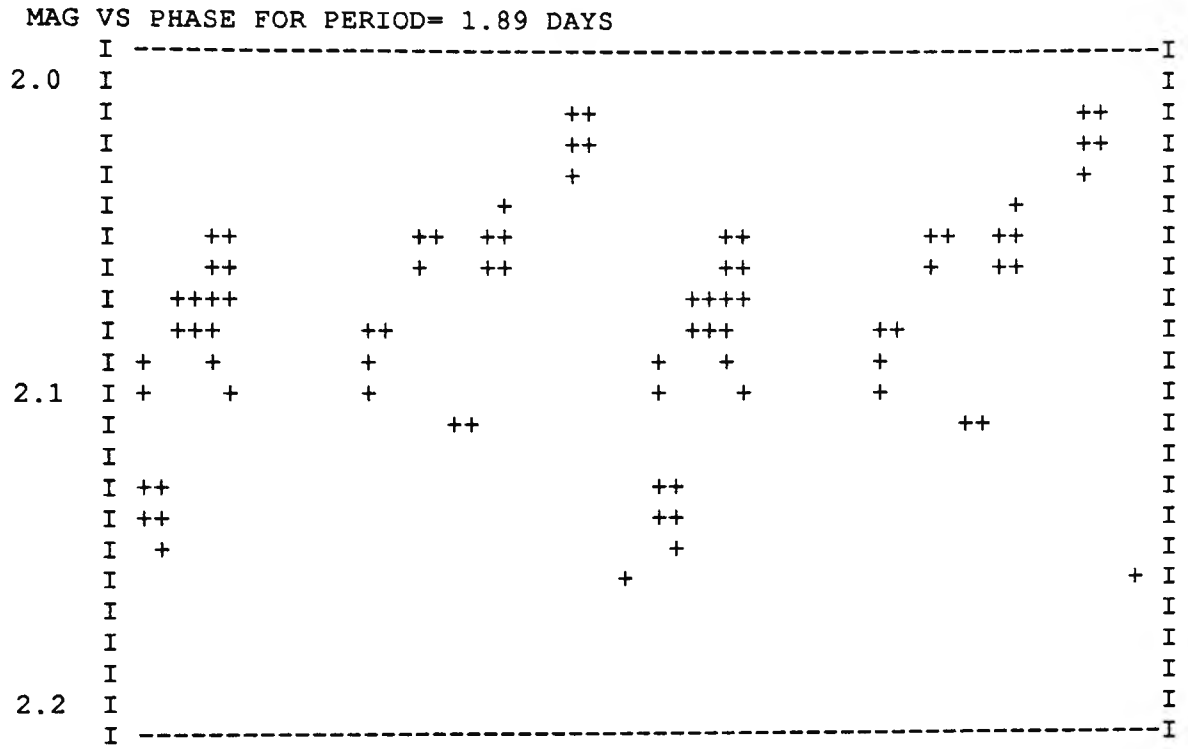

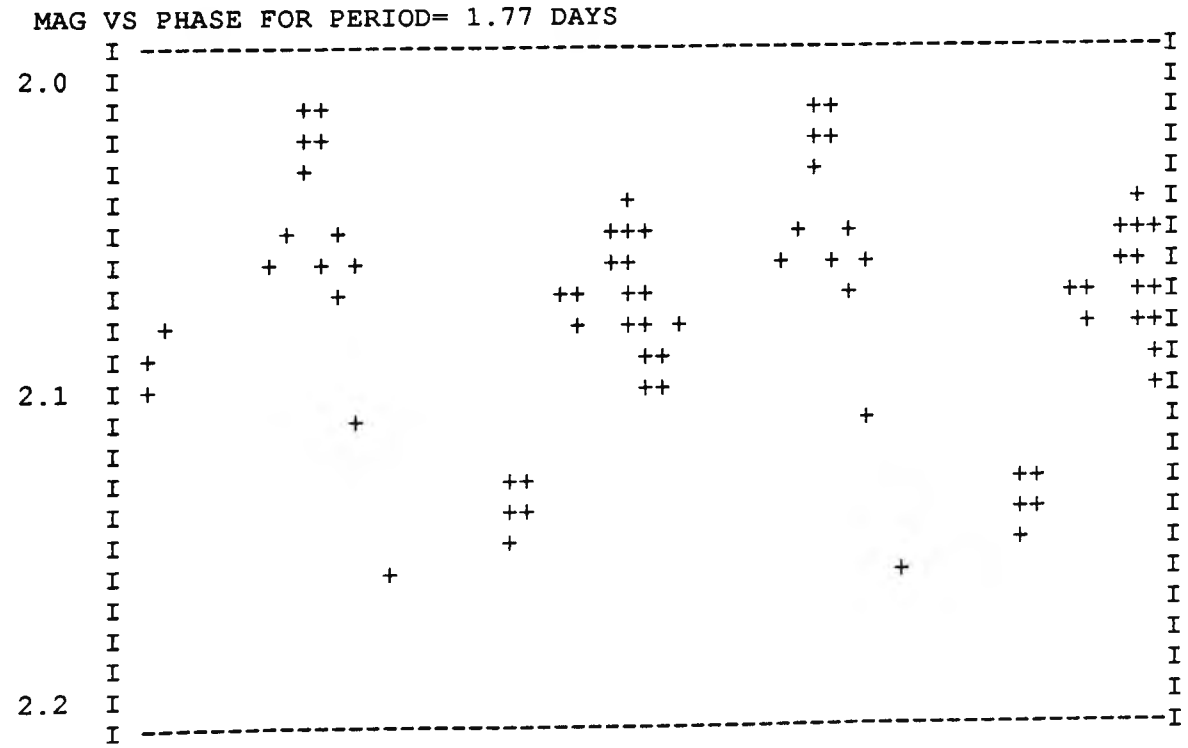

Strom. b Filter

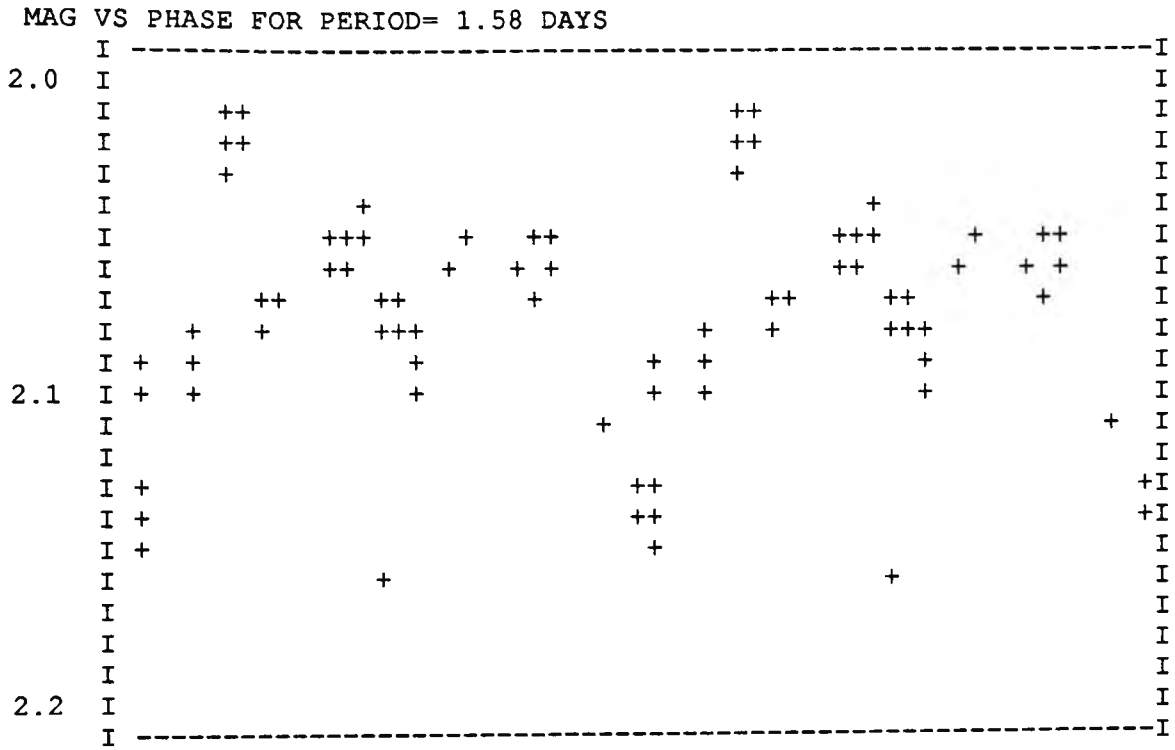

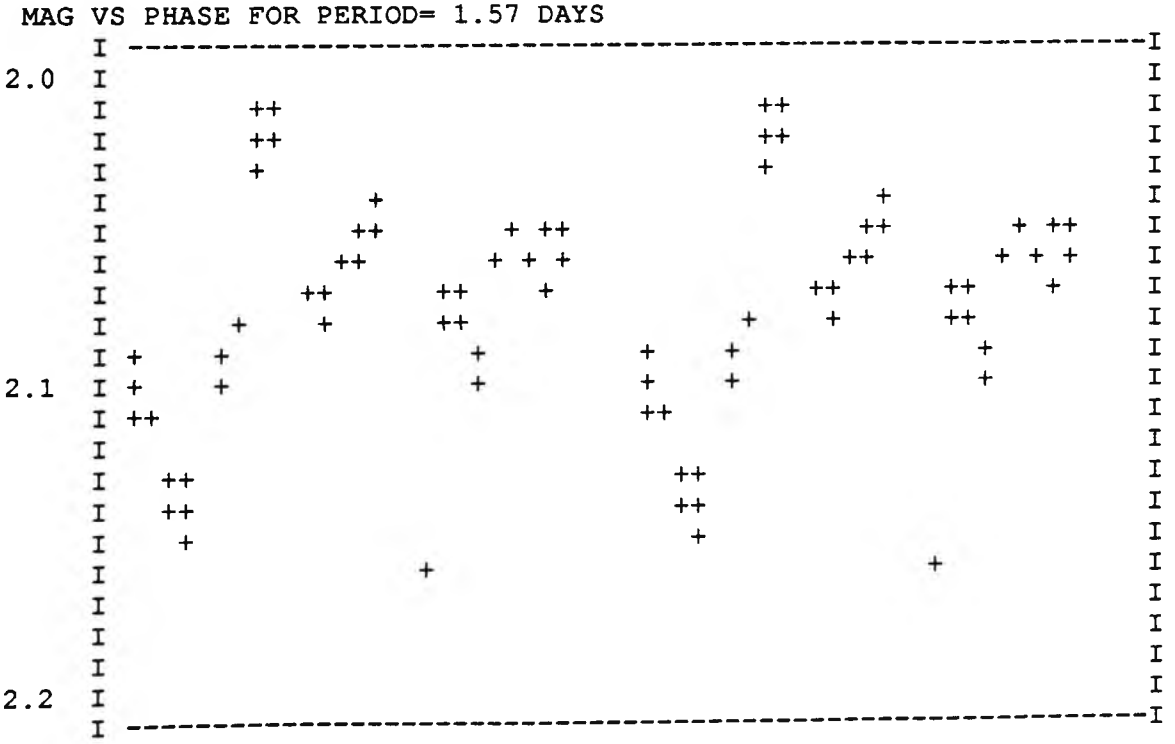

Strom. b Filter

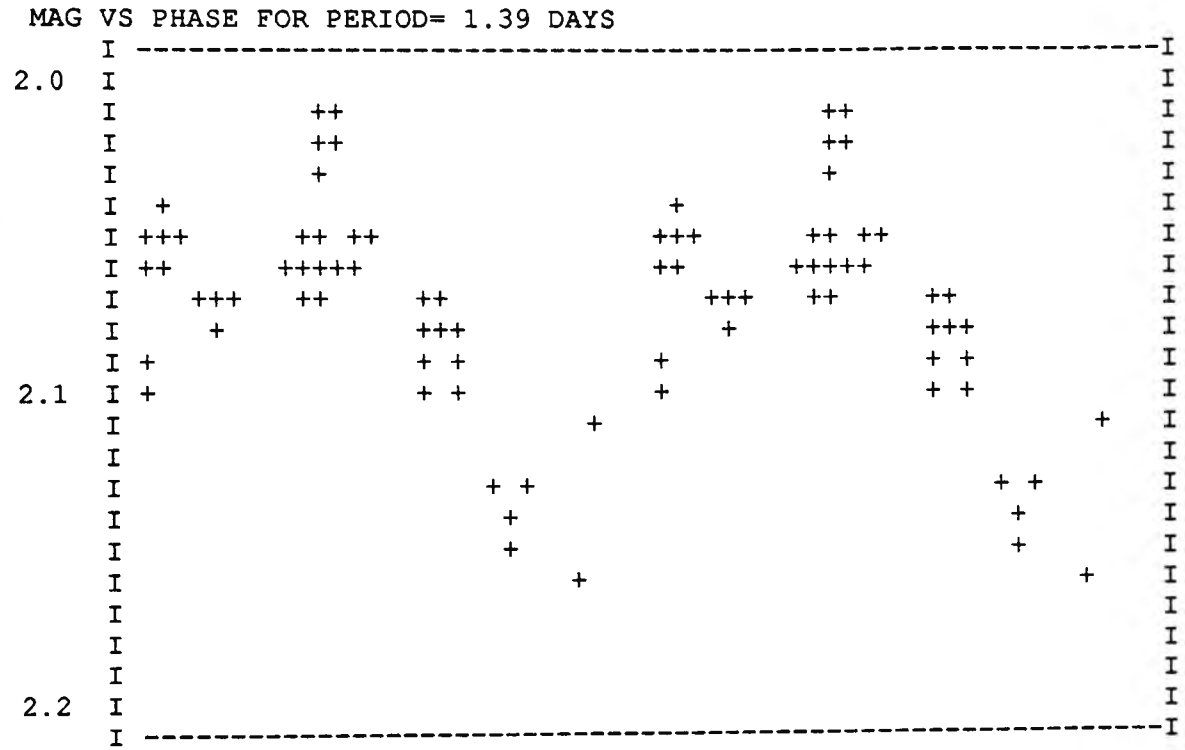

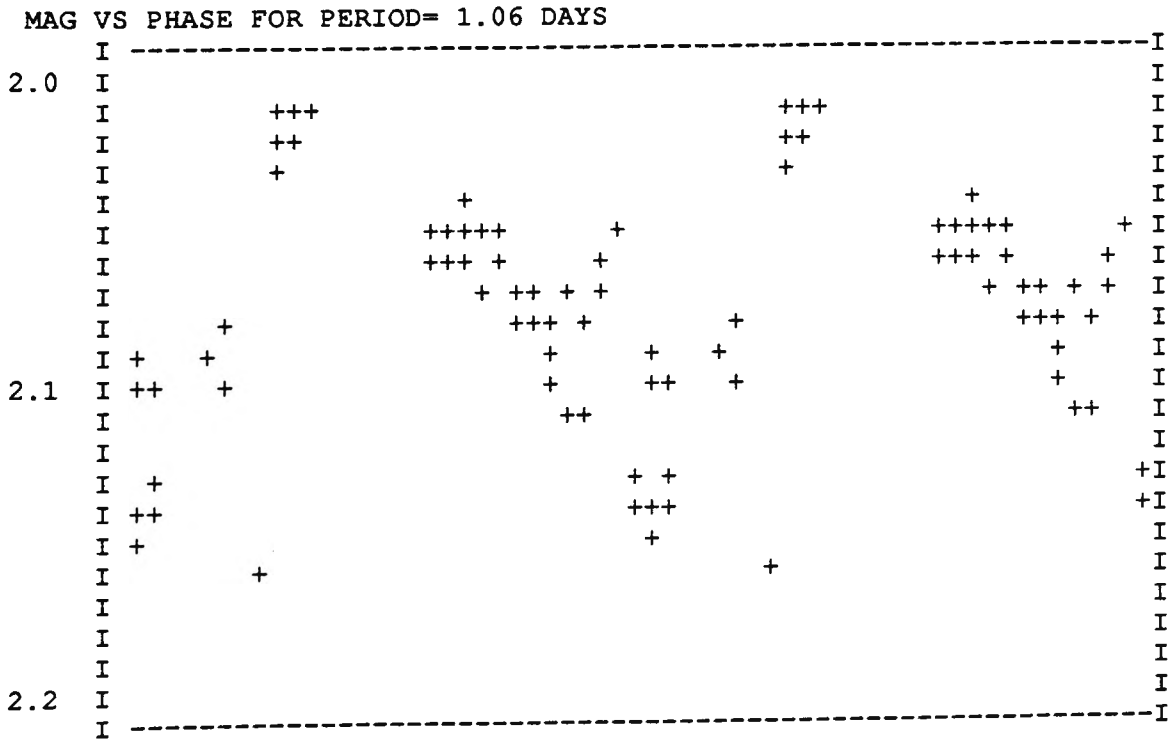

Strom. b Filter

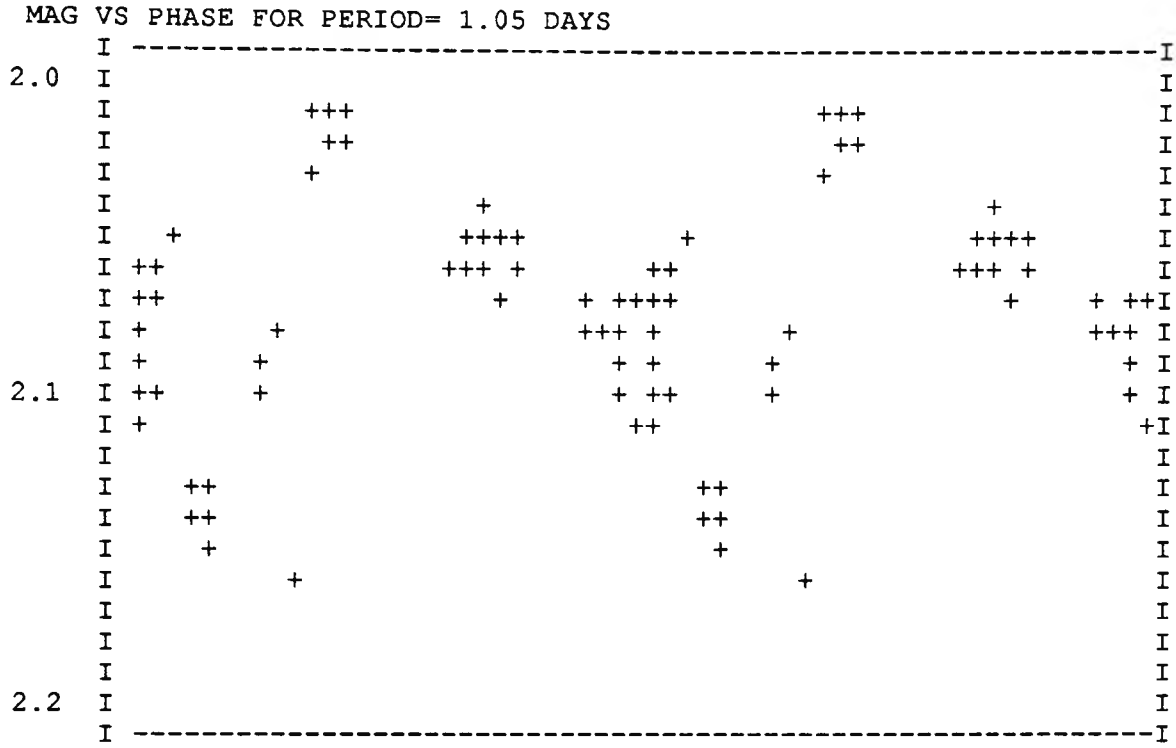

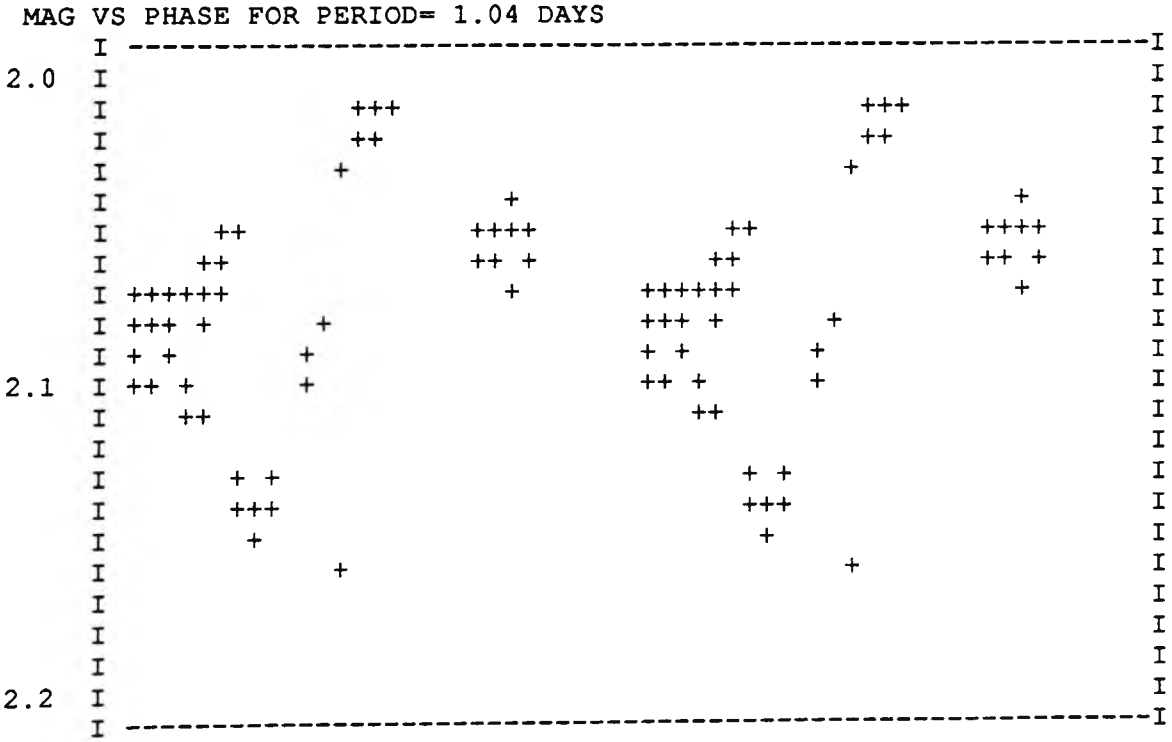

Strom. b Filter

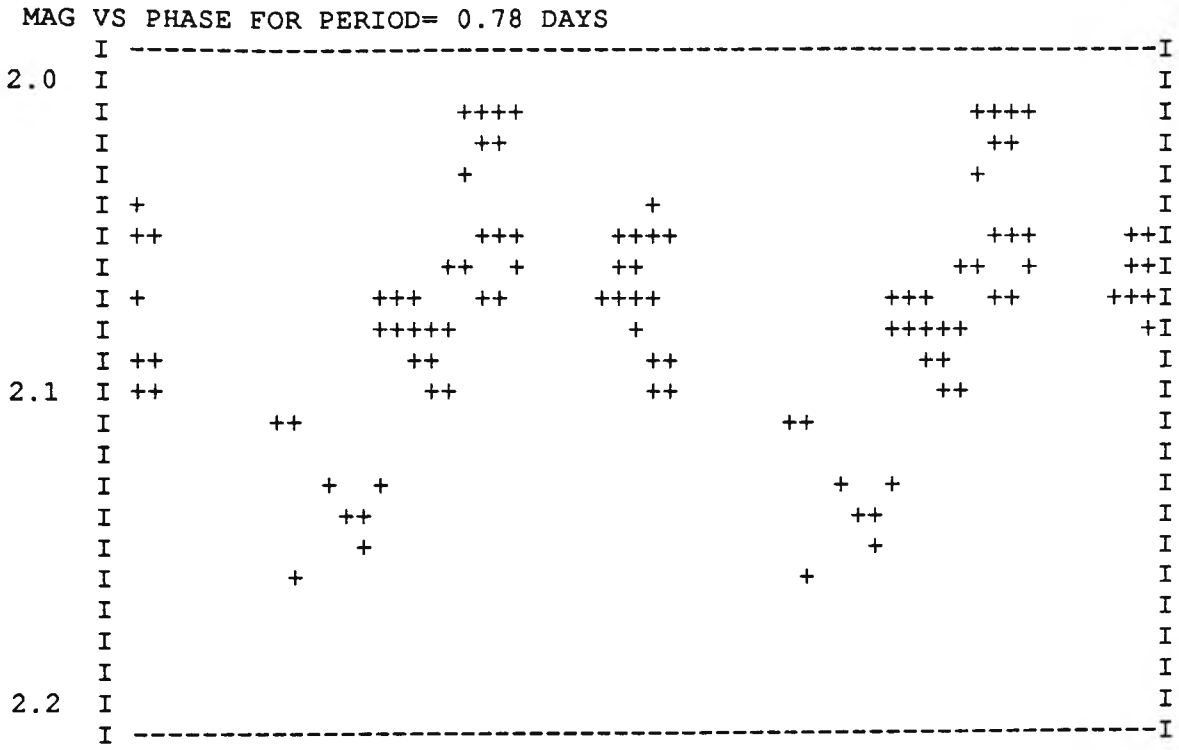

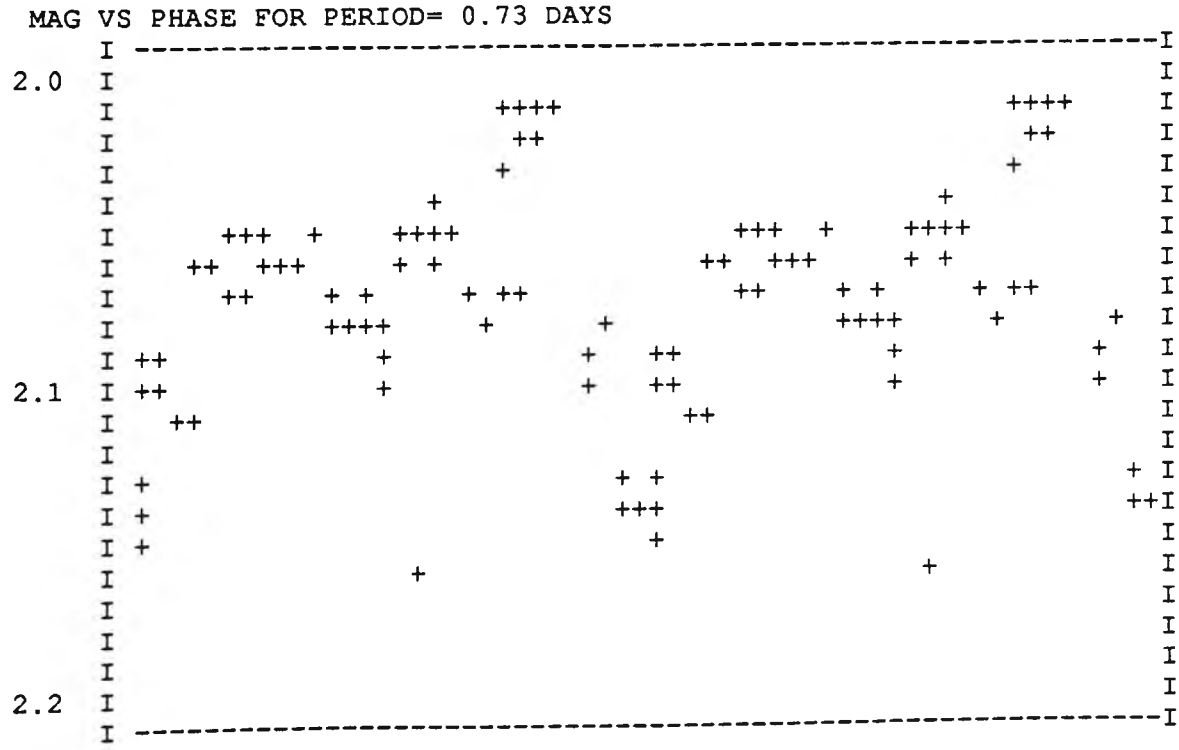

Data Points (John. V Filter)

JD=2448124+	Mag.
7.74844	1.730752
7.75398	1.727568
7.7822	1.729663
7.78798	1.732515
8.72063	1.737605
8.72657	1.736249
8.73765	1.740836
8.74336	1.741256
8.75428	1.741043
8.75982	1.740626
8.77083	1.743171
8.77639	1.743187
8.78738	1.739706
8.79294	1.742263
9.70947	1.727207
9.72619	1.749163
9.73183	1.731853
9.74293	1.737171
9.7486	1.737493
9.76527	1.733315
9.77637	1.739682
9.78275	1.73584
9.79373	1.738111
13.73146	1.81726
13.74263	1.80192
13.77644	1.81516
13.78198	1.83442
14.68887	1.77736
14.70575	1.76589
14.7168	1.76242
14.72258	1.76139
14.73406	1.76569
14.73988	1.761078
14.75096	1.754914
14.75656	1.763245
14.76749	1.76406
14.7733	1.765108
17.75878	1.844923
17.76482	1.840617
17.77593	1.839499
17.78162	1.853109
20.68521	1.73
20.70178	1.727
20.70738	1.726
20.71838	1.726
20.74081	1.726
20.7518	1.723
20.75735	1.723
20.76837	1.727
21.68189	1.801
21.6876	1.809
21.69878	1.804
21.70456	1.807
21.71558	1.807
21.7212	1.806
21.73303	1.8
21.73986	1.799
21.75088	1.801
21.75645	1.799481
21.76734	1.802032
21.77283	1.804969
22.70145	1.729094
22.70727	1.709921
22.71844	1.721073

JD=2448124+	Mag.
22.72416	1.717745
22.73649	1.713
22.74214	1.728
22.75317	1.729
22.75873	1.73
23.70793	1.736565
23.71363	1.740813
23.72476	1.741128
23.73046	1.739695
23.74149	1.733693
23.74713	1.740934
23.75816	1.738015
24.63801	1.72144
24.64367	1.74874
24.67297	1.77136
24.67872	1.747
24.69045	1.742
24.6965	1.741
24.7077	1.734
24.71345	1.736
24.76098	1.733504

Data Points (John, B Filter)

PLATE 64

JD=2448124+	Mag.
1.77951	1.778328
1.79087	1.77807
1.79683	1.777275
7.73101	1.746898
7.73655	1.728392
7.74762	1.747096
7.75317	1.741521
7.76485	1.743217
7.77038	1.728981
7.78139	1.741208
7.78717	1.748051
7.79809	1.741451
8.70301	1.710855
8.70857	1.72552
8.71982	1.73229
8.72574	1.74181
8.77002	1.73592
8.77555	1.727844
8.78657	1.724026
8.79213	1.711391
14.68246	1.678725
14.70493	1.690424
14.71598	1.68176
14.72177	1.697102
14.73905	1.698823
14.75014	1.70803
14.75573	1.69591
14.76669	1.699495
16.76338	1.75268
17.74107	1.753888
17.74679	1.756521
17.75795	1.740312
17.77512	1.757843
20.71756	1.811224
20.72325	1.815988
20.7344	1.8245
20.73999	1.8092
20.75098	1.810045
20.75653	1.808588
20.76756	1.795584
21.68109	1.72646
21.6868	1.73554
21.69796	1.74171
21.70374	1.73079
21.71477	1.72119
21.72039	1.74747
21.73221	1.72682
21.73905	1.74253
21.75006	1.7434
21.75561	1.7429
21.76653	1.74361
21.77201	1.74268
22.6838	1.75312
22.68945	1.76187
22.70062	1.7435
22.72333	1.76714
22.73568	1.7552
22.74132	1.76417
22.75234	1.76404
23.72394	1.79146
23.72965	1.803998
23.74068	1.80316
23.74631	1.80454
23.75734	1.80048
23.76291	1.768

Data Points (Strom. b Filter)

PLATE 65

JD=2448124+	Mag.
1.77349	2.109655
1.77951	2.104354
1.79683	2.104052
1.80832	2.1072
7.69651	2.072465
7.70204	2.072006
7.71299	2.072865
7.71855	2.074258
7.73655	2.064213
7.74762	2.077787
7.75317	2.063788
7.76485	2.075273
7.77038	2.062273
7.78139	2.062657
7.78717	2.068
8.70857	2.0683
8.71982	2.05999
8.73684	2.061141
8.74255	2.063344
8.75347	2.063781
8.75901	2.068906
8.77002	2.05926
8.77555	2.053866
8.78657	2.06104
8.79213	2.061592
14.69926	2.035875
14.70493	2.023876
14.71598	2.028613
14.72177	2.021615
14.73325	2.02327
14.73905	2.0295
14.75014	2.022096
14.75573	2.0293
14.76669	2.022052
14.77249	2.0239
16.76338	2.167755
17.74107	2.095301
17.74679	2.1089
17.75795	2.0937
17.76363	2.091405
17.77512	2.085305
20.71756	2.13576
20.72325	2.15044
20.7344	2.14828
20.75098	2.15576
20.75653	2.15016
20.76756	2.14612
20.7731	2.14276
21.6868	2.06882
21.69796	2.069779
21.70374	2.06727
21.73221	2.063076
21.73905	2.0619
22.6838	2.079
22.68945	2.078
22.71762	2.092
22.73568	2.076
22.74132	2.077
22.75234	2.07569
22.75789	2.077853
23.74068	2.115
23.74631	2.12
23.75734	2.116
23.76291	2.116

JD=2448124+	Mag.
24.67215	2.08421
24.67791	2.08921
24.68965	2.07895
24.69569	2.09105
24.70687	2.08577
24.72507	2.08801
24.73098	2.08288
24.74243	2.08964
24.74855	2.09988
24.76015	2.1071